SPS 2019, Zurich
26-30 August 2019

Recent Measurements of Vacuum Muonium

Narongrit Ritjoho

PSI and ETH Zurich

* A. Antognini, P. Crivelli, T. Hume, K. Kirch, J. Nuber, D. Taqqu (ETH Zurich)
* M. Bartkowiak, A. Knecht, A. Papa, N. Ritjoho, R. Scheuermann, A. Soter, B. van den Brandt, L. Ziegler (Paul Scherer Institut)
* M. F. L. De Volder (University of Cambridge)
* D.M. Kaplan and T. J. Phillips (Illinois Institute of Technology)

Motivations

* Muonium atom (μ^+e^-)
* Aim : To build a high-brightness muonium beam for the gravity measurement of muonium

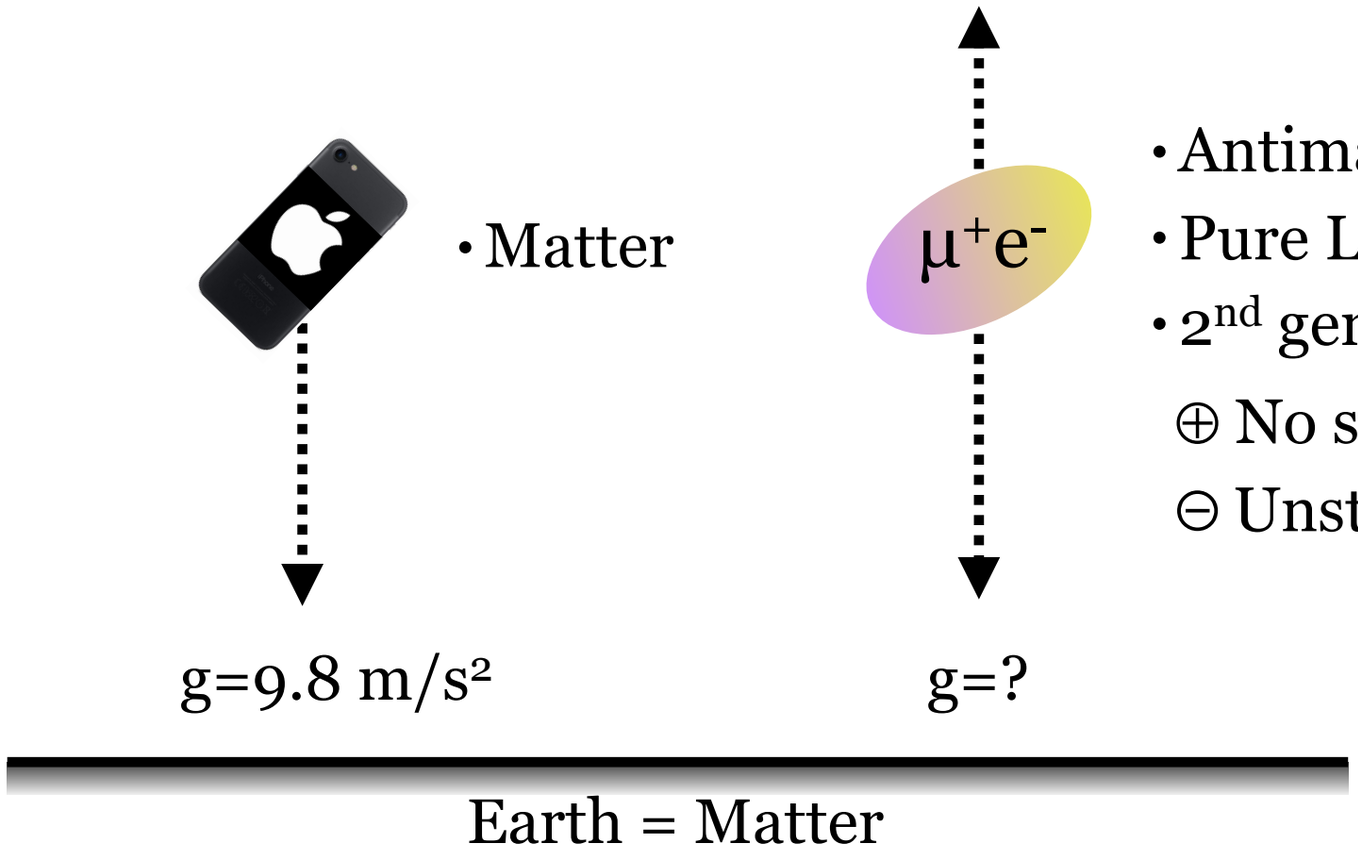

- Antimatter (✔Anti-H) (✔Ps)
- Pure Lepton (✘Anti-H) (✔Ps)
- 2^{nd} gen. particles (✘Anti-H) (✘Ps)

⊕ No strong interaction

⊖ Unstable, Lifetime=2.2 μs

WANTED
Vacuum Muonium

Gravity of muonium measurement

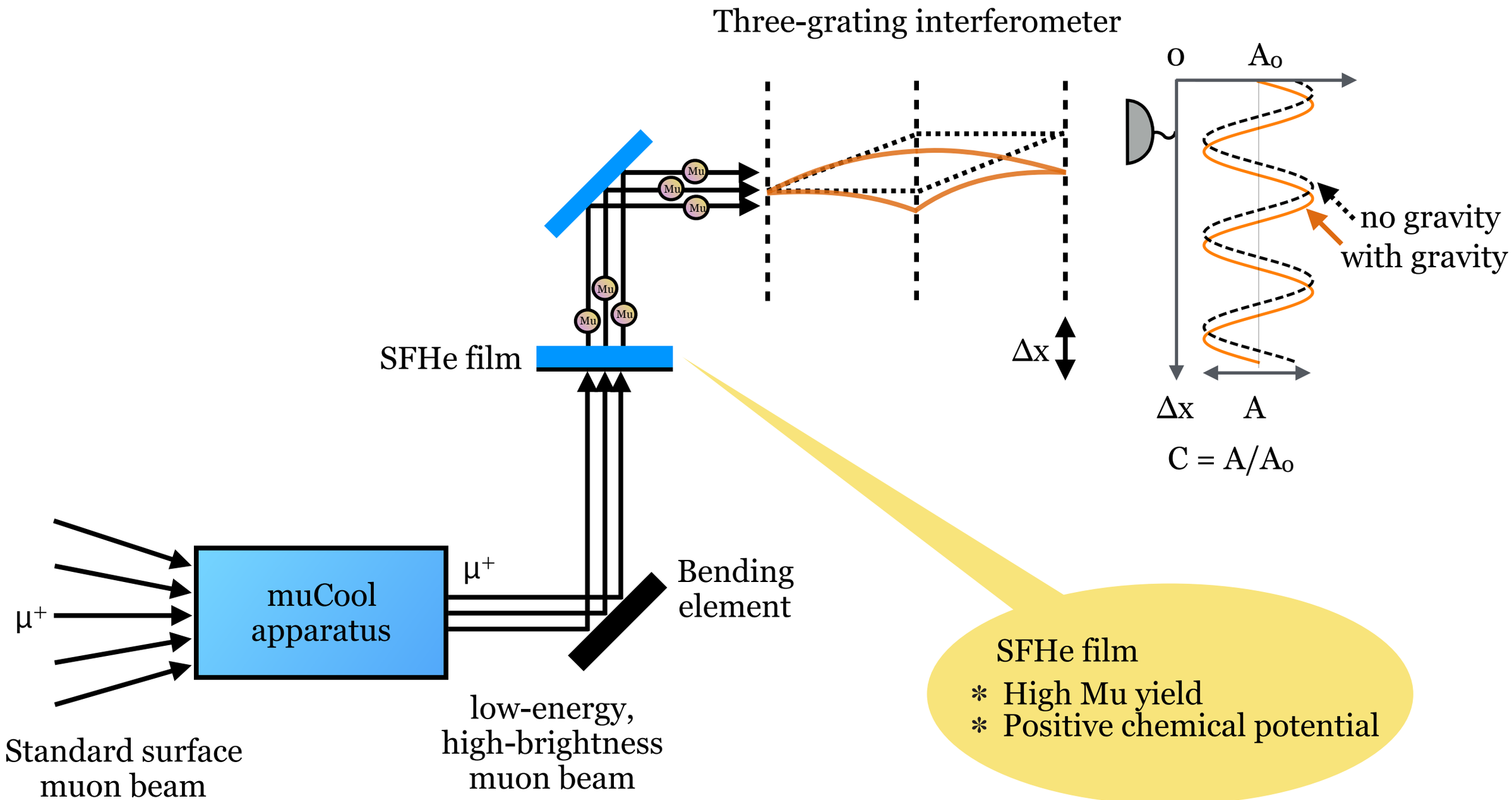

Gravity of muonium measurement

This project:
Development of
a high-brightness
muonium beam

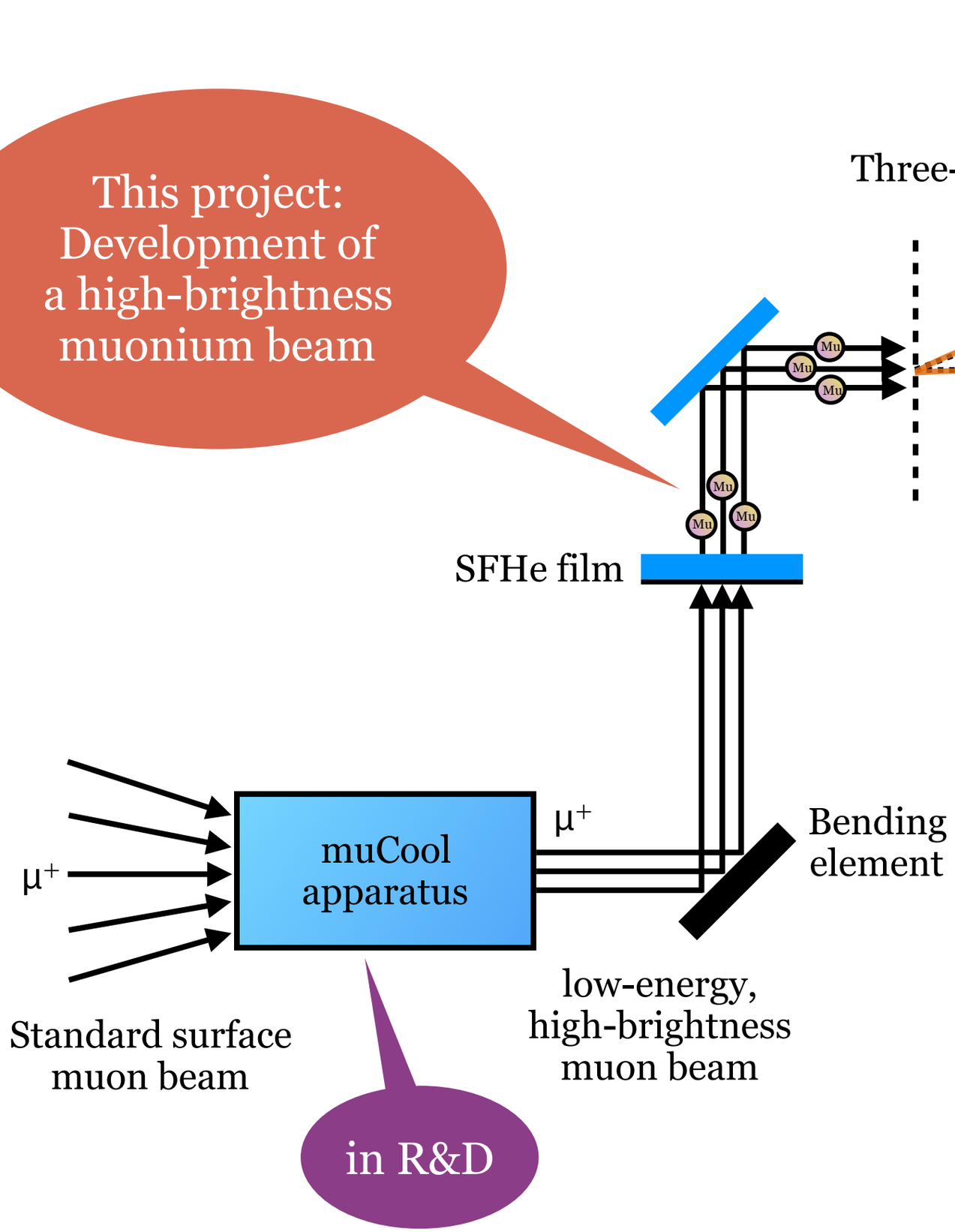

in R&D

Three-grating interferometer

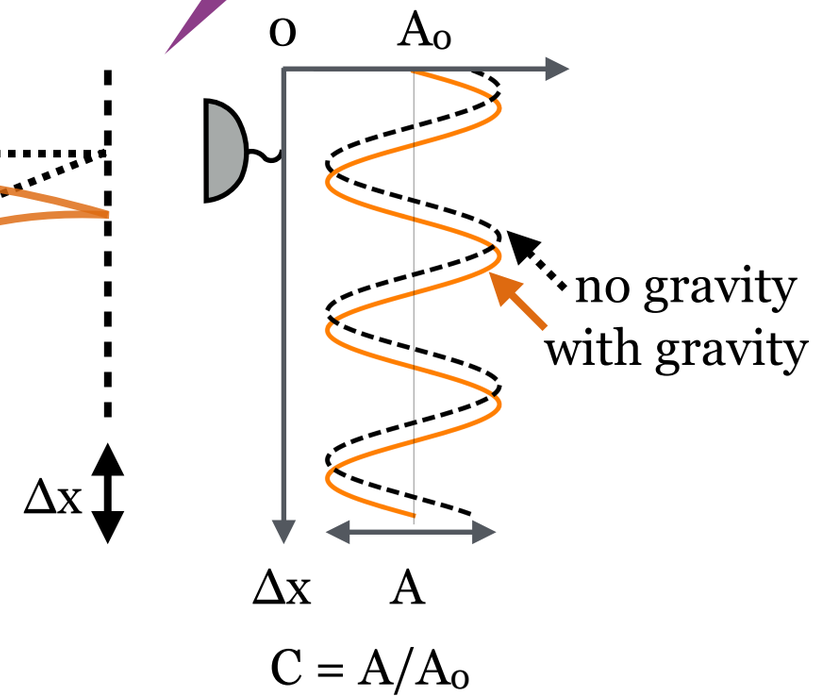

SFHe film

- High Mu yield
- Positive chemical potential

Experiments regarding muonium

This project: Development of a high-brightness muonium beam

1. Vacuum muonium from Aerogel, Zeolite, Semiconductor-CNT
2. Vacuum muonium from SFHe film coated nanostructure materials, and free-surface
3. Muonium emission into helium gas

Experiments regarding muonium

1. Vacuum muonium from Aerogel, Zeolite, Semiconductor-CNT

① Vacuum muonium from Aerogel, Zeolite, Semiconductor-CNT

SPS 2019, Zurich
26-30 August 2019

Aim

* To observe the vacuum muonium atoms from alternative porous materials at room temperature
* To test the detection technique of vacuum muonium by exploiting atomic electrons

Experimental Setup

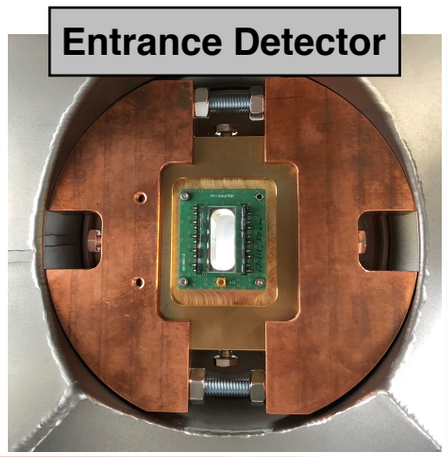

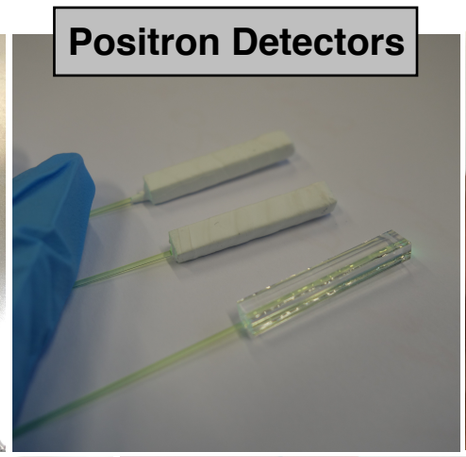

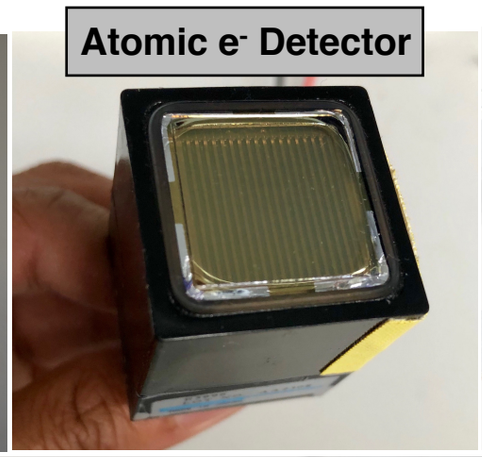

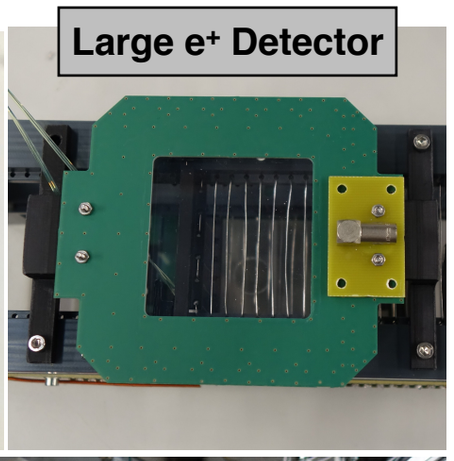

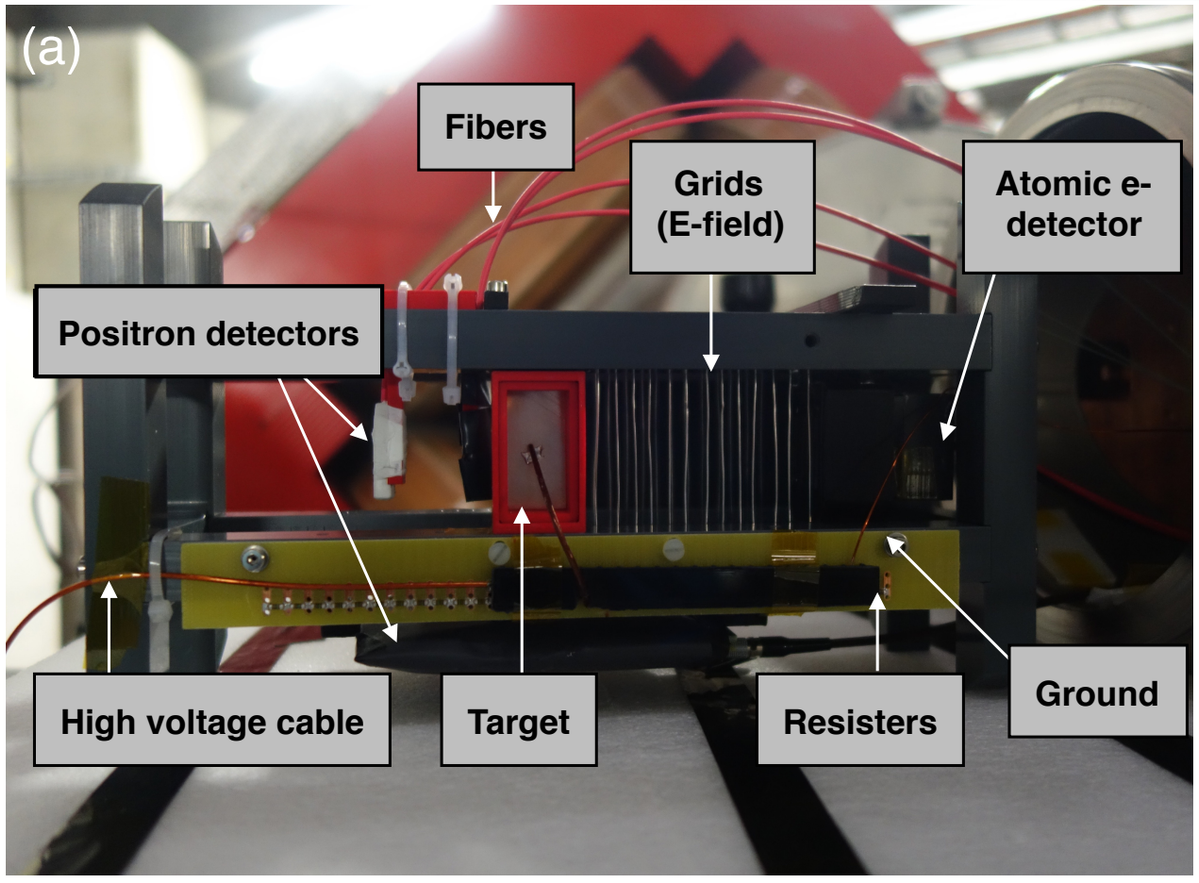

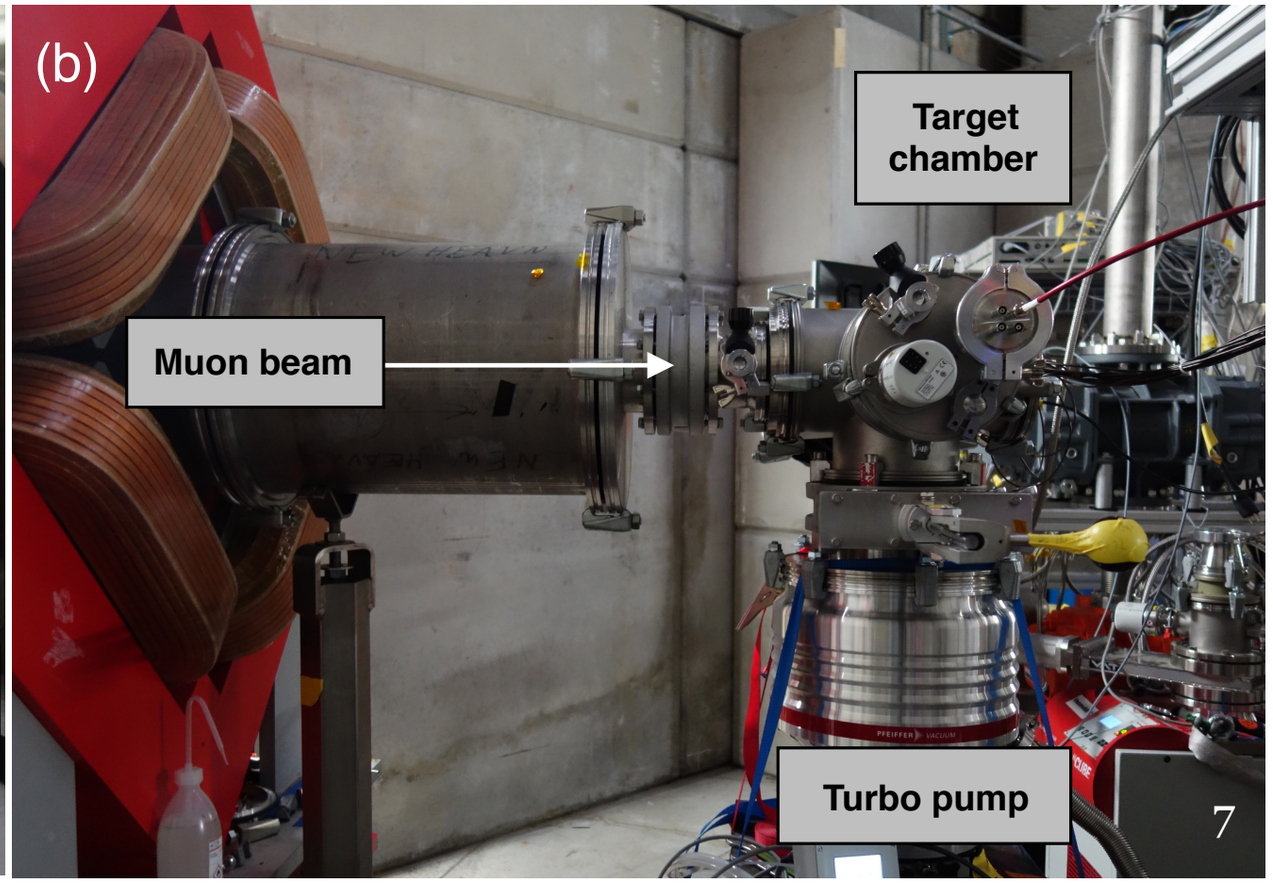

Experimental Setup

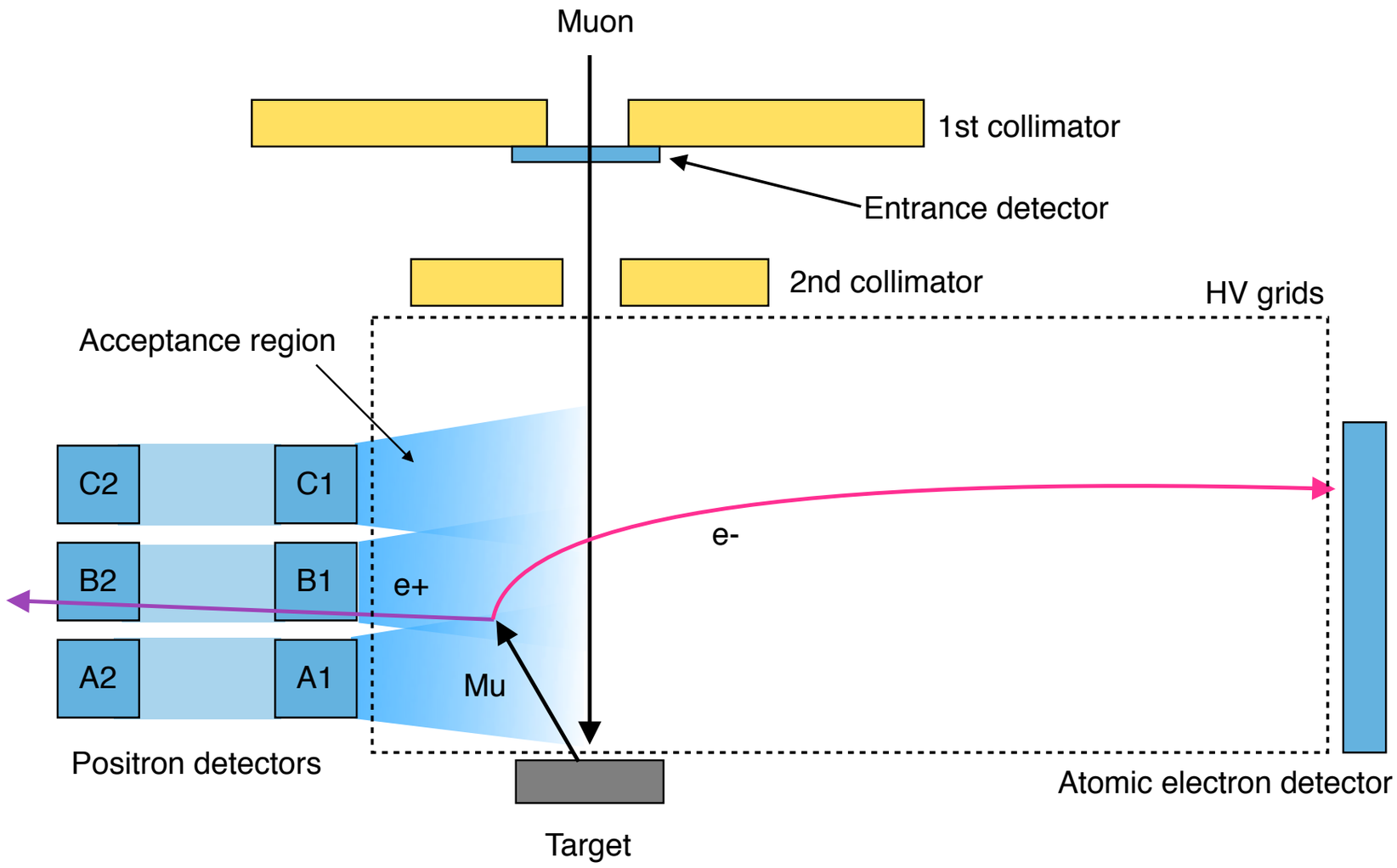

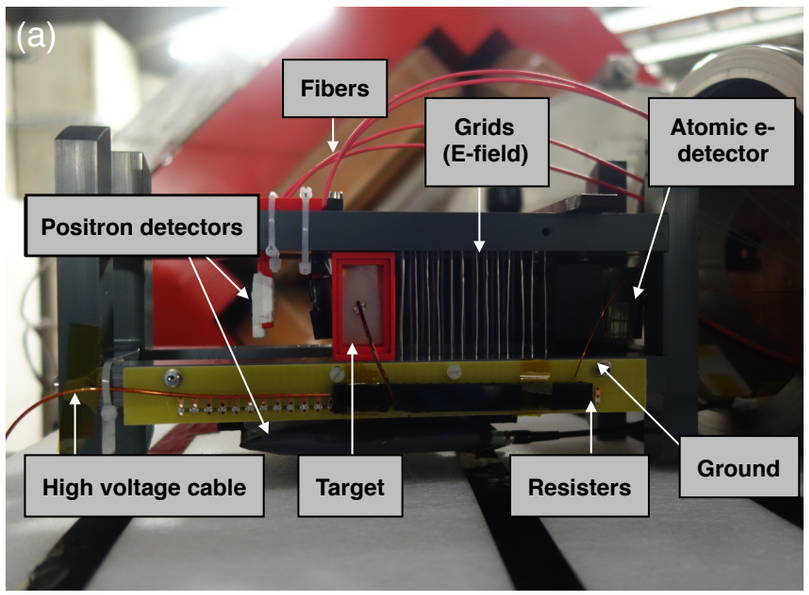

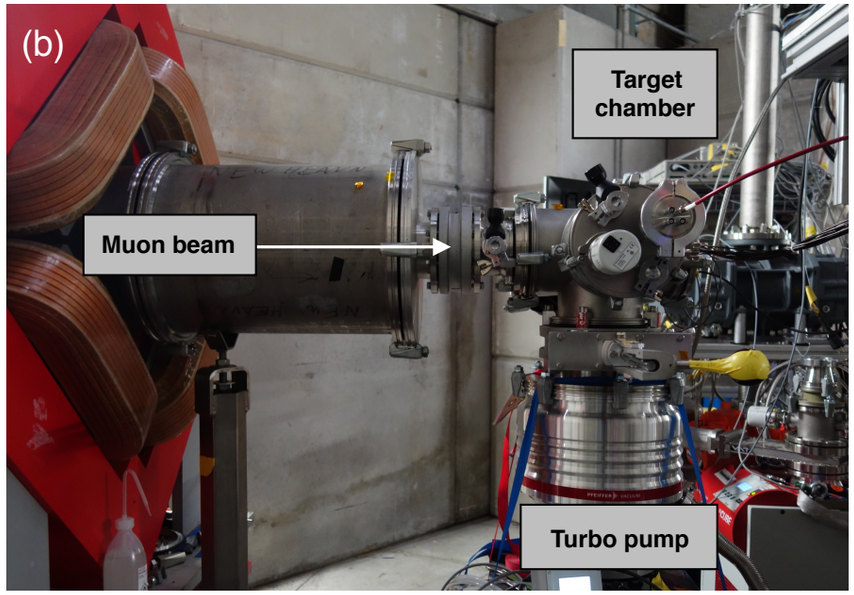

Detection methods

1. Double coincidence of decay e^+

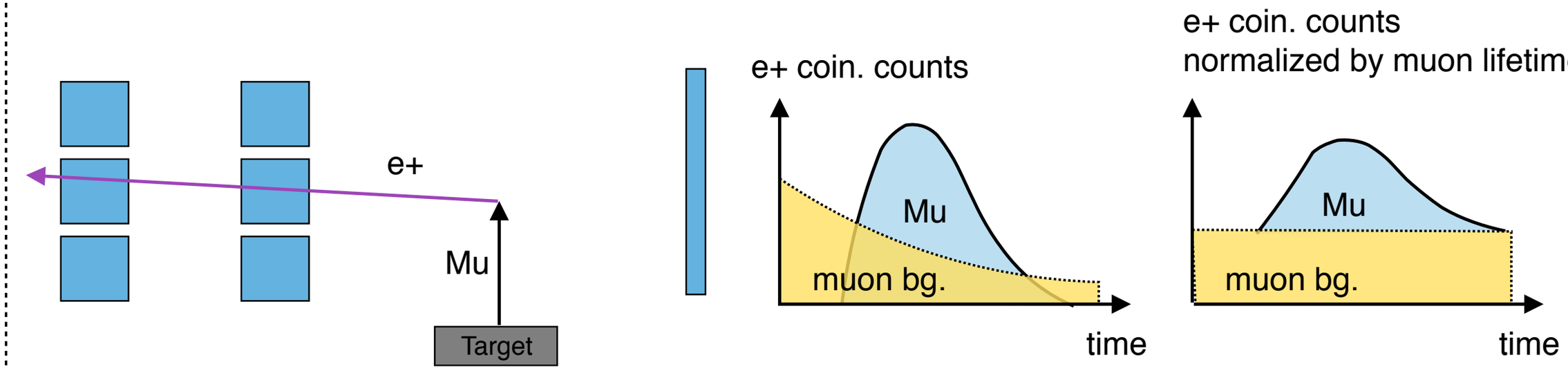

2. Triple coincidence of decay e^+ and atomic e^-

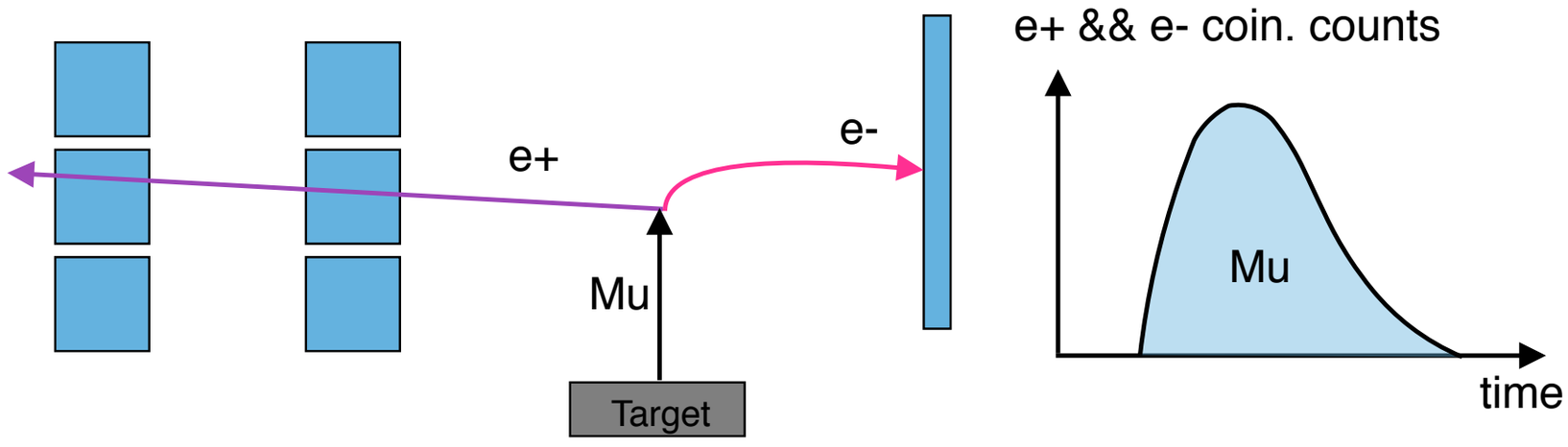

Vacuum muonium from Aerogel, Zeolite, Semiconductor-CNT

Targets

1. Laser ablated aerogel

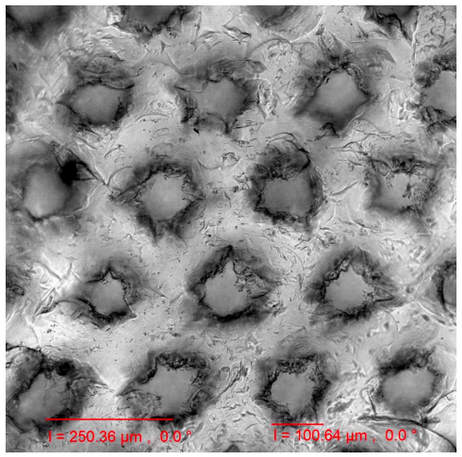

†

2. Zeolite powder

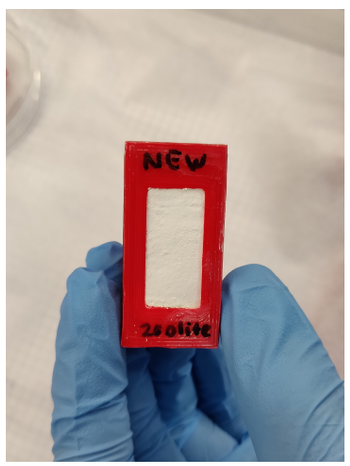

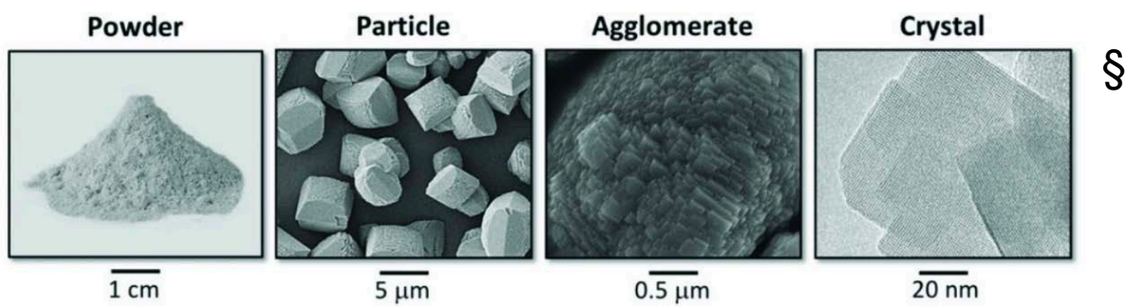

§

3. Semiconductor carbon nanotubes

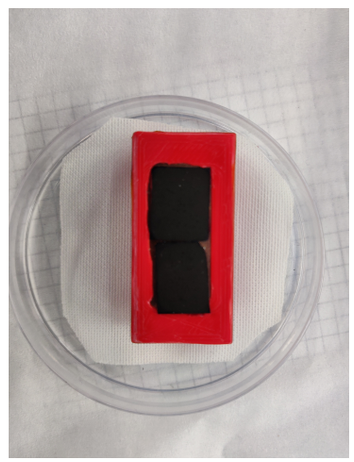

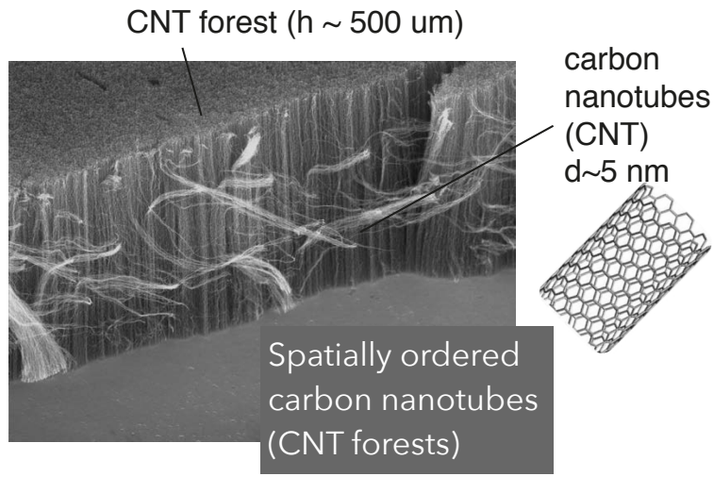

¶

† courtesy of S. Kamal and G. Marshall from TRIUMF,
§ courtesy of L. Gerchow, P. L. Begona, and P. Crivelli from ETH,
¶ courtesy of M. De Volder and C. Valentine from Cambridge.

Vacuum muonium from Aerogel, Zeolite, Semiconductor-CNT

Results of vacuum muonium

Triple coincidences of middle detectors from different types of targets

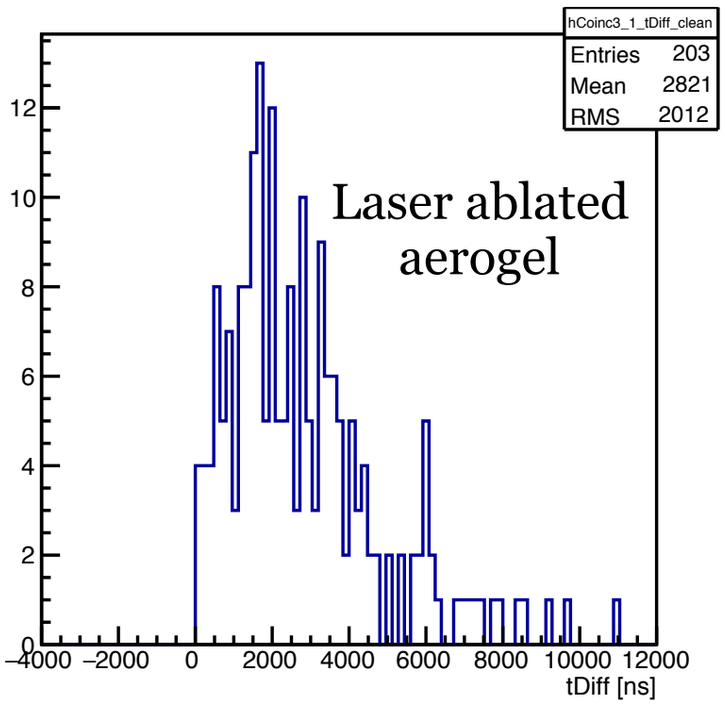

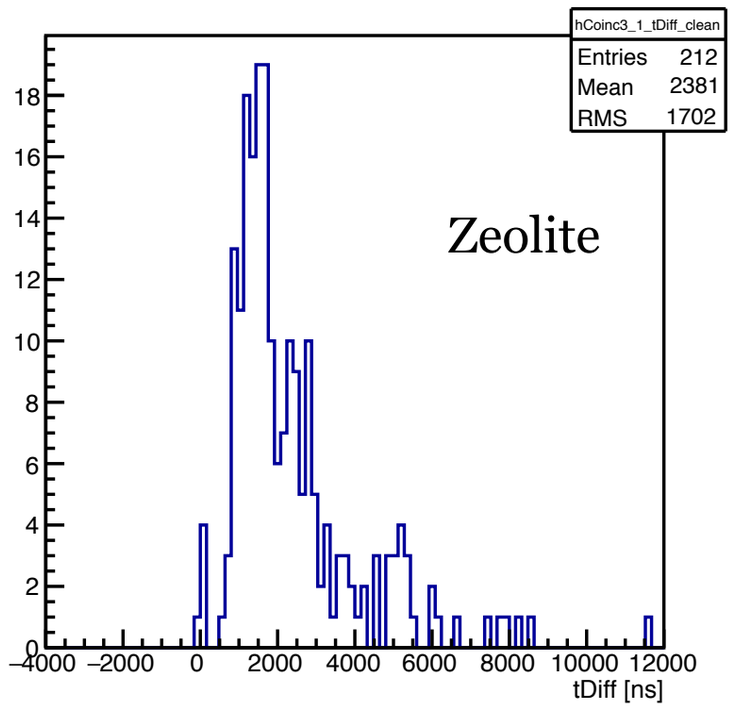

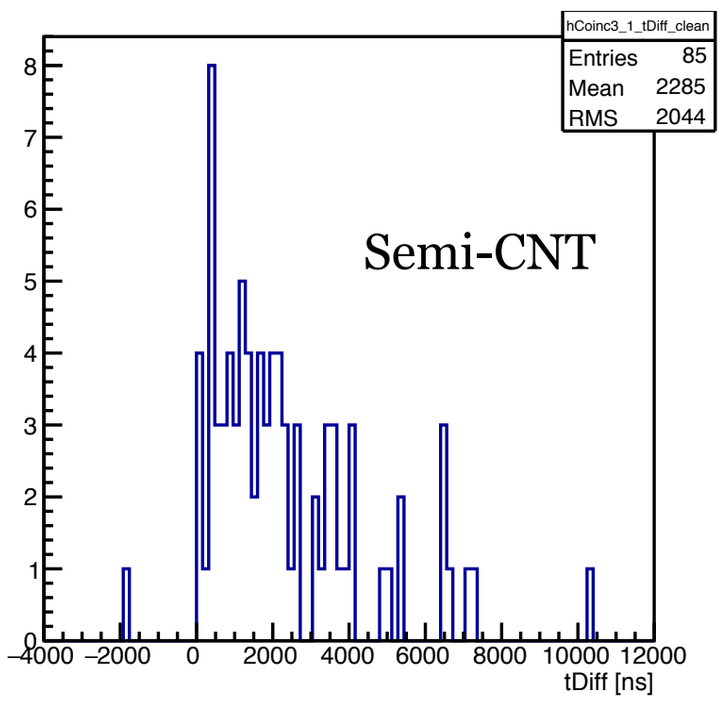

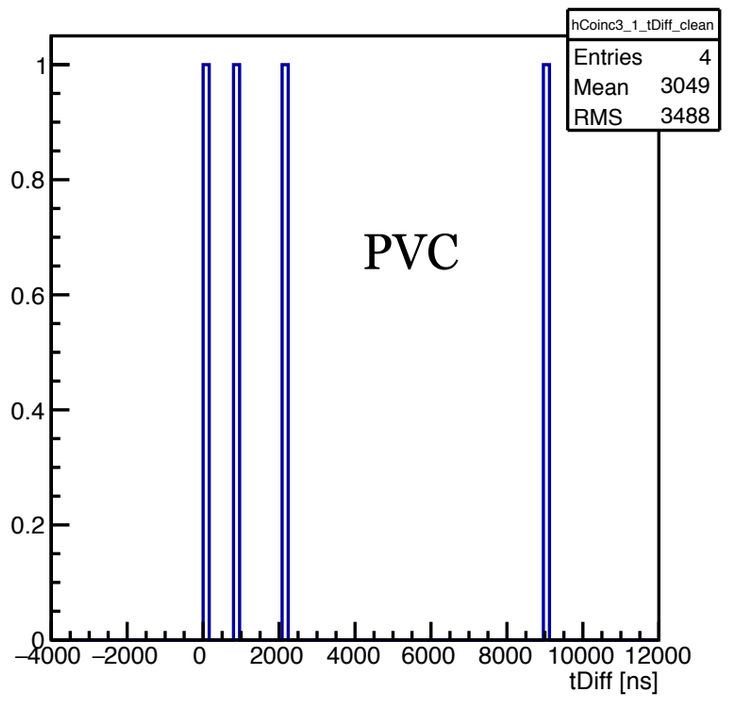

Vacuum muonium yield from aerogel ~50% larger than the yield from zeolite

Vacuum muonium from Aerogel, Zeolite, Semiconductor-CNT

Results of vacuum muonium

Triple coincidences

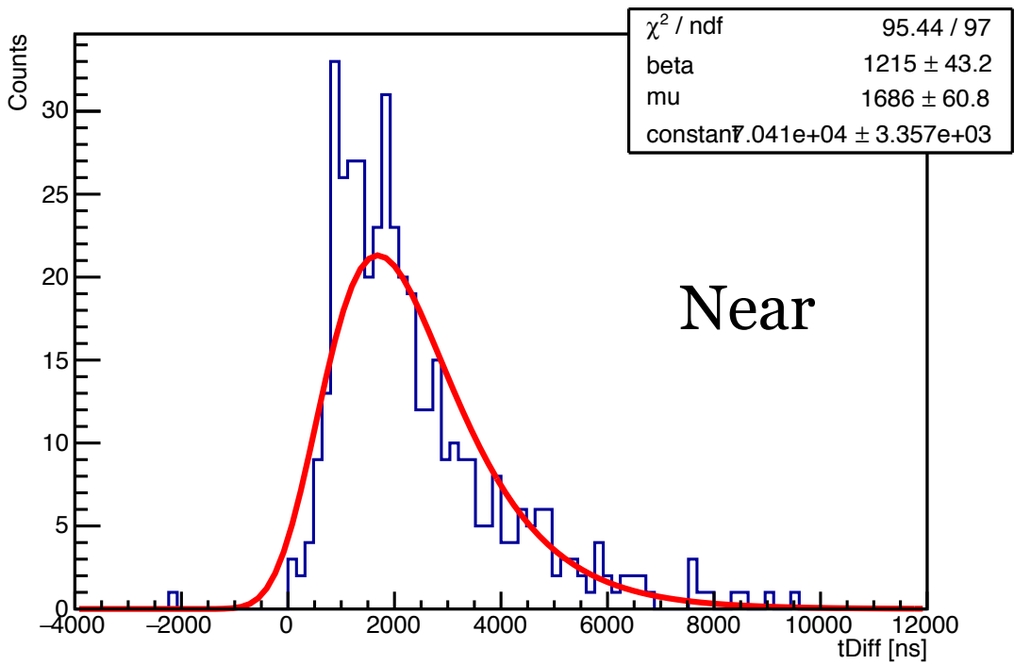

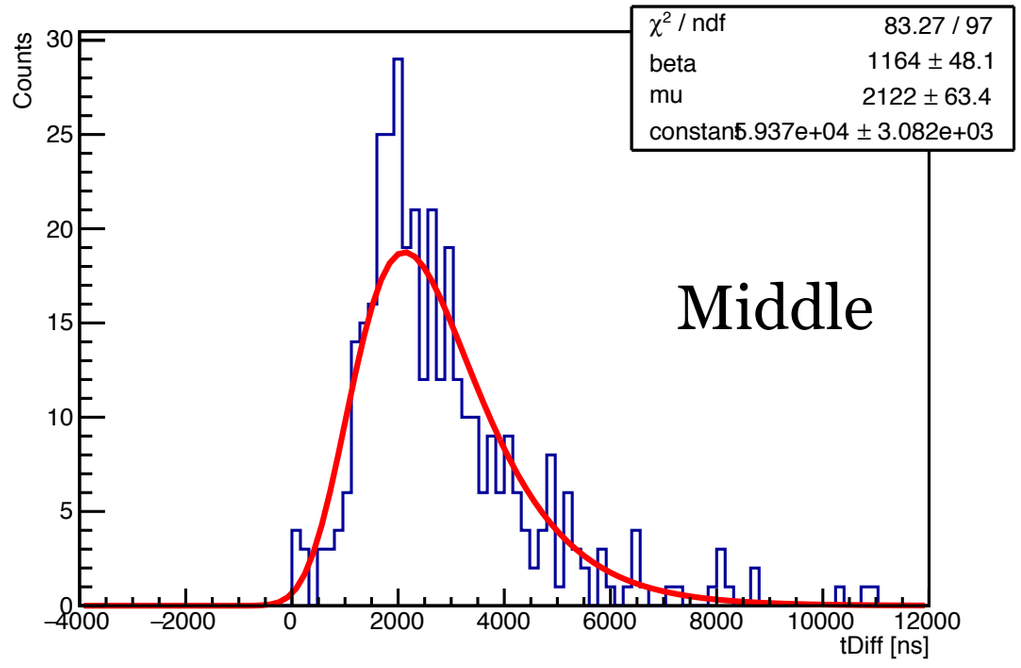

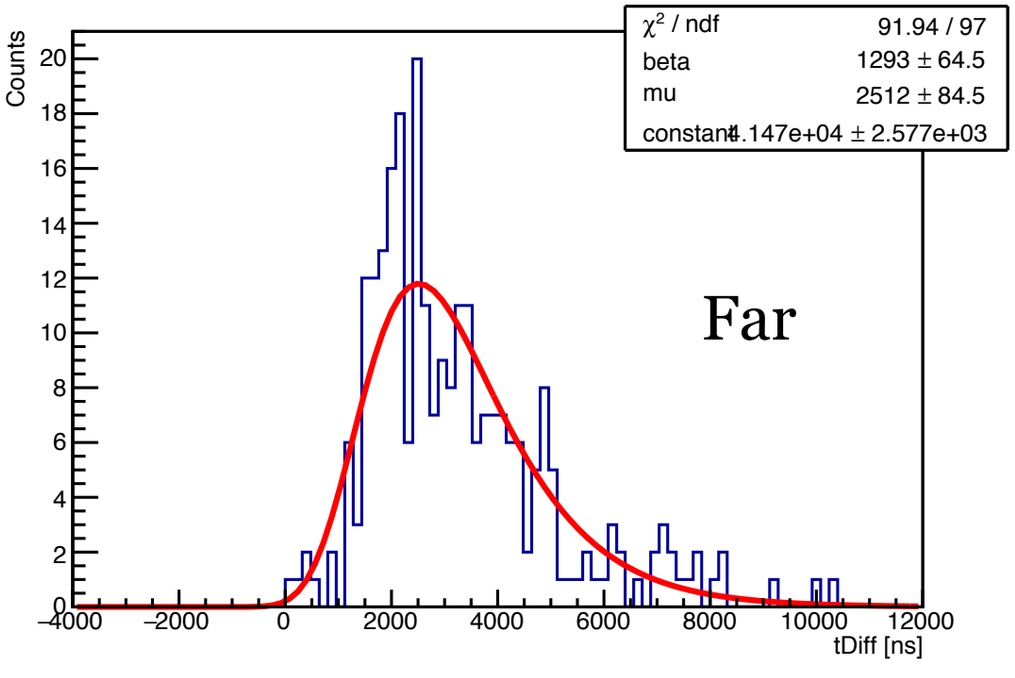

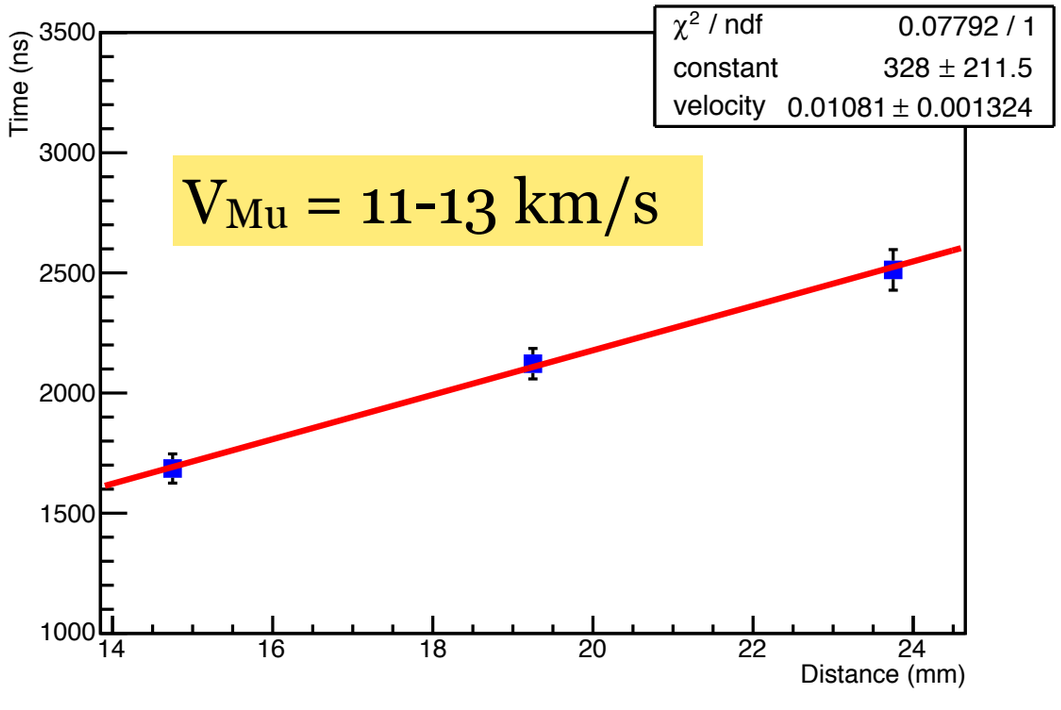

V_{Mu} = 11-13 km/s

2. Vacuum muonium from SFHe film coated nanostructure materials, and free-surface SFHe bath

② Vacuum muonium from SFHe film coated nanostructure materials, and free-surface SFHe

Aim

To observe emission of muonium atoms formed in SFHe into vacuum (expected temperature was 0.3 K)

Experimental Setup

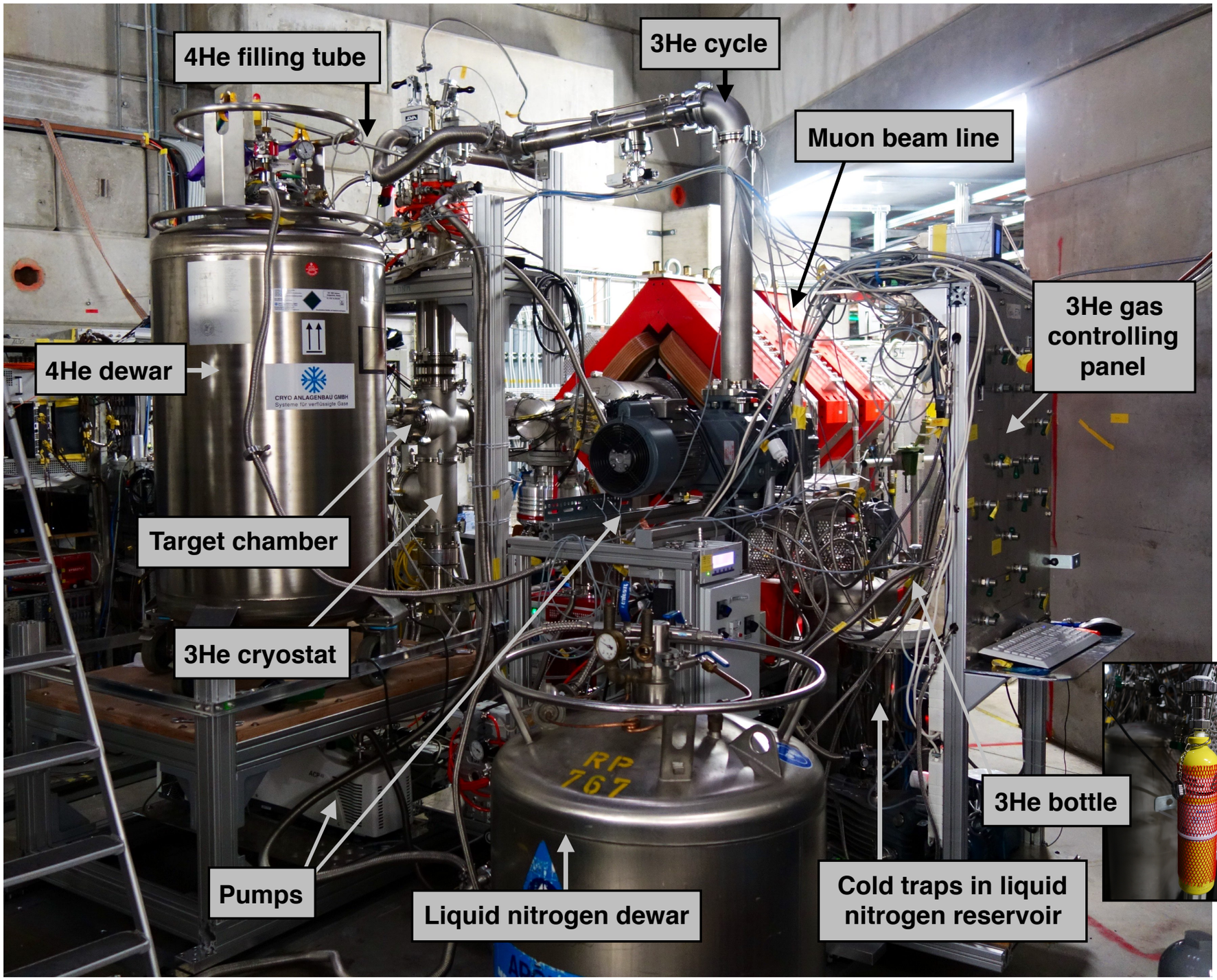

Experimental Setup

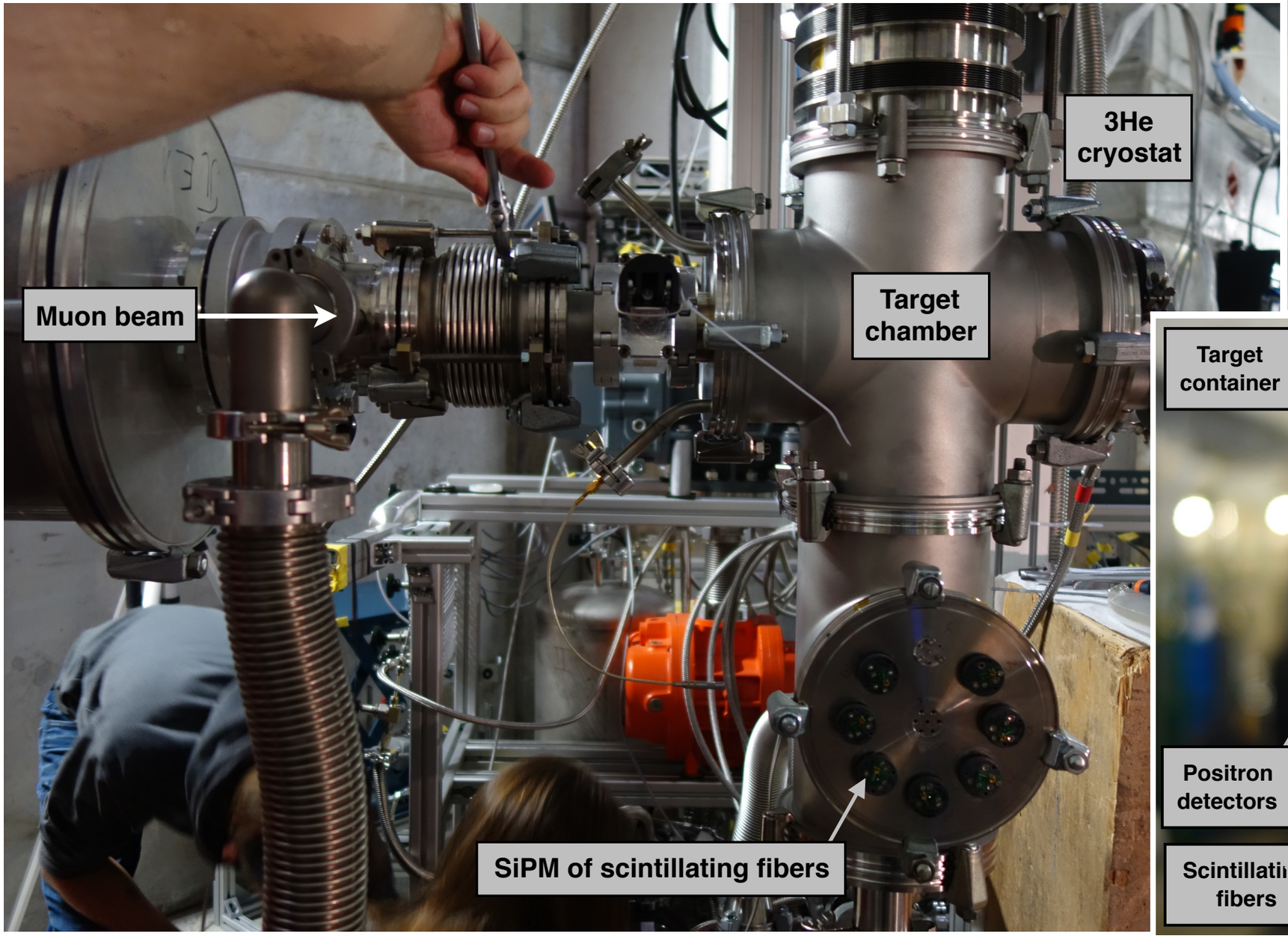

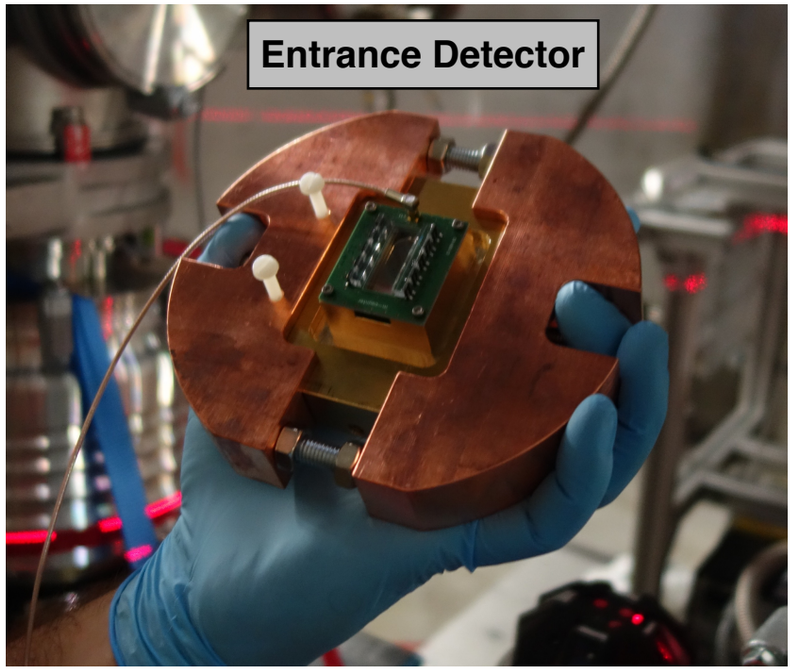

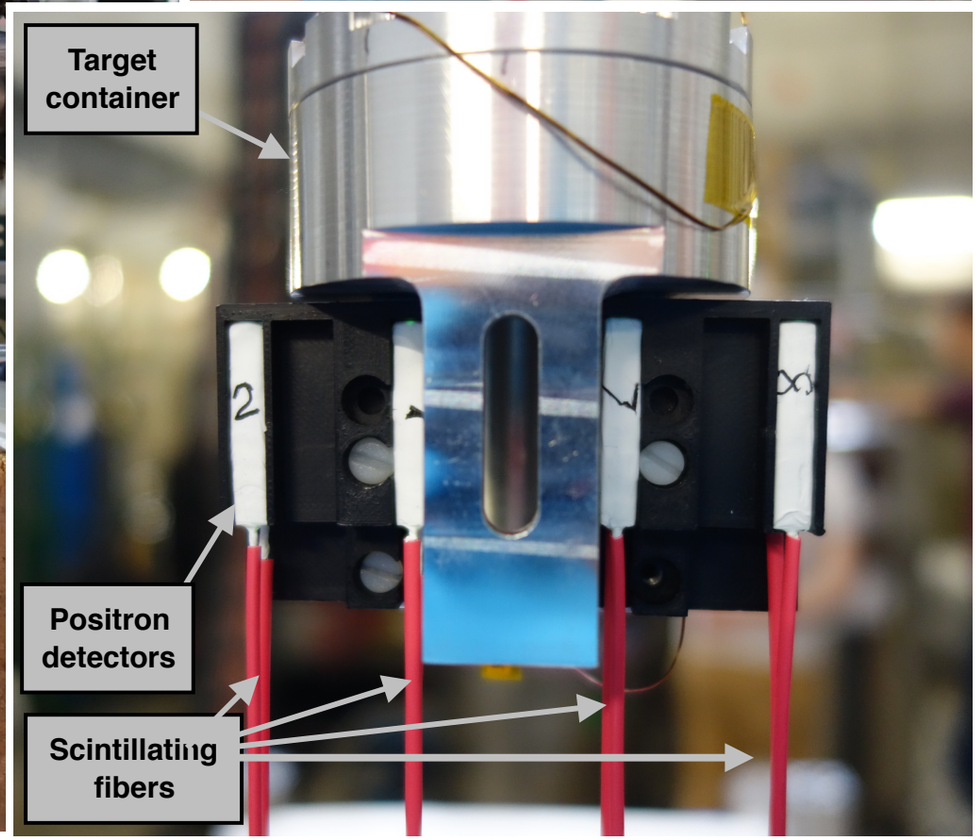

Experimental Setup

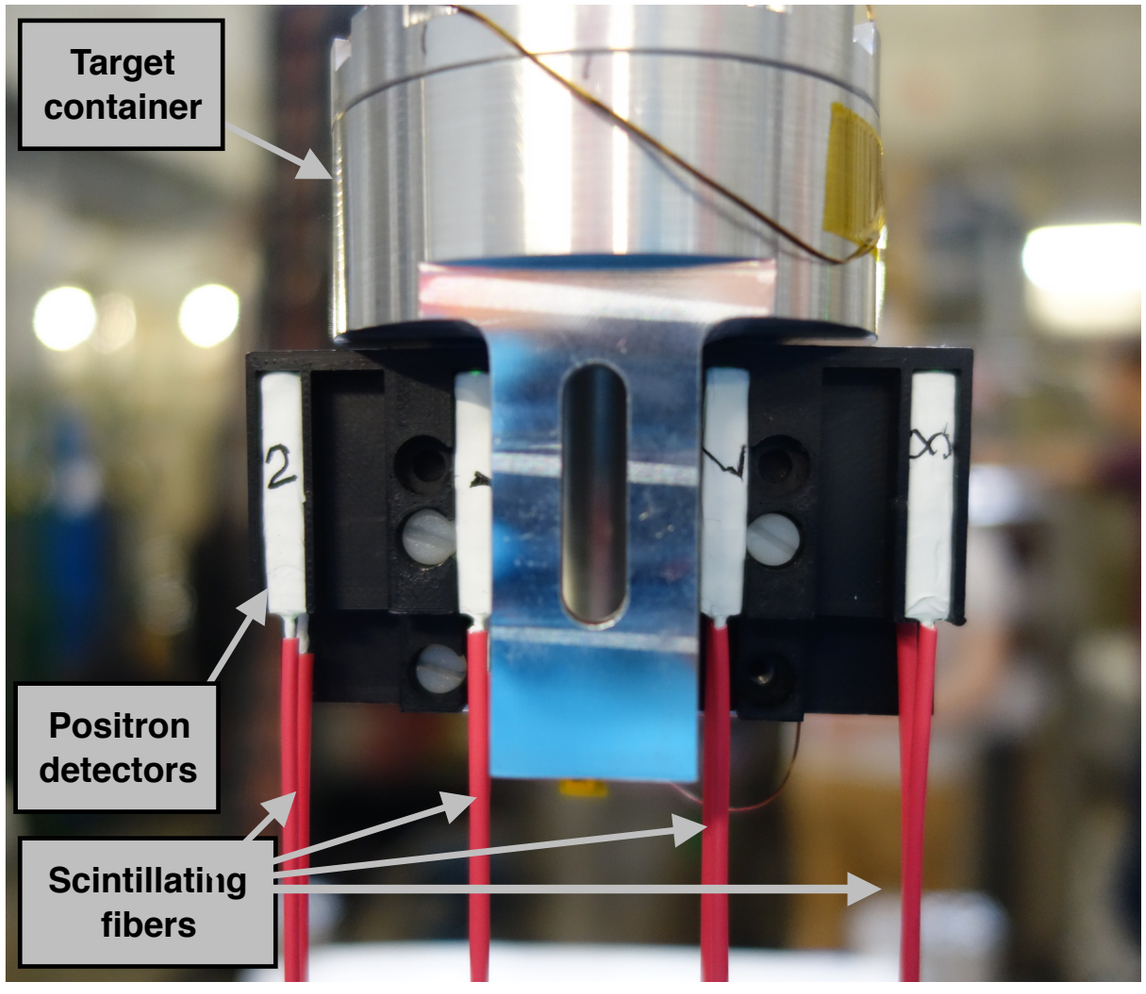

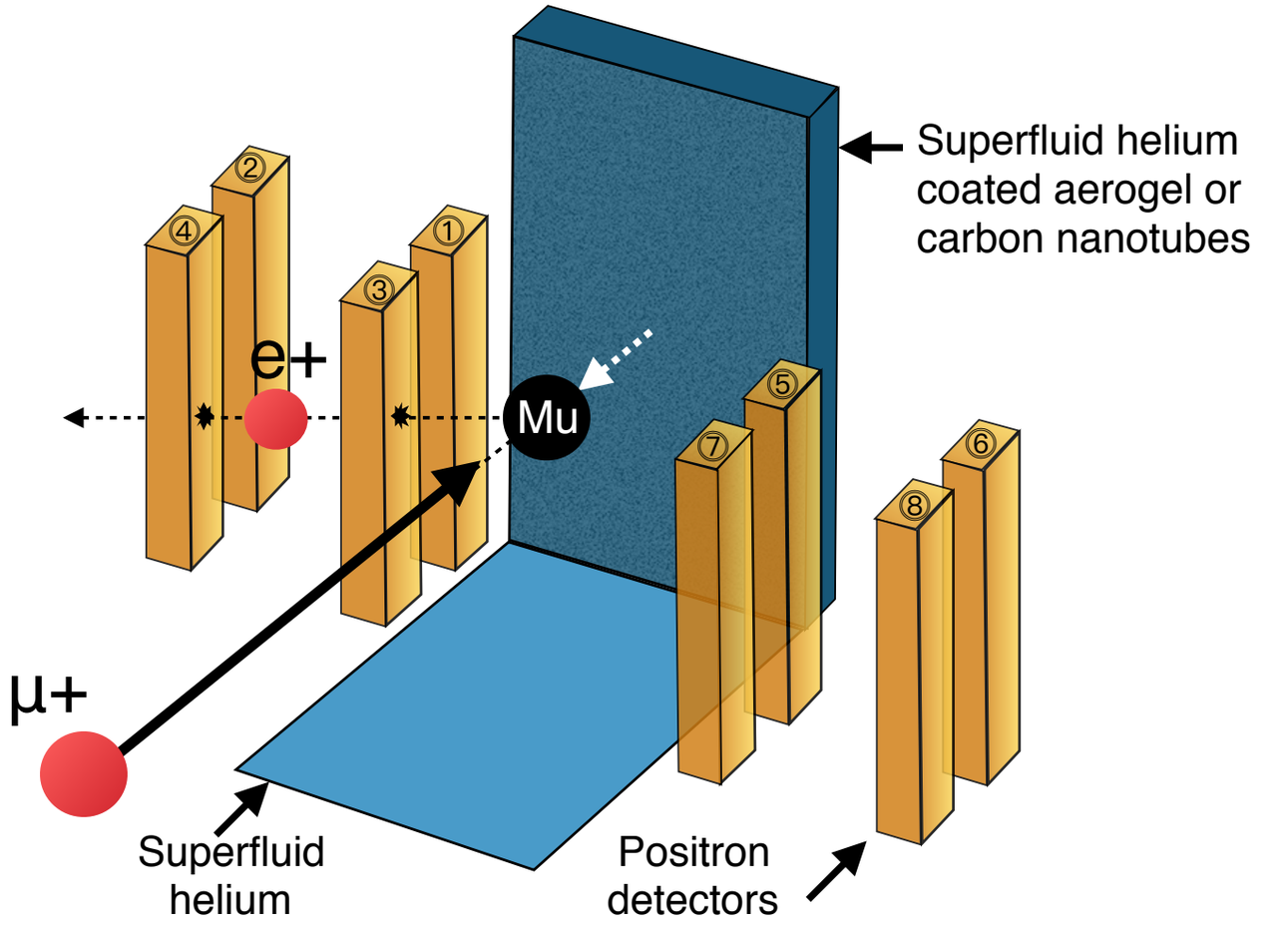

Results of vacuum muonium

⇒ No vacuum muonium atoms was observed from different wet targets and film of SFHe

⇒ Only background from muon decay, e.g.

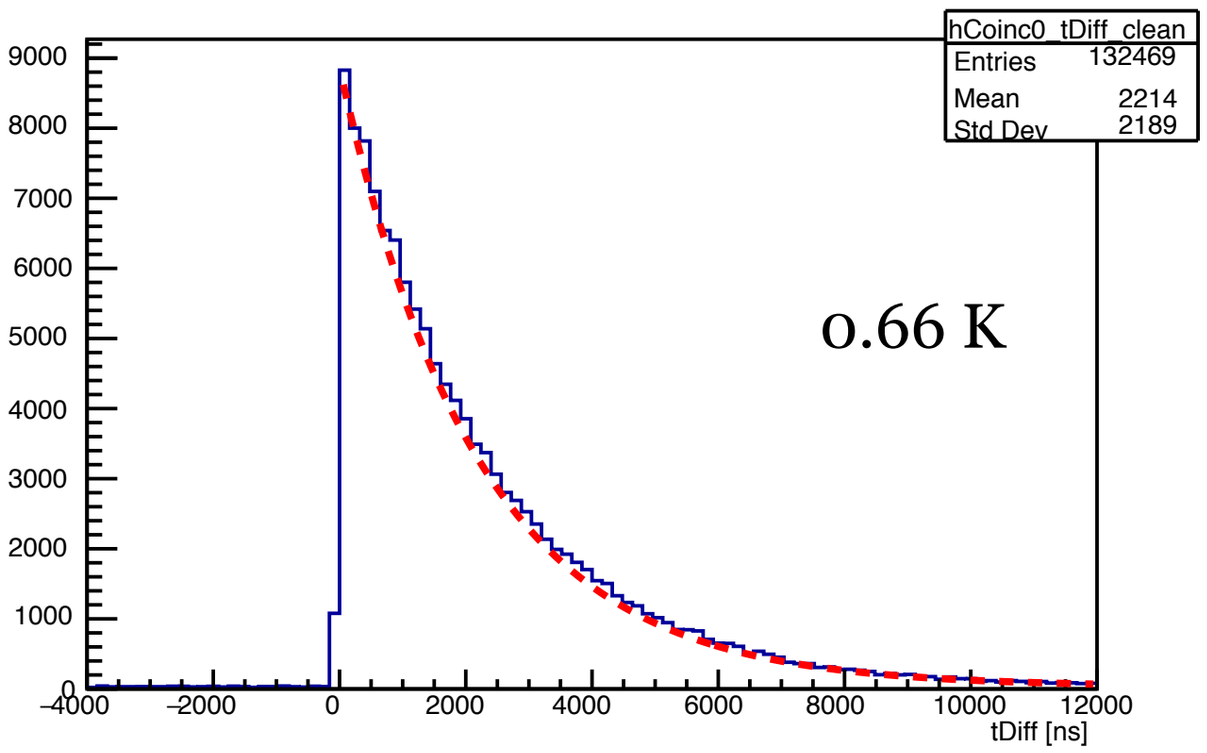

Wet aerogel

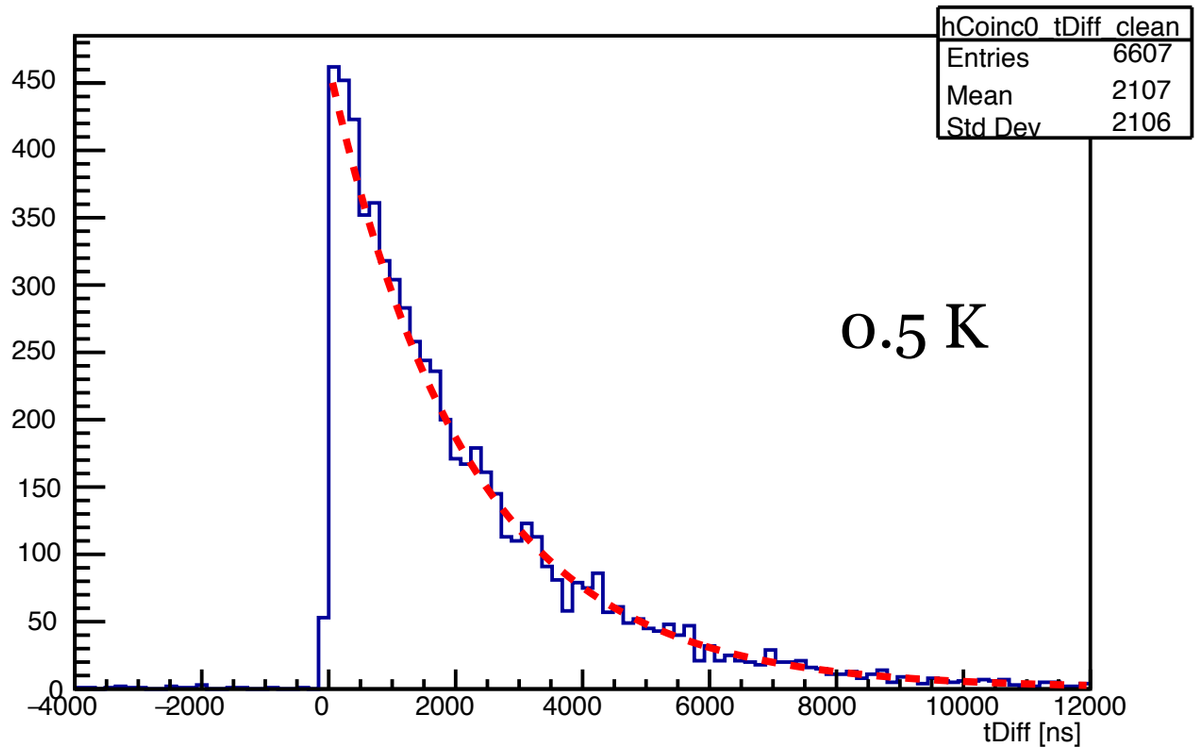

Wet CNT

⇒ Problem due to too high helium vapor pressure?

3. Muonium emission into helium gas

③ Muonium emission into helium gas

Aim

* To study the effect of helium gas on the propagation of emitted muonium atoms

Experimental Setup

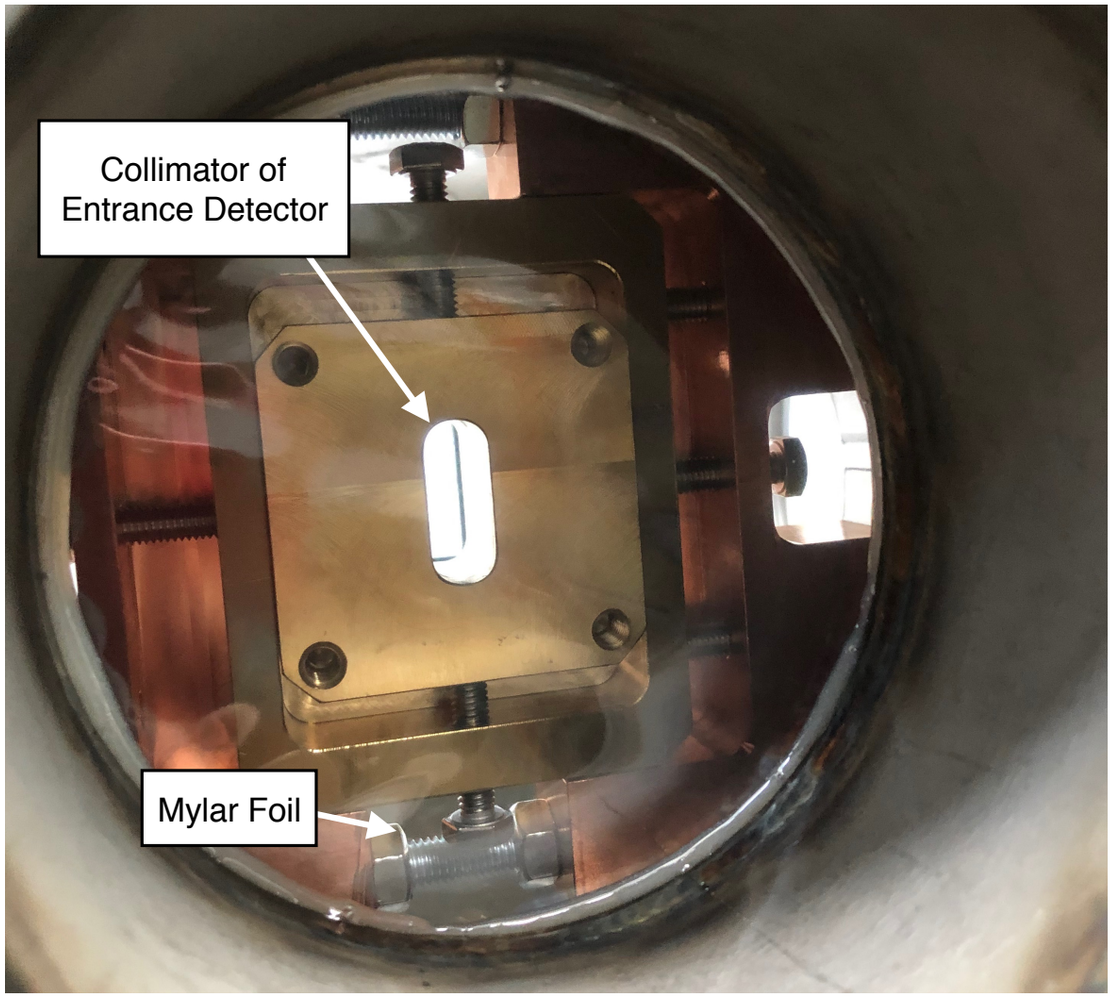

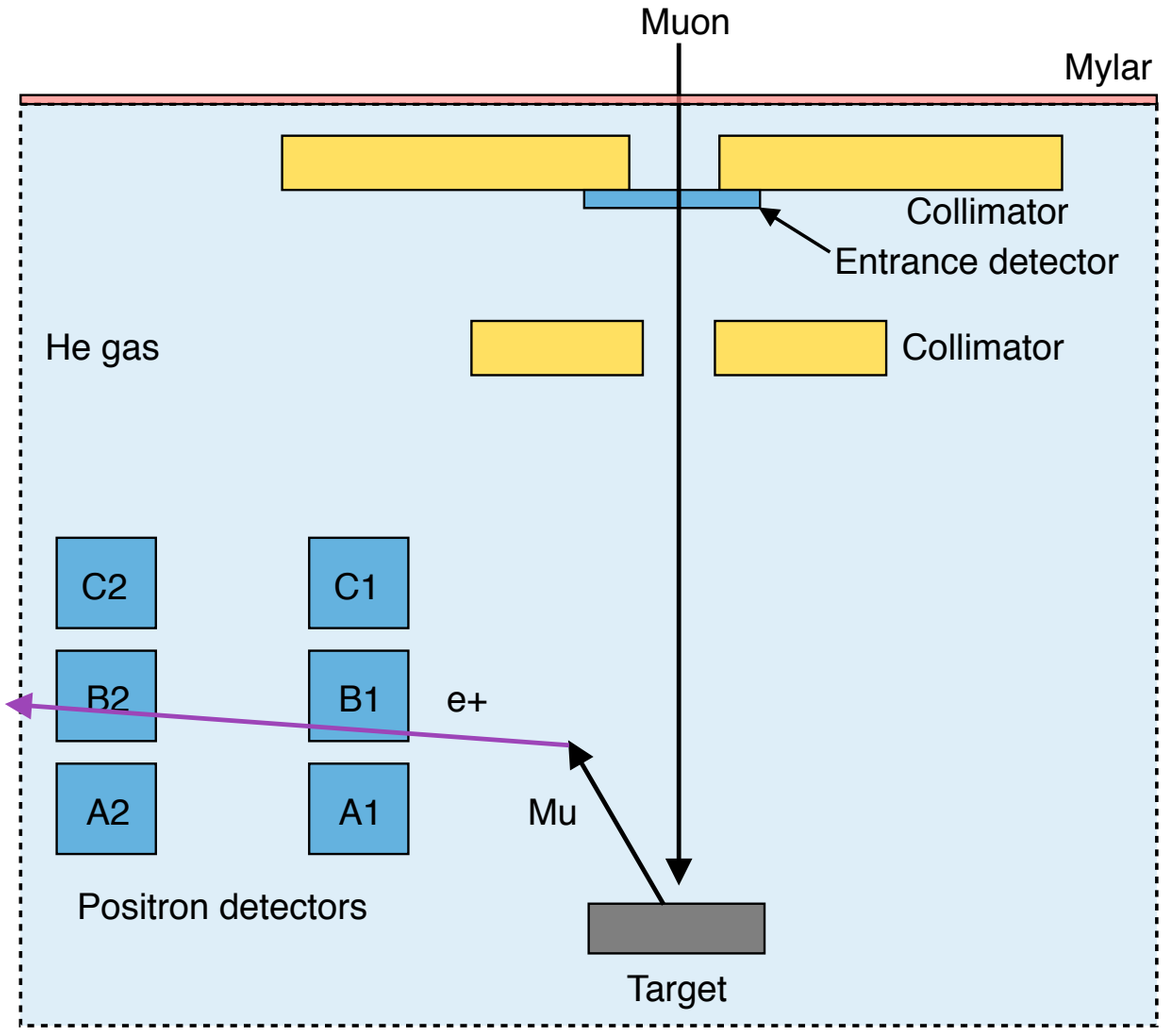

③ Muonium emission into helium gas

Results and discussions

Double coincidences of middle detector

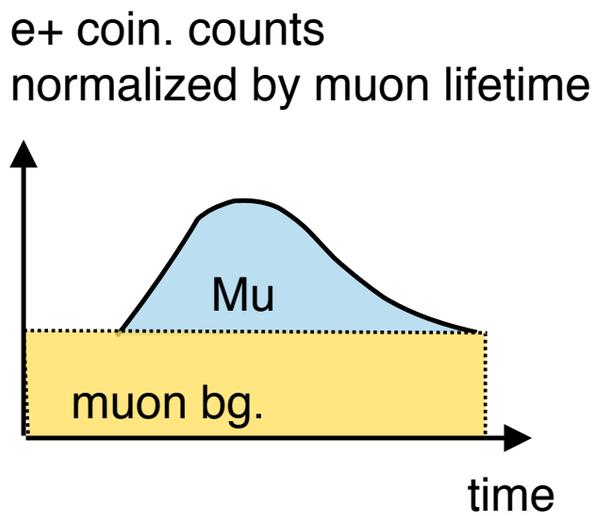

* P~10^{-6} mbar is consistent with T_{vap} = 0.3 K, P_{vap} = 5×10^{-10} mbar
* P~0.01 mbar is consistent with T_{vap} = 0.5 K, P_{vap} = 2×10^{-5} mbar
* P~0.1 mbar is consistent with T_{vap} = 0.6 K, P_{vap} = 2×10^{-3} mbar

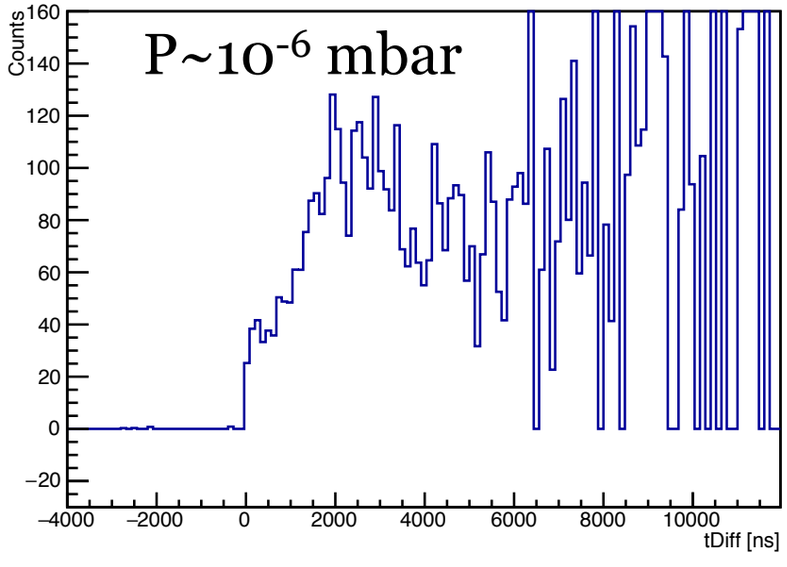

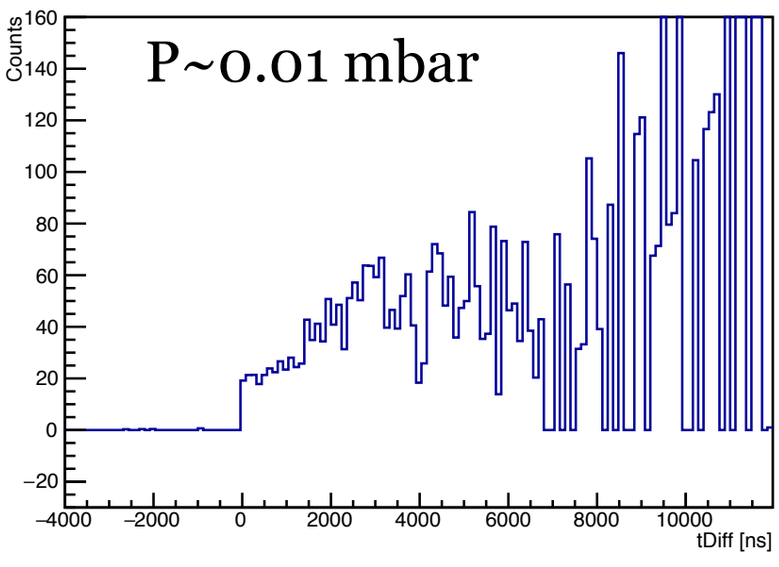

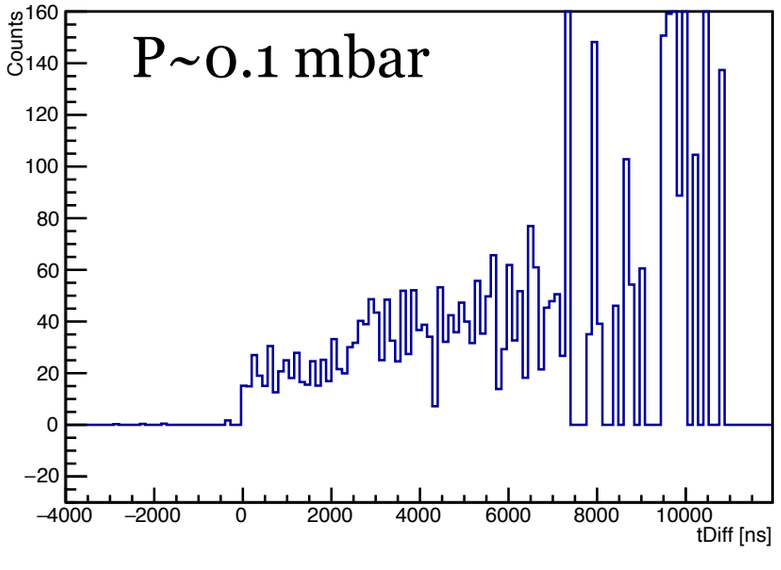

* The number of muonium signals detected by the middle detectors decreased when the pressure of helium increased
* These results are consistent with the calculation of muonium mean free path in helium gas

Conclusions

* Muonium atoms can be formed in an ablated aerogel, zeolite power, semiconductor carbon nanotubes
* High vacuum muonium yield observed in aerogel. Zeolite is also a promising conversion target
* No vacuum muonium atoms was observed from the SFHe thin film coated nanostructure materials or free-surface of SFHe bath due to too high helium vapor pressure
* Outlook : development of the cryostat with lower base temperature is necessary

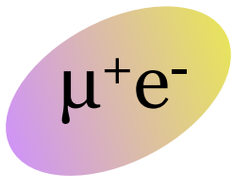

Thank you

ETH Zurich

A. Antognini, P. Crivelli, T. Hume, K. Kirch, J. Nuber, D. Taqqu

Paul Scherer Institut

M. Bartkowiak, A. Knecht, A. Papa, N. Ritjoho,
R. Scheuermann, A. Soter, B. van den Brandt, L. Ziegler

University of Cambridge

M. F. L. De Volder

Illinois Institute of Technology

D.M. Kaplan and T. J. Phillips

Backup

Velocity of vacuum muonium

* From aerogel : V_{Mu} = 11.3 ± 0.6 km/s
* From zeolite : V_{Mu} = 13.3 ± 2.5 km/s

Relative yield of vacuum muonium

* The vacuum muonium yield from aerogel was higher than the one from zeolite ~50%

Vacuum muonium from SFHe film coated nanostructure materials, and free-surface SFHe

Detection Regimes

1. Horizontal vacuum muonium

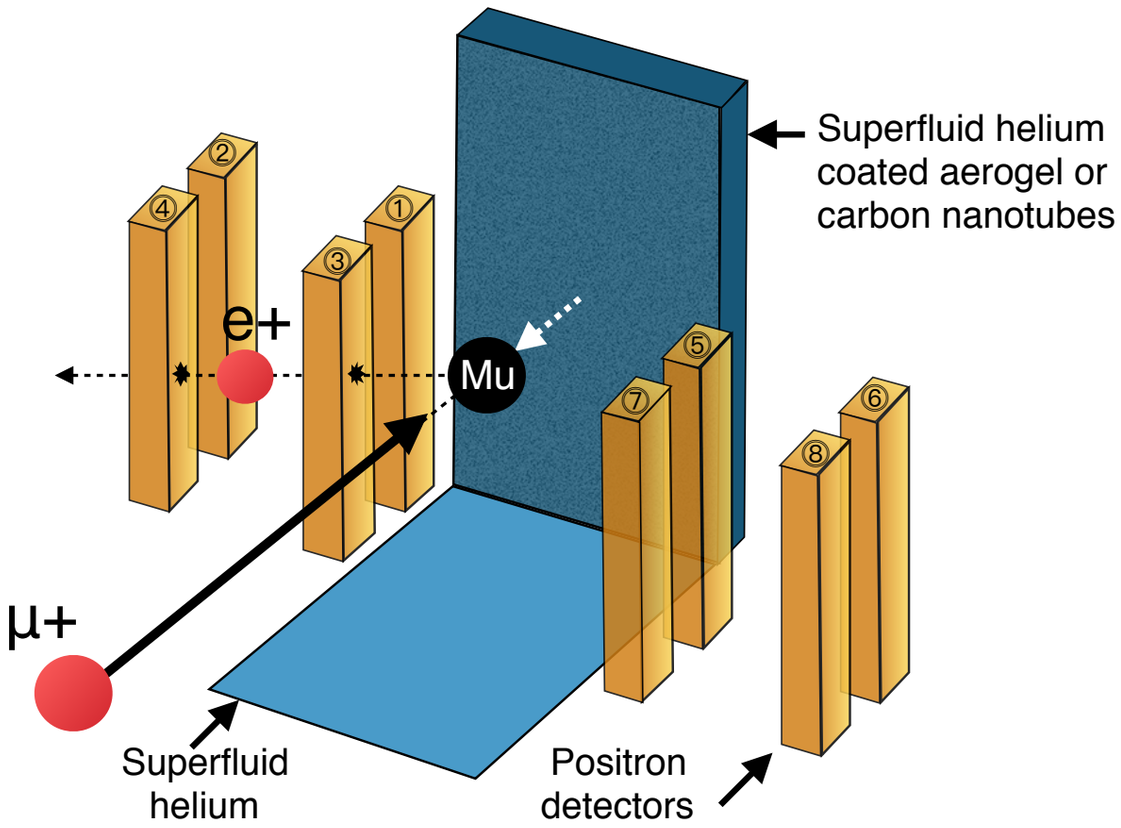

2. Vertical vacuum muonium

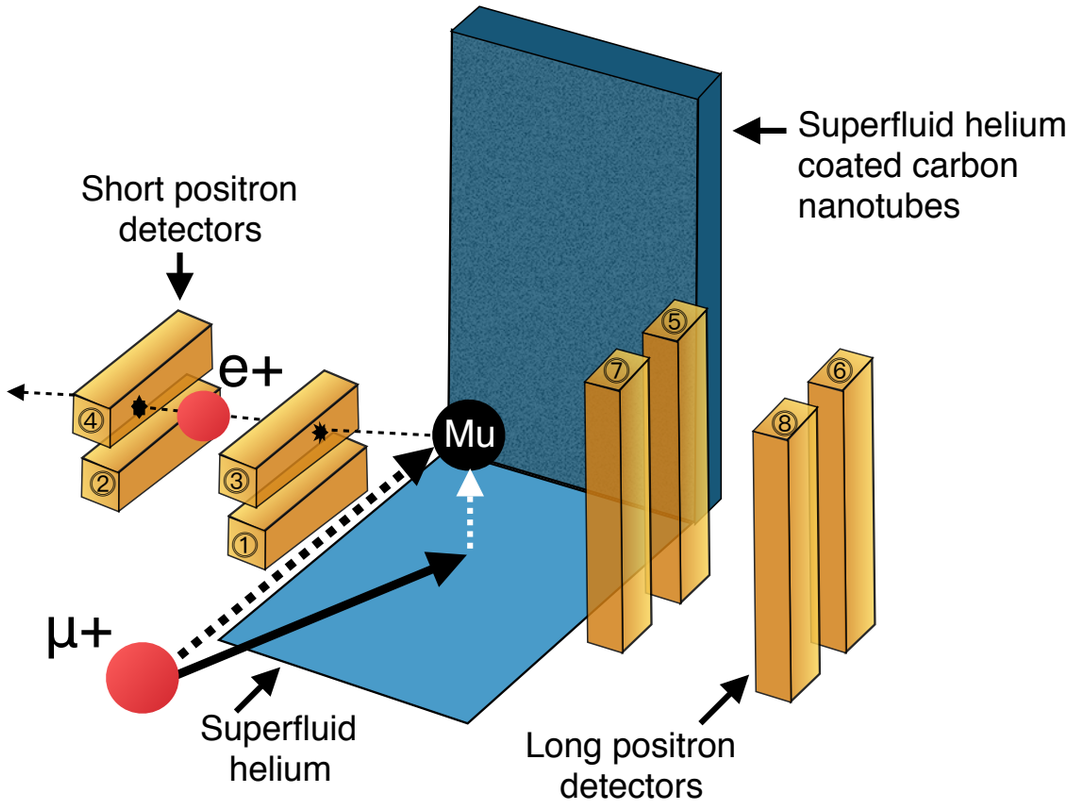

Vacuum muonium signal from double coincidence of e^+

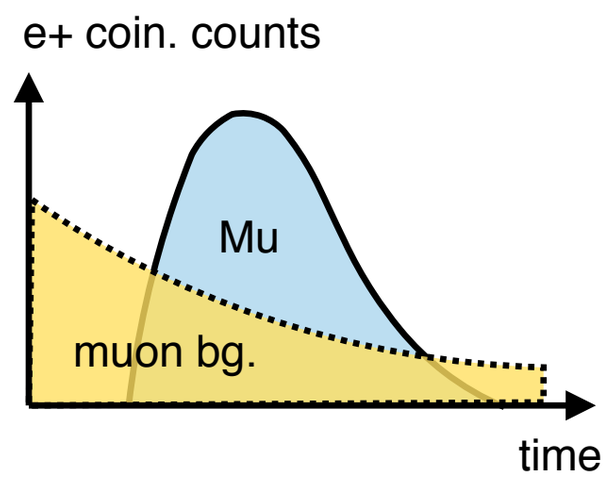

Vacuum muonium from SFHe film coated nanostructure materials, and free-surface SFHe

Targets

1. Warm aerogel : Ablated aerogel at room temperature
2. Dry aerogel : Ablated aerogel at 1 K
3. Wet aerogel : Ablated aerogel coated by SFHe film at 0.66 K
4. Wet CNT : Conductive carbon nanotubes coated by SFHe film at 0.5 K
5. Free surface SFHe : Muon beam was slated and impinged on free-surface of SFHe bath

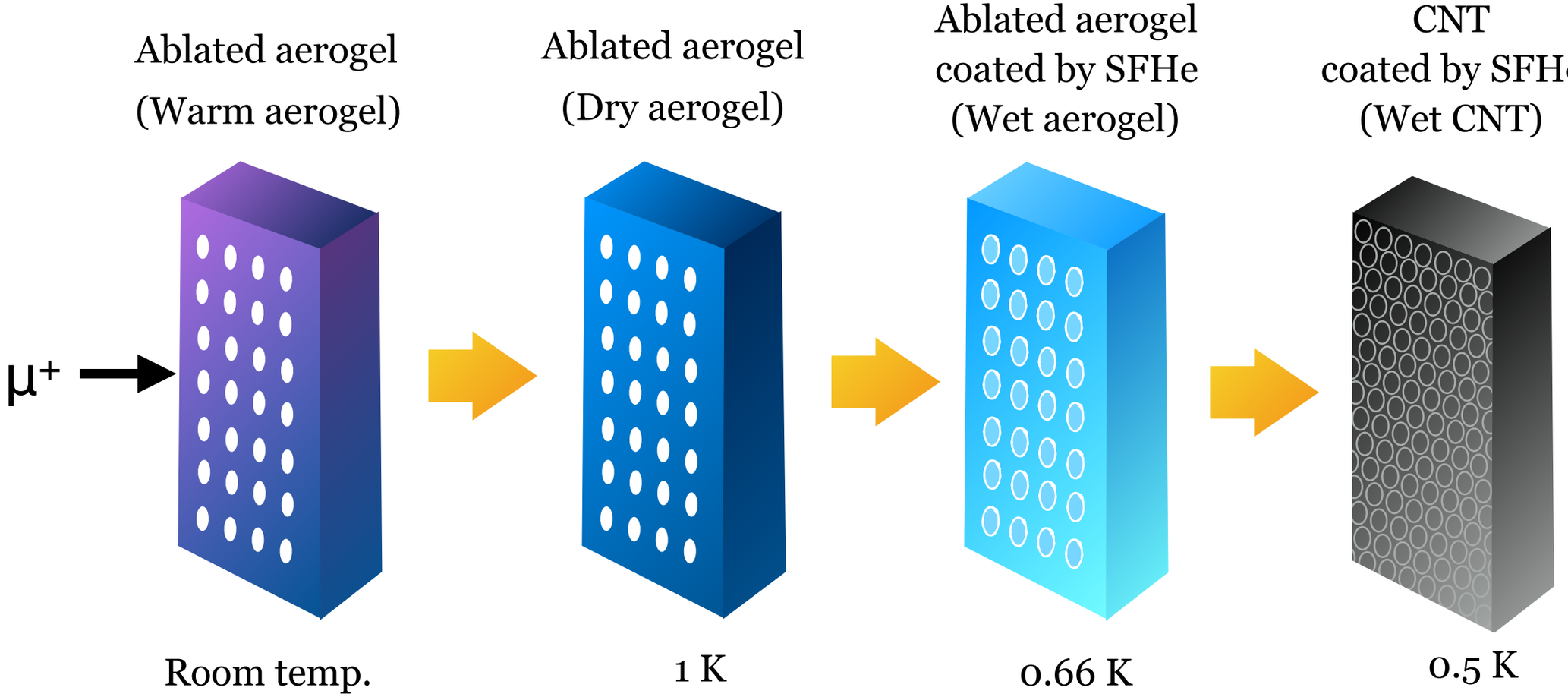

Results of muonium formation

⇒ We observed the muonium spin rotation signals (Mu-SR)

⇒ Took an advantage of stray magnetic field

⇒ Detected by individual positron detector

⇒ An evidence of muonium formation in the targets but do not emit into vacuum

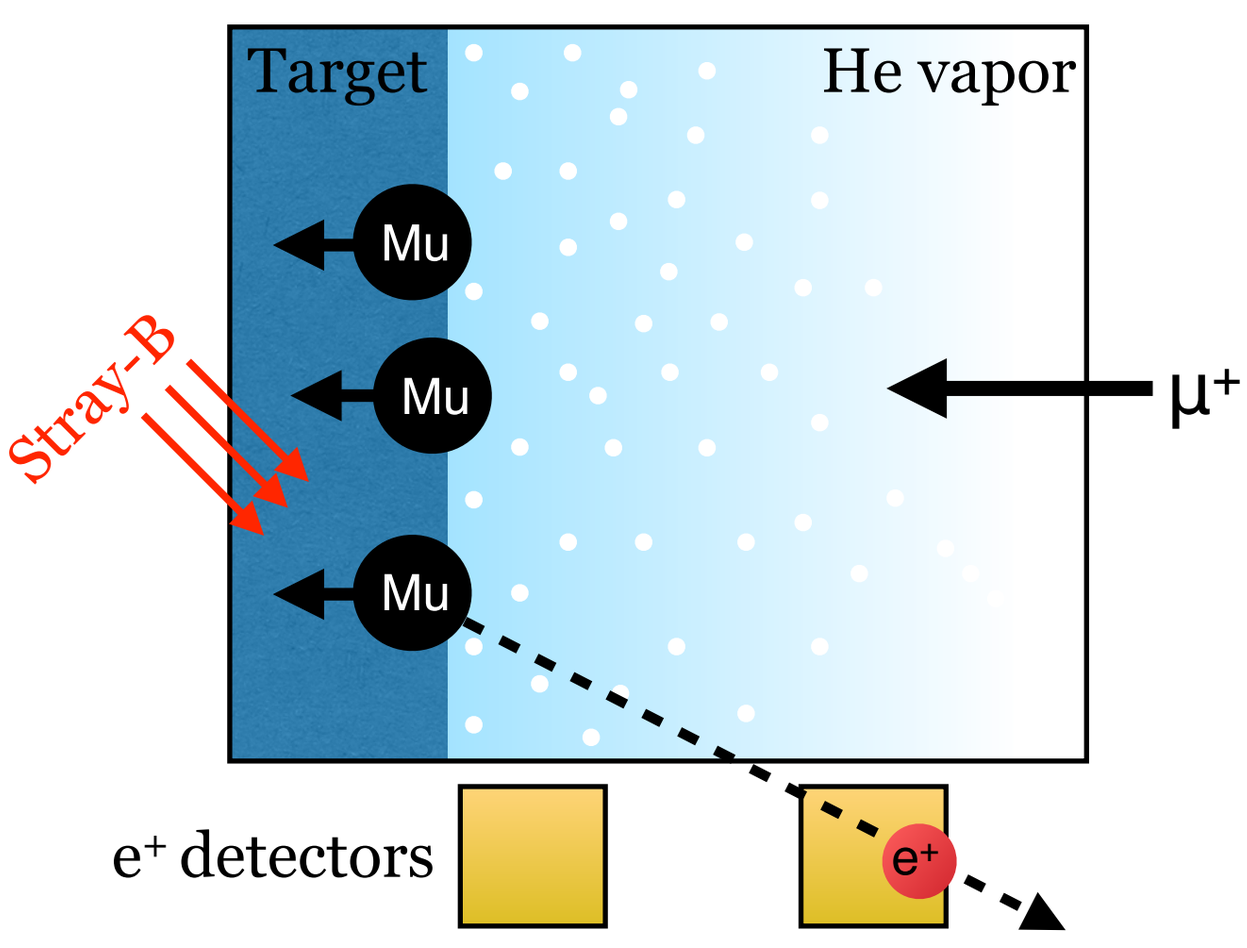

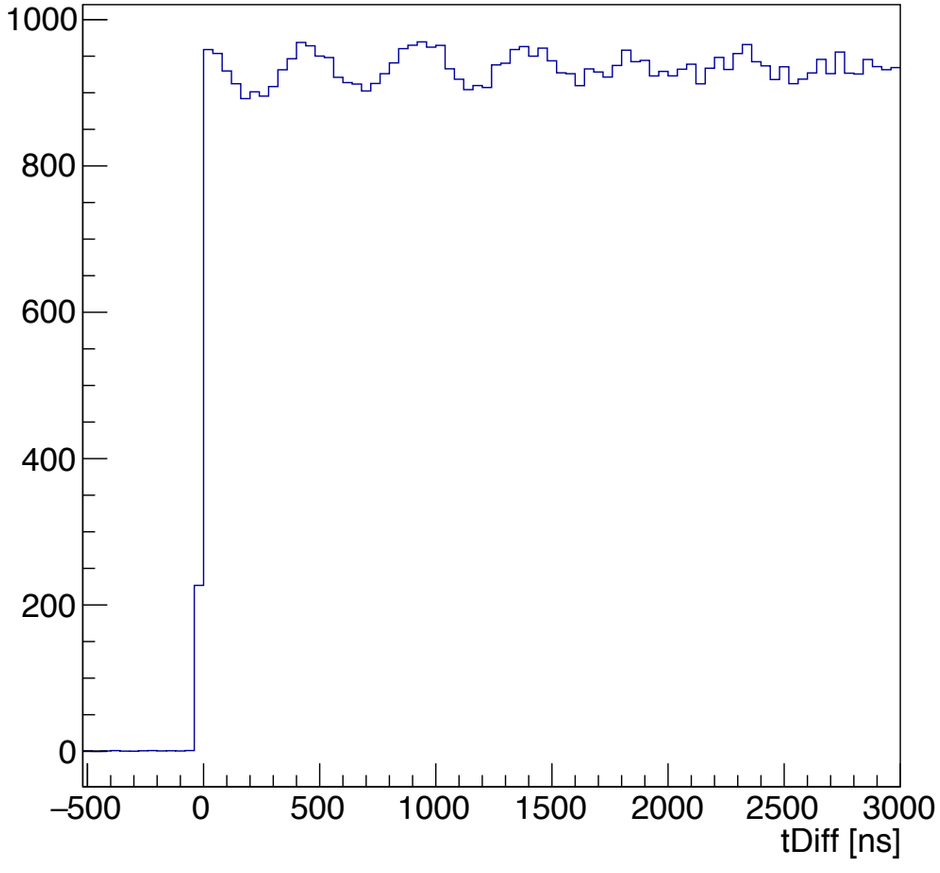

Vacuum muonium from SFHe film coated nanostructure materials, and free-surface SFHe

Results of muonium formation

Warm aerogel (Room temp.)

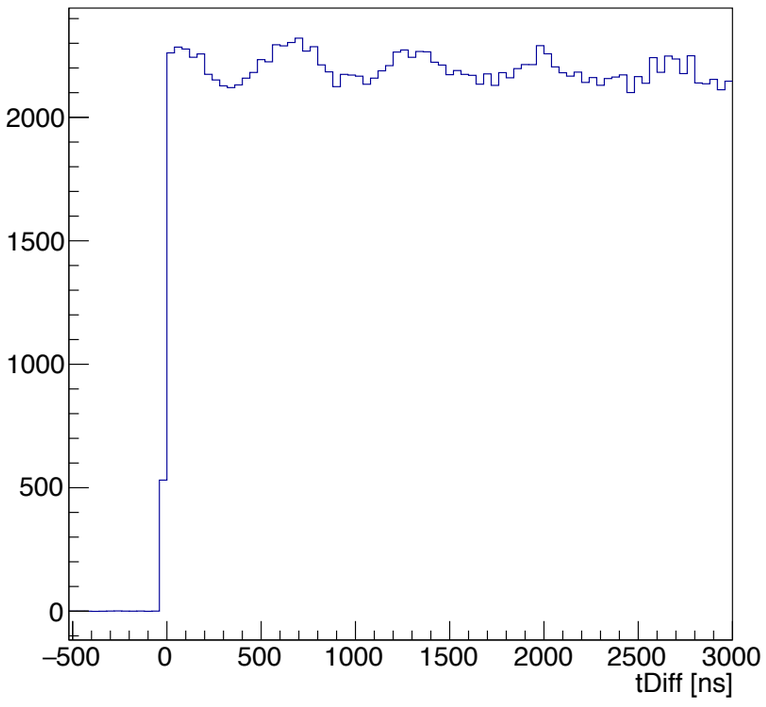

Dry aerogel (1 K)

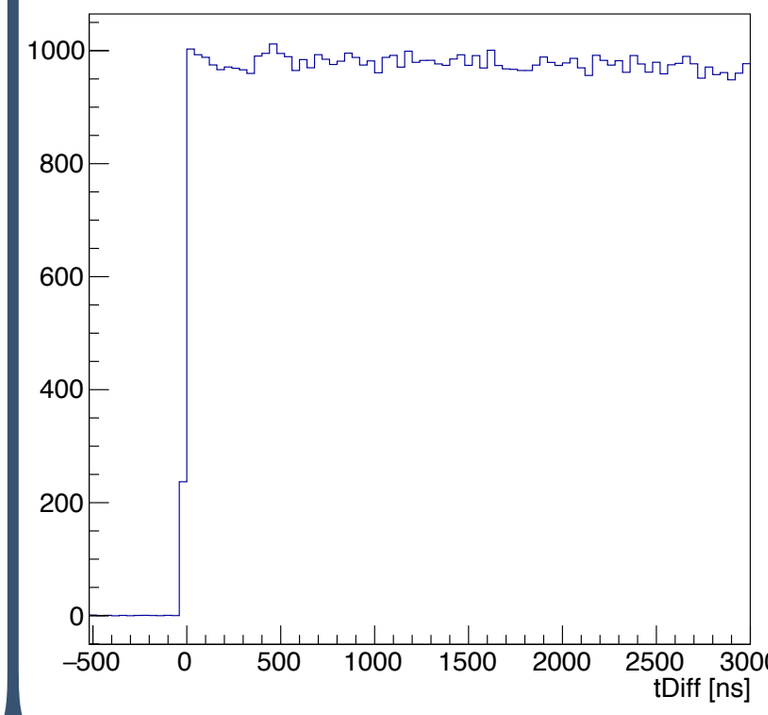

Wet aerogel (0.66 K)

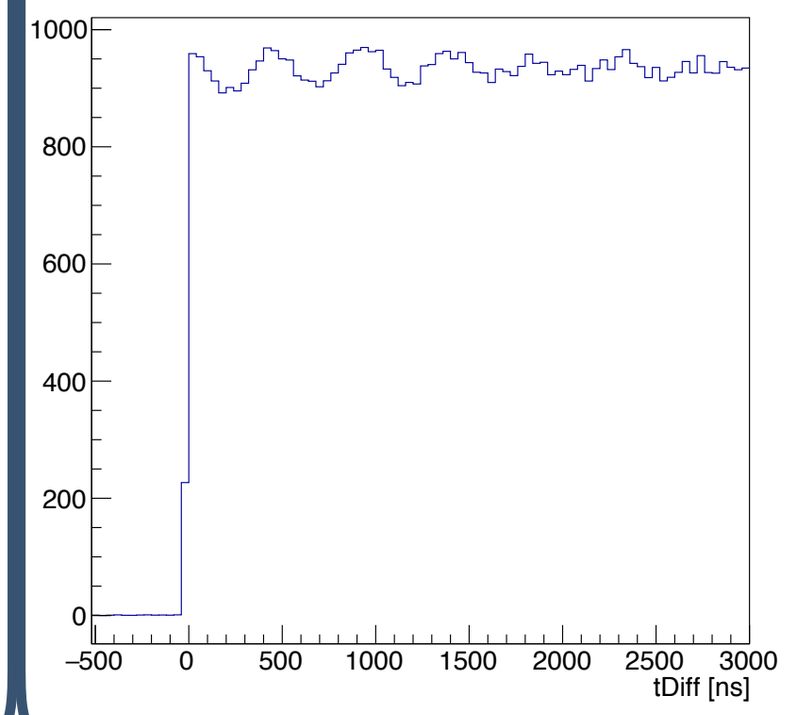

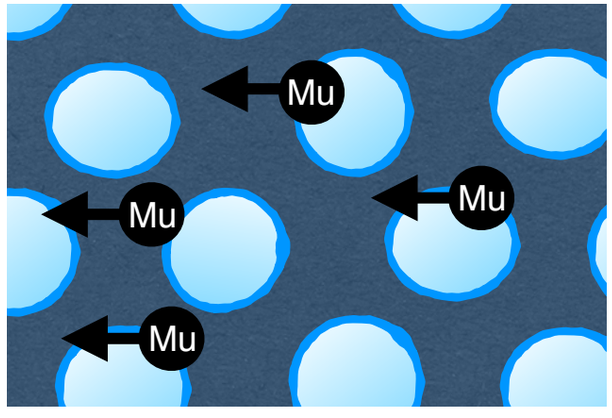

Results and discussions

1. Warm aerogel : No vacuum muonium was observed but Mu-SR existed. The target was not in vacuum due to the pumping difficulty.

2. Dry aerogel (1 K) : No vacuum muonium and no Mu-SR were observed. The helium vapor pressure was too high at 1 K and the formed muonium atoms probably were frozen at the surface of the aerogel.

3. Wet aerogel (0.66 K) : No vacuum muonium was observed due to the high helium pavor pressure. The introduced SFHe film coated the dry aerogel presumably lubricated the frozen muonium atoms to be precessing again

4. Wet CNT (0.5 K) : No vacuum muonium and no Mu-SR were observed. Muonium atoms cannot be formed inside the conductive-CNT and the SFHe film was too thin to stop and form muonium atoms

5. Free surface SFHe (0.5 K) : No vacuum muonium and no Mu-SR were observed. Too high background was measured because of a possibility that muon did not stop inside the SFHe bath only but also on backside target and the target container was too small.

Results and discussions

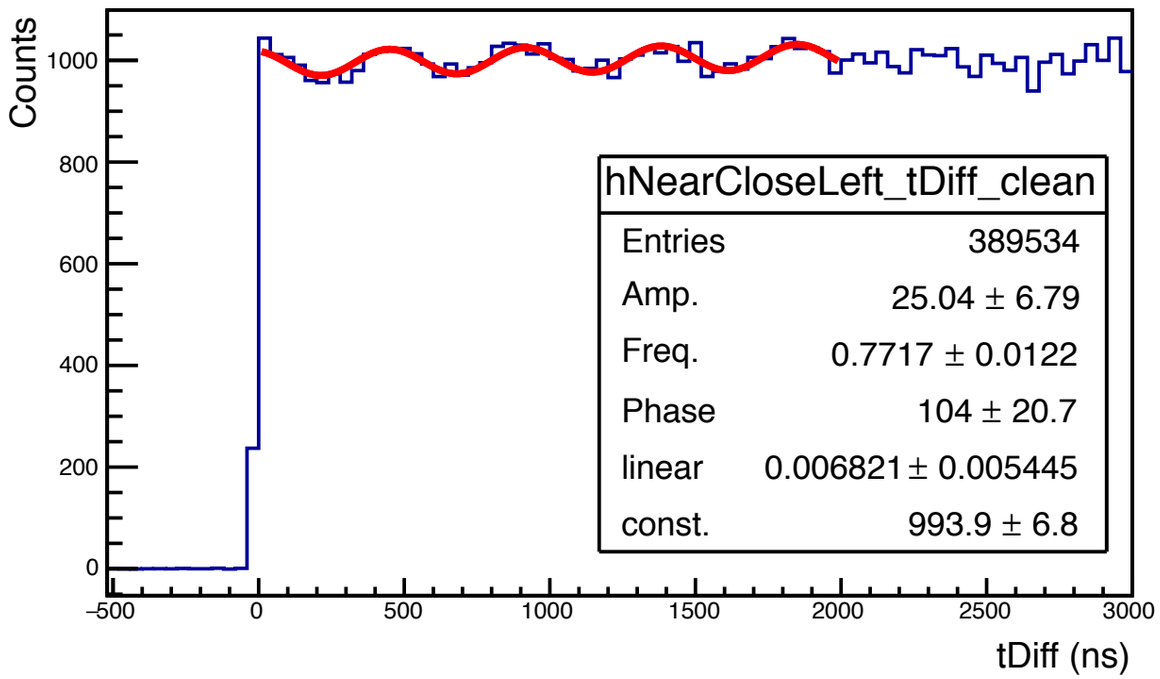

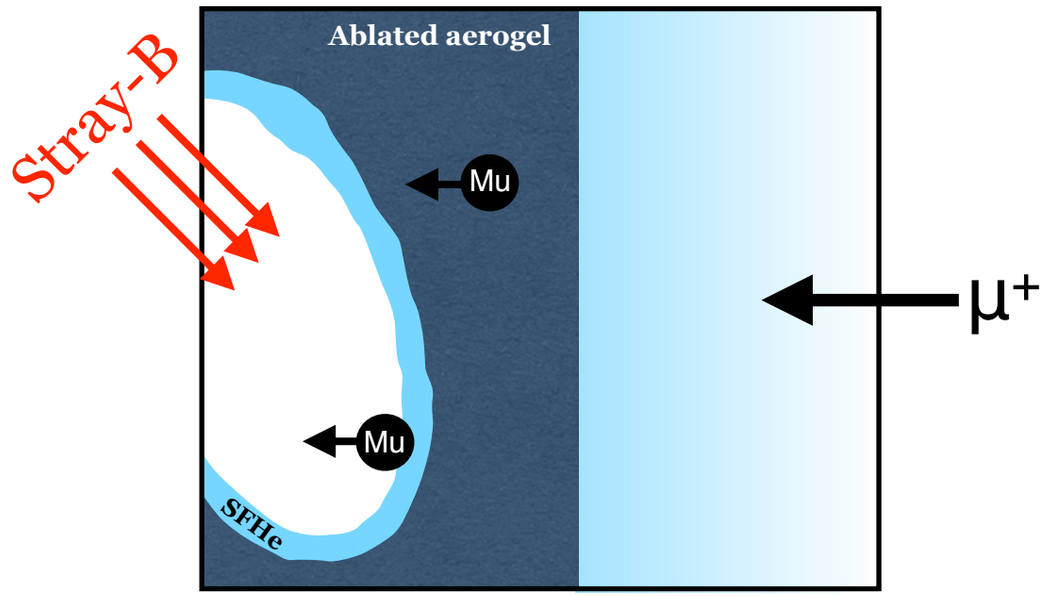

* The Mu-SR results were fitted with $N = N_0 \sin(\omega_{Mu}t+\phi_{Mu}) + N_{BG}$
* The muonium phase (ϕ_{Mu}) can tell whether muonium atoms were formed inside the ablated aerogel or SFHe film coating.
* Assuming that muonium atoms formed in the aerogel follow the direct capture processes, while muonium atoms formed in the SFHe time-dependently, the ϕ_{Mu} of the *warm aerogel* should differ from the one of the *wet aerogel* ($\Delta\phi_{Mu} = |\phi_{Mu,Warm} - \phi_{Mu,Wet}| \neq 0$).
* At temperature = 0.5 K, magnetic field = 1.55 G, mean formation time (τ) ≈ 47 ns, the expected $\Delta\phi_{Mu} \approx 30$ degree.
* However, from the analyzed data we found that $\Delta\phi_{Mu} \approx 0$. This gave a hint that the muonium atoms were probably formed in the aerogel (not SFHe film).

Mu in bulk SFHe

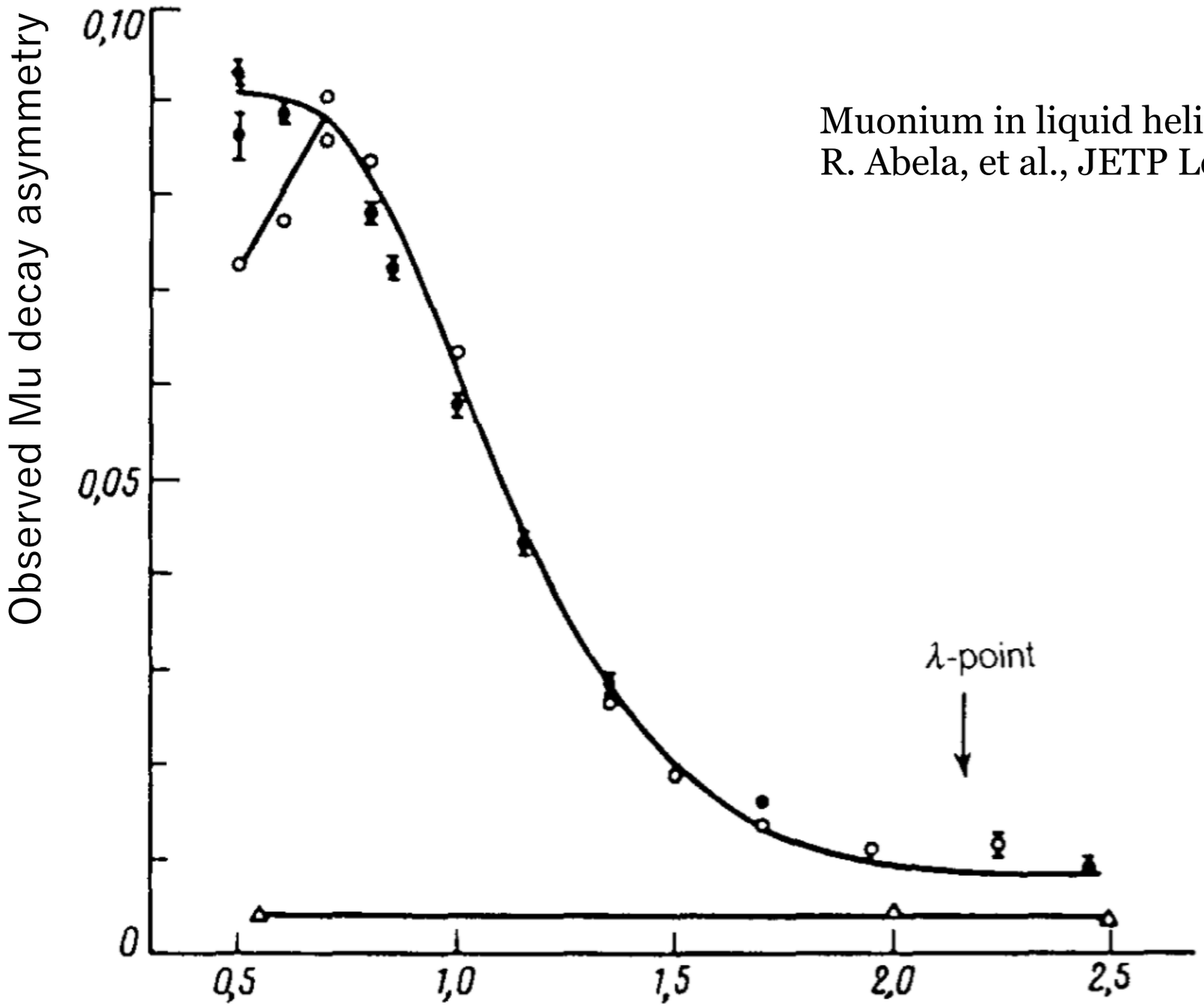

Muonium in liquid helium isotopes
R. Abela, et al., JETP Letter, Vol. 57, No. 3, 10 Feb 1993

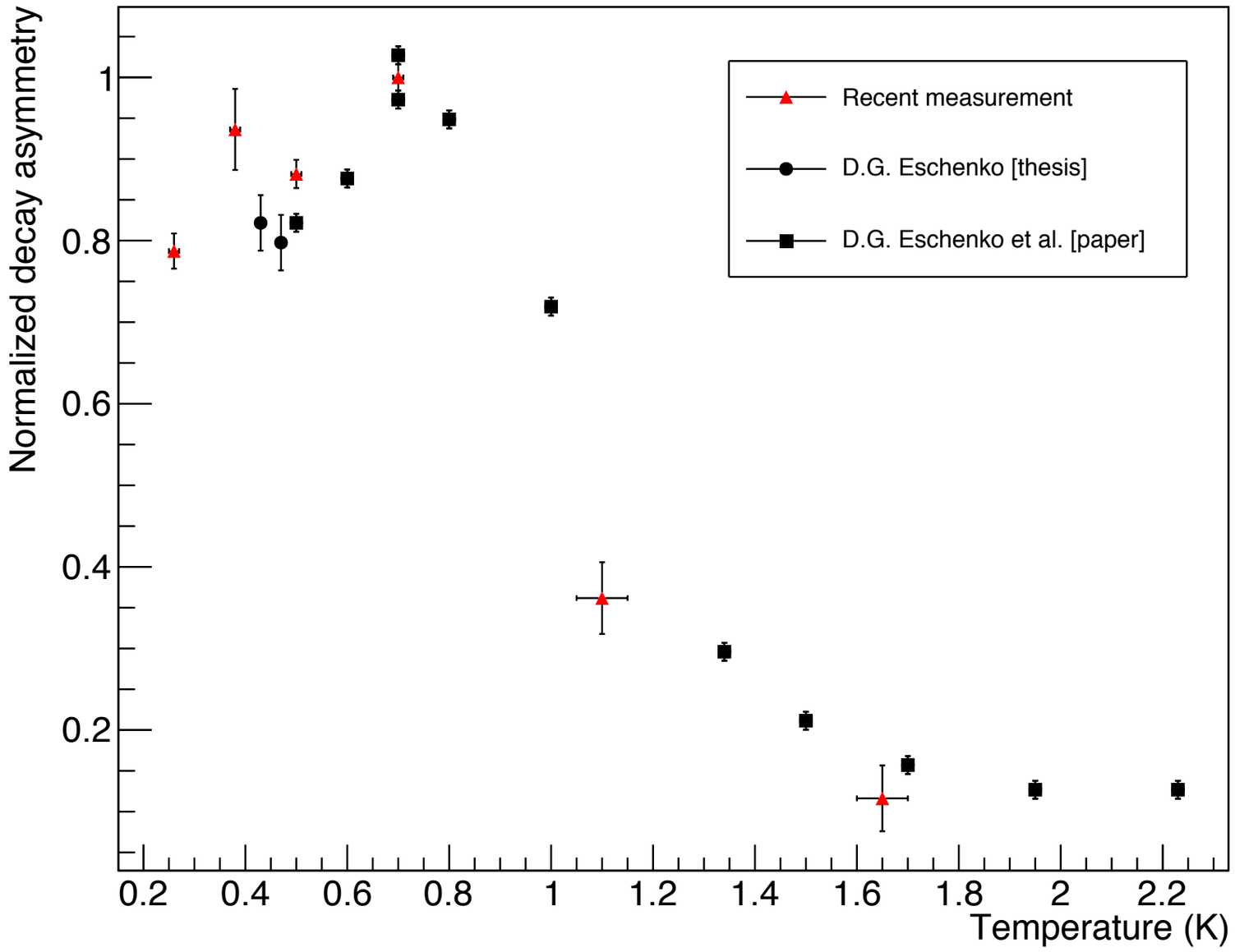
Normalized decay asymmetry
1
0.8
0.6
0.4
0.2
0.2
0.4
0.6
0.8
1
1.2
1.4
1.6
1.8
2
2.2
Temperature (K)
Recent measurement
D.G. Eschenko [thesis]
D.G. Eschenko et al. [paper]

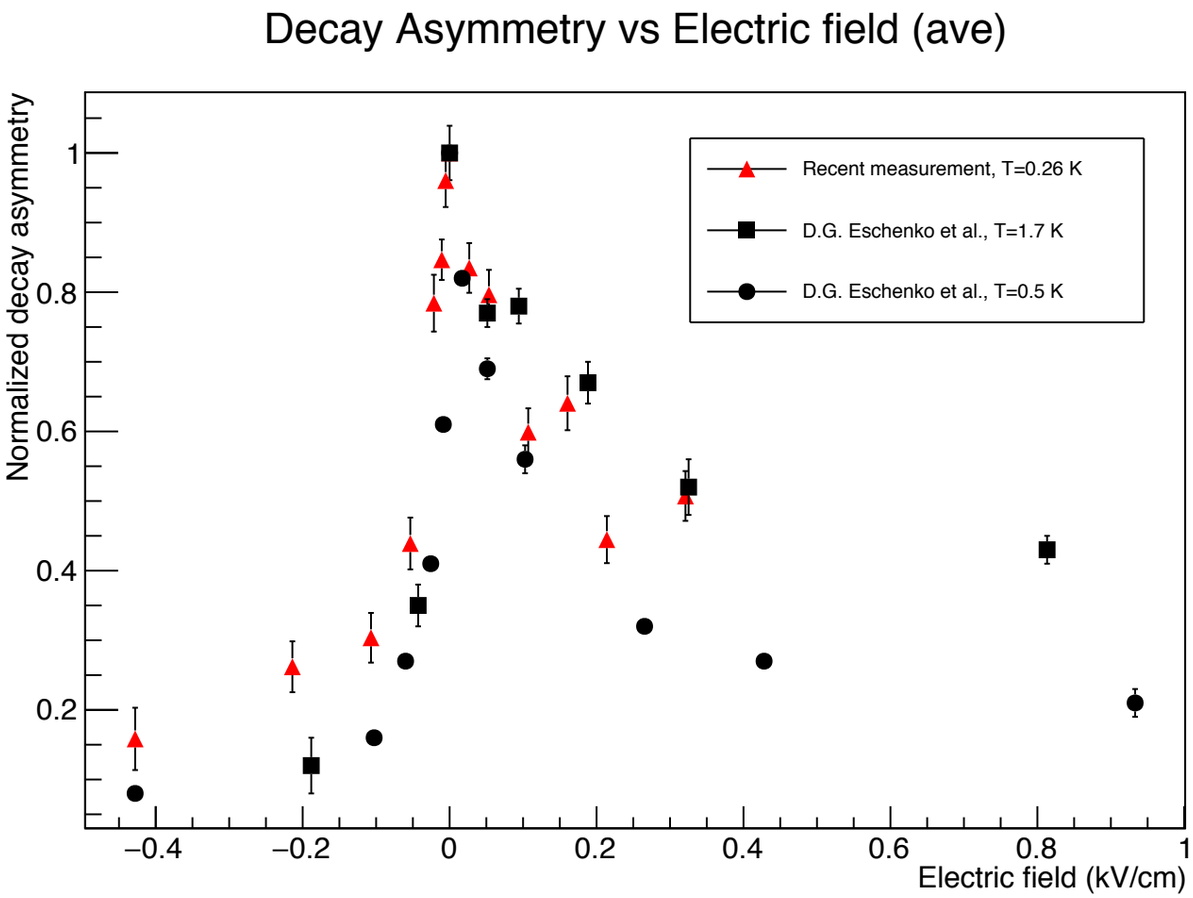
Decay Asymmetry vs Electric field (ave)
Normalized decay asymmetry
1
0.8
0.6
0.4
0.2
−0.4
−0.2
0
0.2
0.4
0.6
0.8
1
Electric field (kV/cm)
Recent measurement, T=0.26 K
D.G. Eschenko et al., T=1.7 K
D.G. Eschenko et al., T=0.5 K

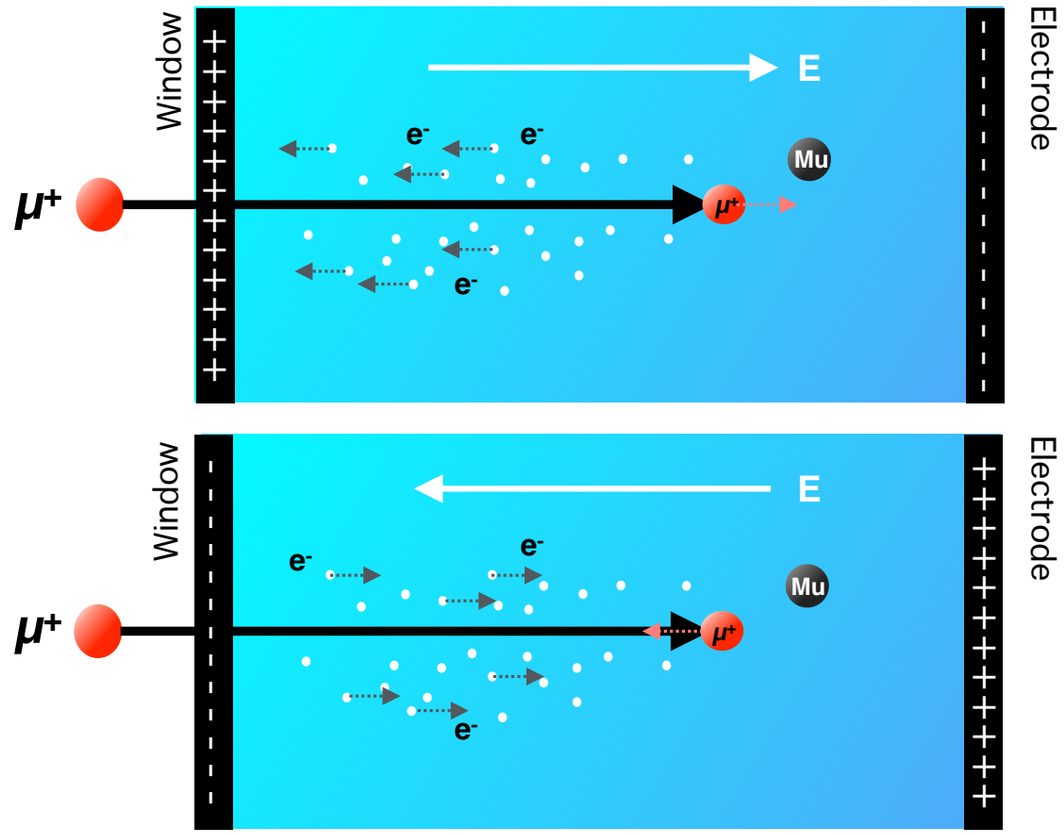
Window
Electrode
E
e-
e-
e-
Mu
μ+
μ+
Window
Electrode
E
e-
e-
e-
Mu
μ+
μ+

Positive Chemical Potential

Hydrogen Isotope and ^{3}He Impurities in Liquid ^{4}He

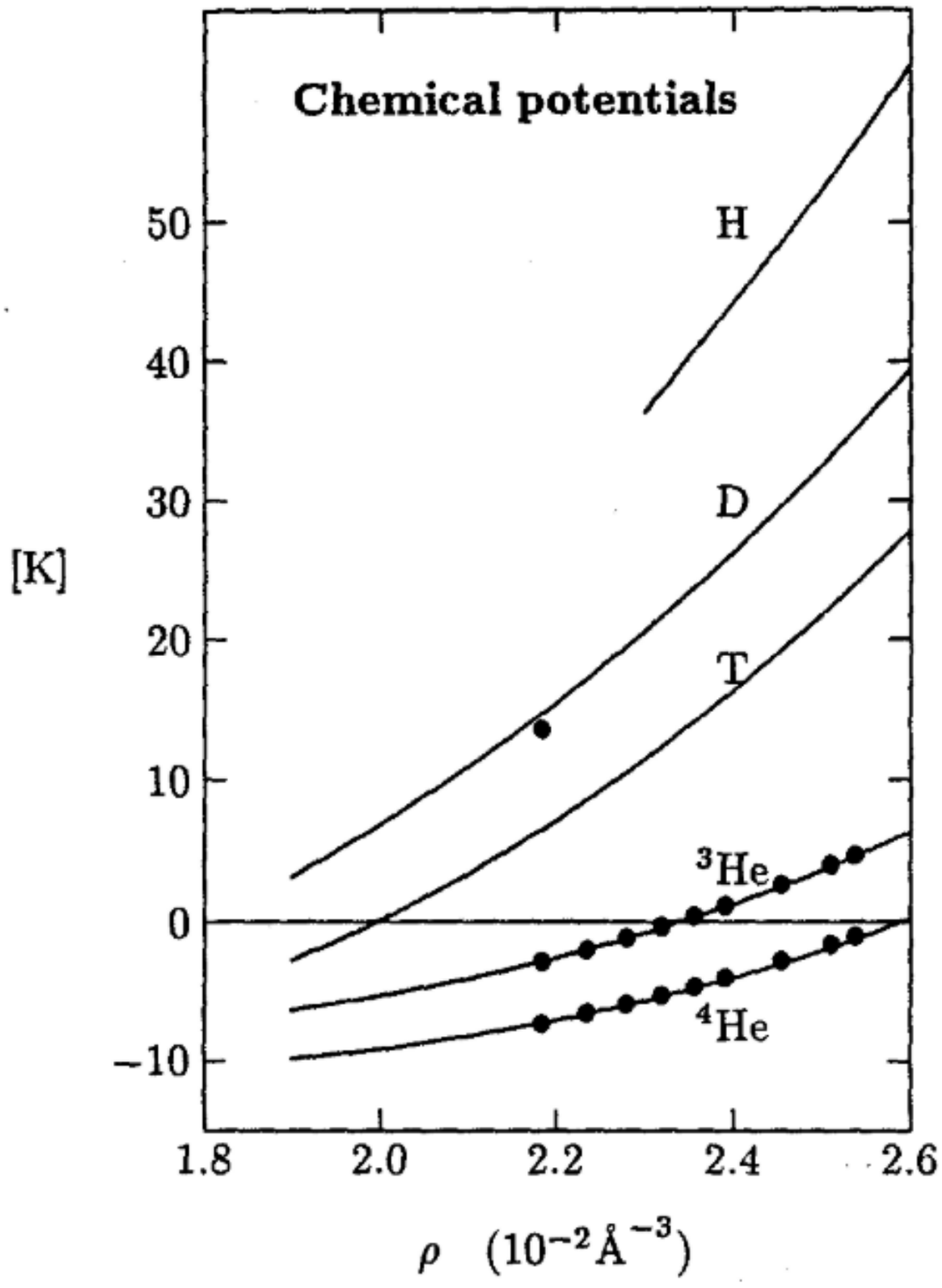

Fig. 9. Chemical potentials for ^{4}He, ^{3}He, and hydrogen isotopes. The solid curves are the theoretical results and the black dots are taken from experiments.[2] Notice the new experimental result for deuterium.[1]

Hydrogen isotopes and 3He impurities in liquid 4He
R. Abela et al., Journal of Low Temperature Physics, Vol. 90 (1993)

muSR

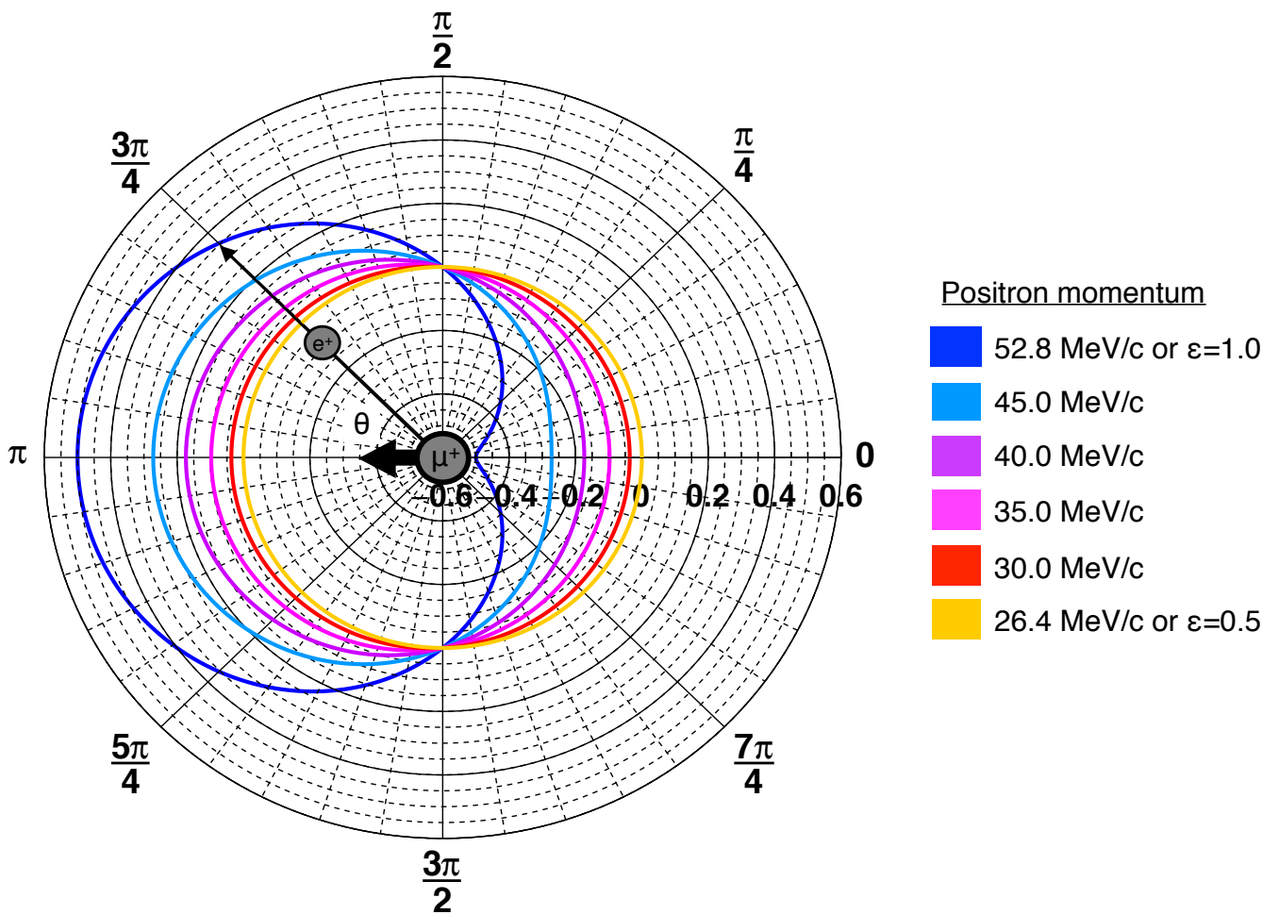
π/2
3π/4
π/4
π
0
5π/4
7π/4
3π/2
e⁺
μ⁺
θ
−0.6 −0.4 −0.2 0 0.2 0.4 0.6
Positron momentum
52.8 MeV/c or ε=1.0
45.0 MeV/c
40.0 MeV/c
35.0 MeV/c
30.0 MeV/c
26.4 MeV/c or ε=0.5

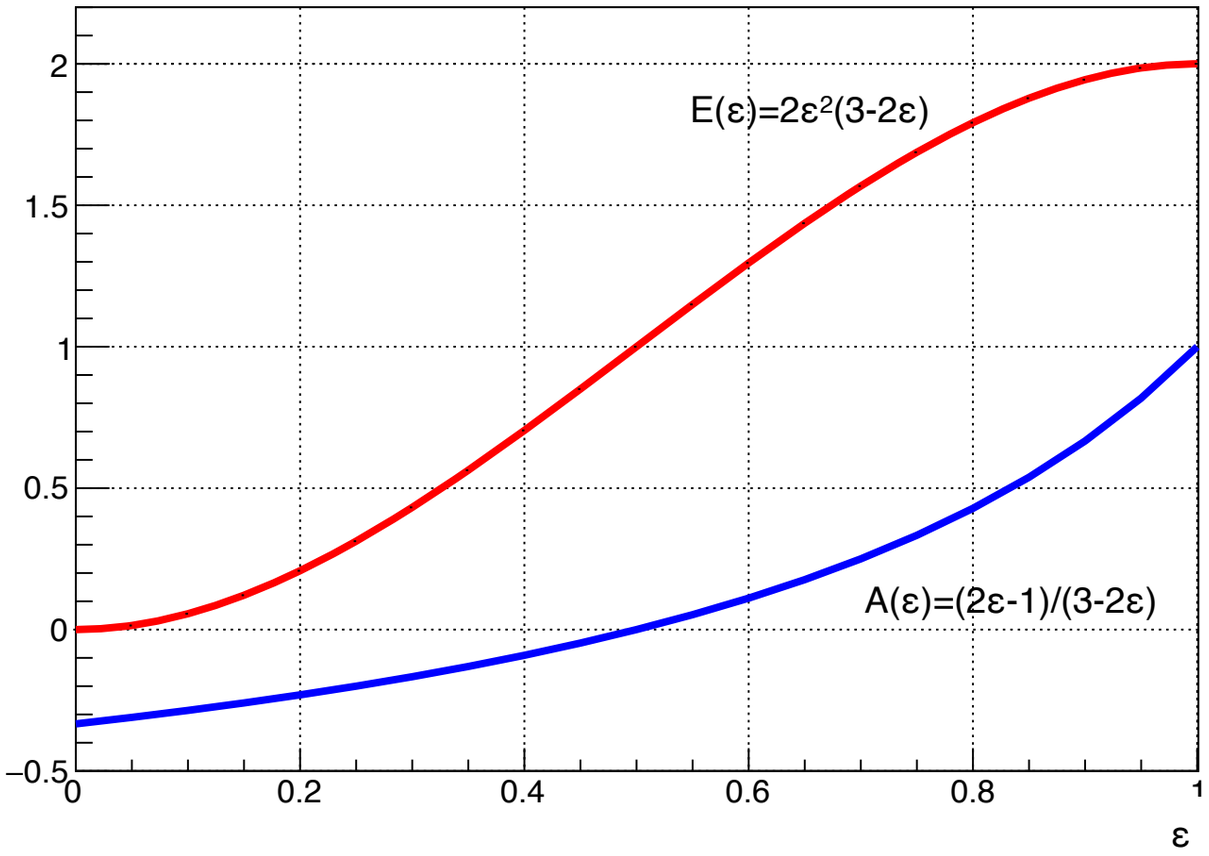
E(ε)=2ε²(3-2ε)
A(ε)=(2ε-1)/(3-2ε)
2
1.5
1
0.5
0
−0.5
0
0.2
0.4
0.6
0.8
1
ε

Mu from various targets

Ar gas

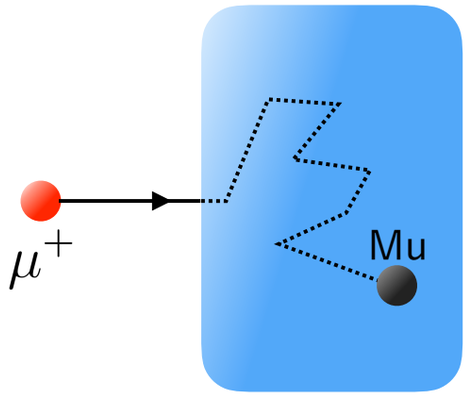

- 100% Muonium yield
- No vacuum yield
- 50% polarisation

Tungsten foil

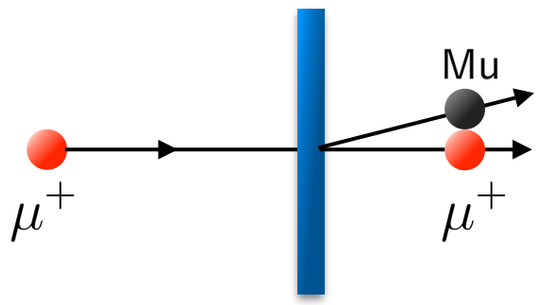

- 4% vacuum yield
  (P_{muon}=23 MeV/c)

SiO_2 powder
or aerogel

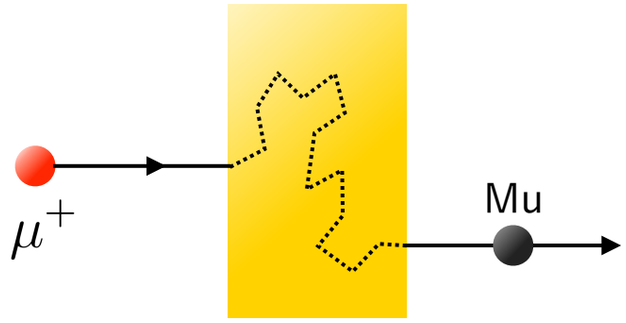

- 19±6% vacuum yield
  (P_{muon}=20 MeV/c)

SiO_2
mesoporous
thin film

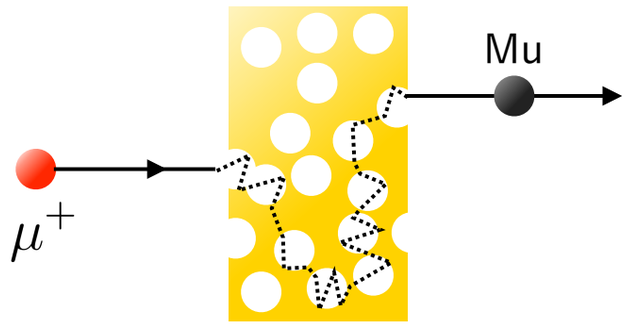

- 38±4% vacuum yield
  (P_{muon}=1 MeV/c or E_{kin}=5 keV)

Necessity for a new $\mu^+ \rightarrow$ vacuum Mu

Conventional Mu source

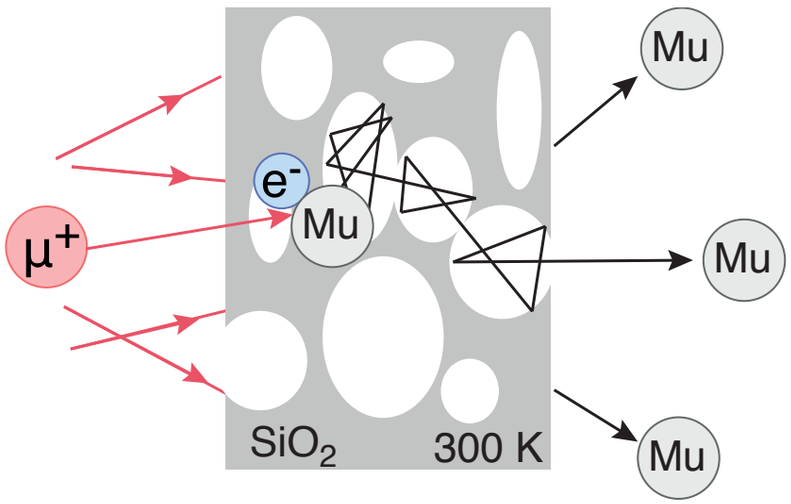

- Large (thermal) energy spread
- Broad angular distribution (~cosθ)
- 3-30 % conversion eff. at T=296 K

Novel Mu source from SFHe

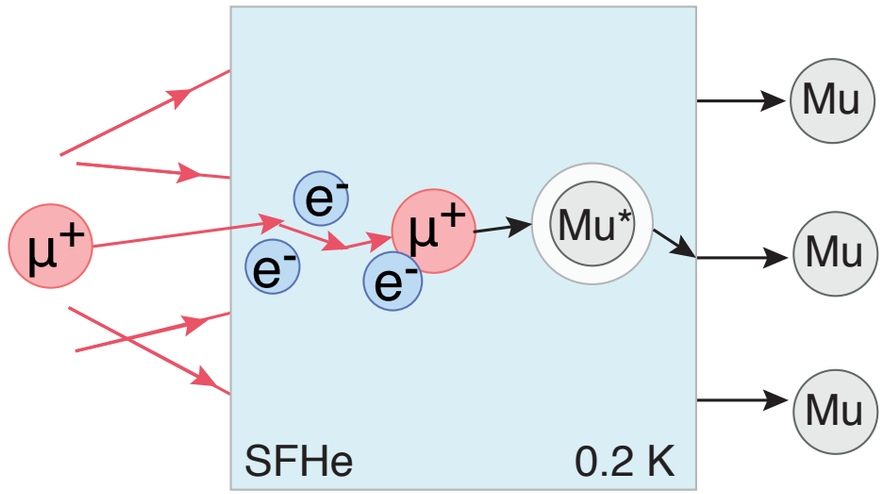

- From **chemical potential** E/k_B~270 K: Mu atoms are ejected from bulk SFHe with v = 6.3 mm/μs

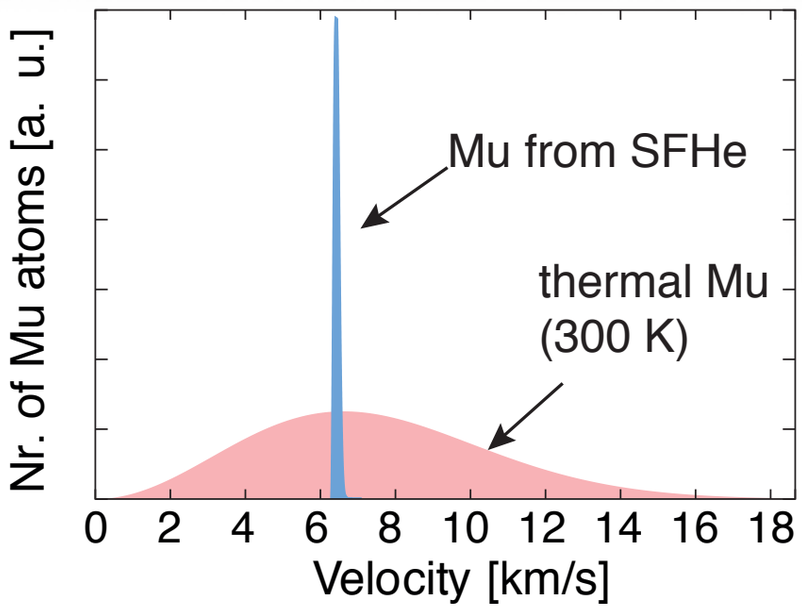

- Narrow energy spread and angular distribution - large transverse coherence ($\ell_0 \sim \lambda/(2\alpha)$ ~10 nm)
- Possibility to Mu diffusion from 100 μm deep SFHe within ~1 μs

Extra - Methods with thick SFHe layers

Horizontal SFHe bath

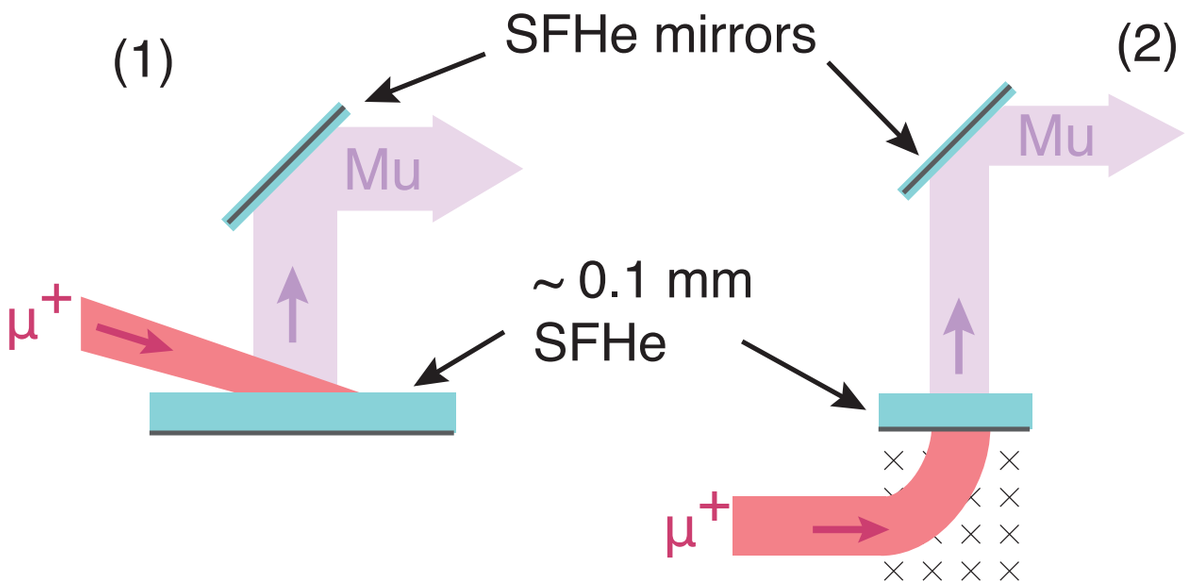

Vertical SFHe sheets

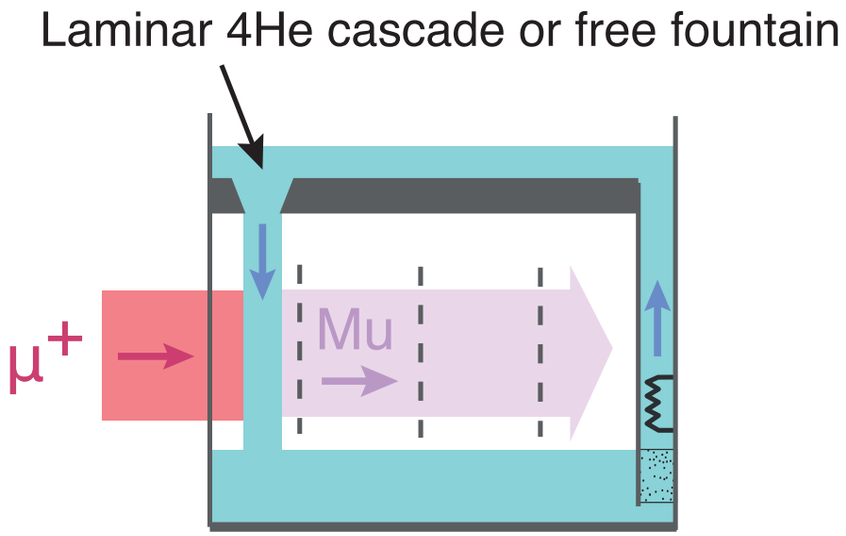

Extra - Contingency extraction methods

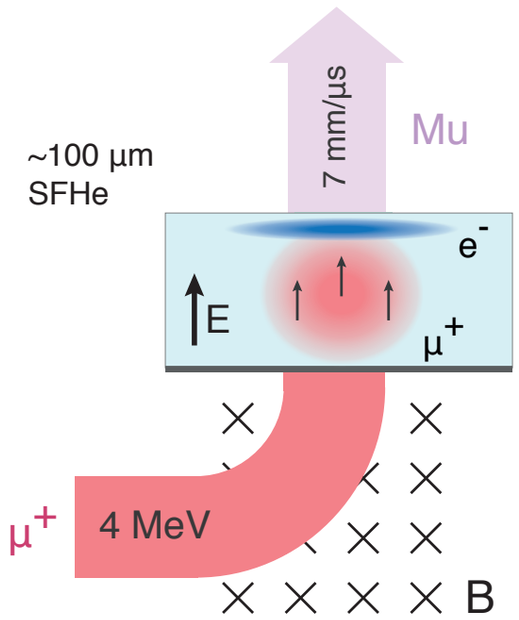

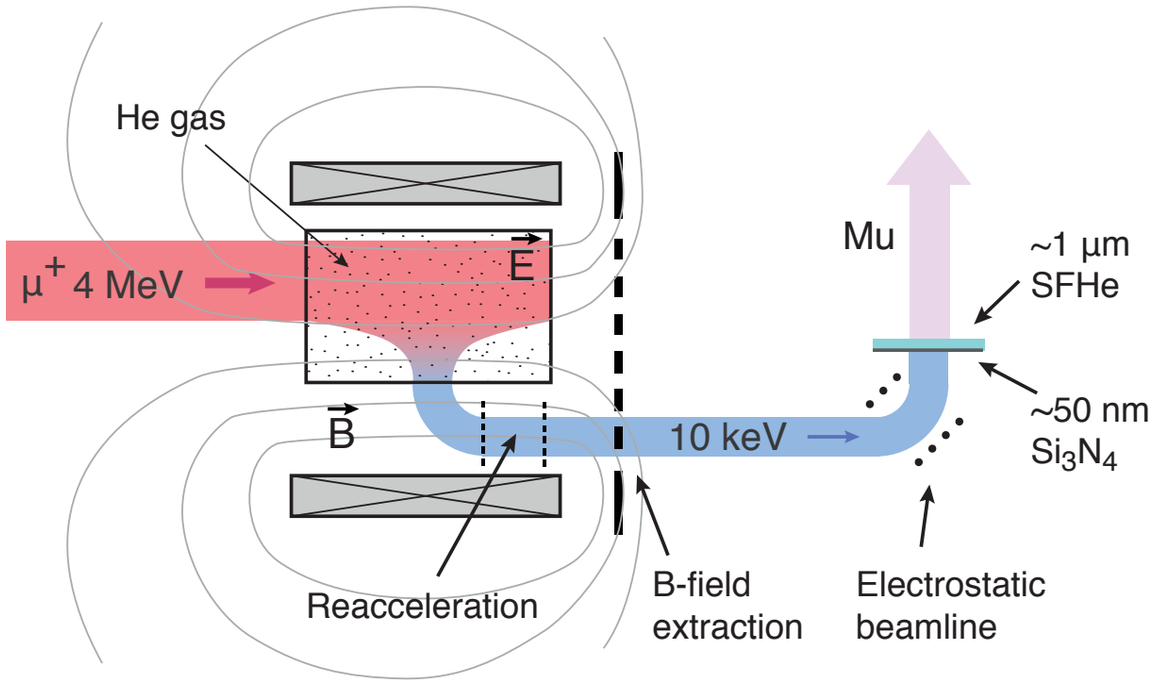

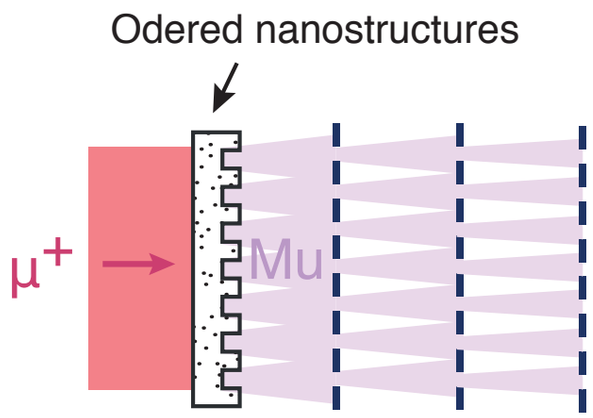

Experiment 1 : Detector layout of the DOLLY

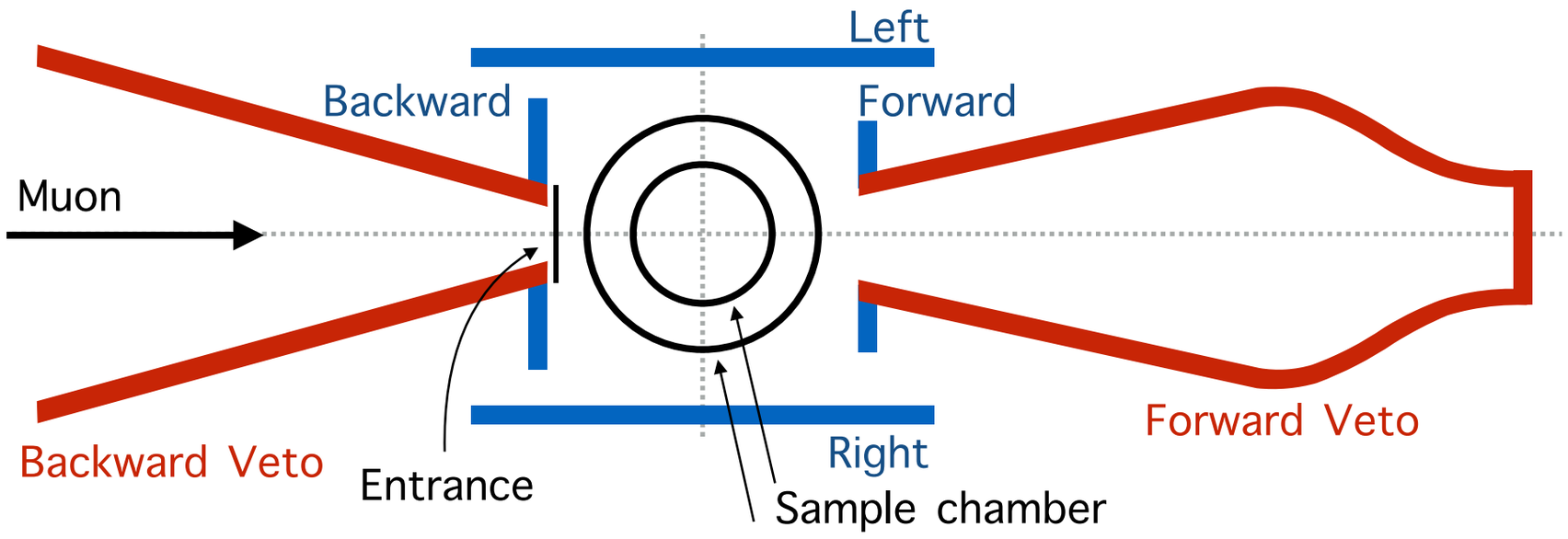

Variox radiation shields

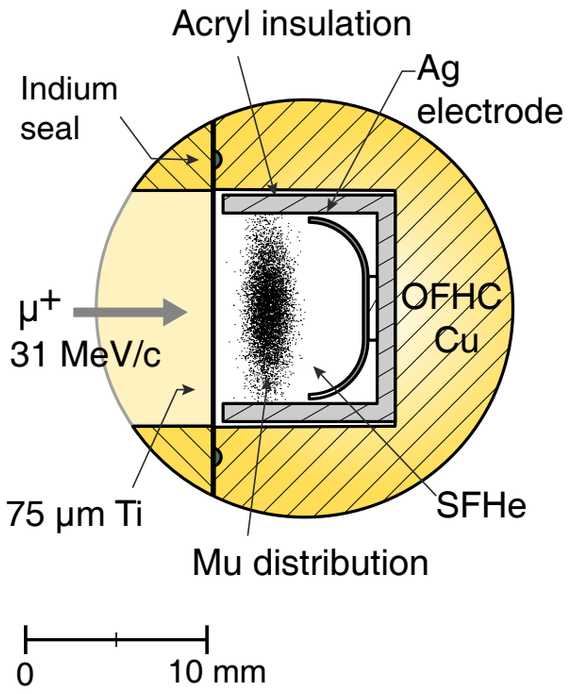

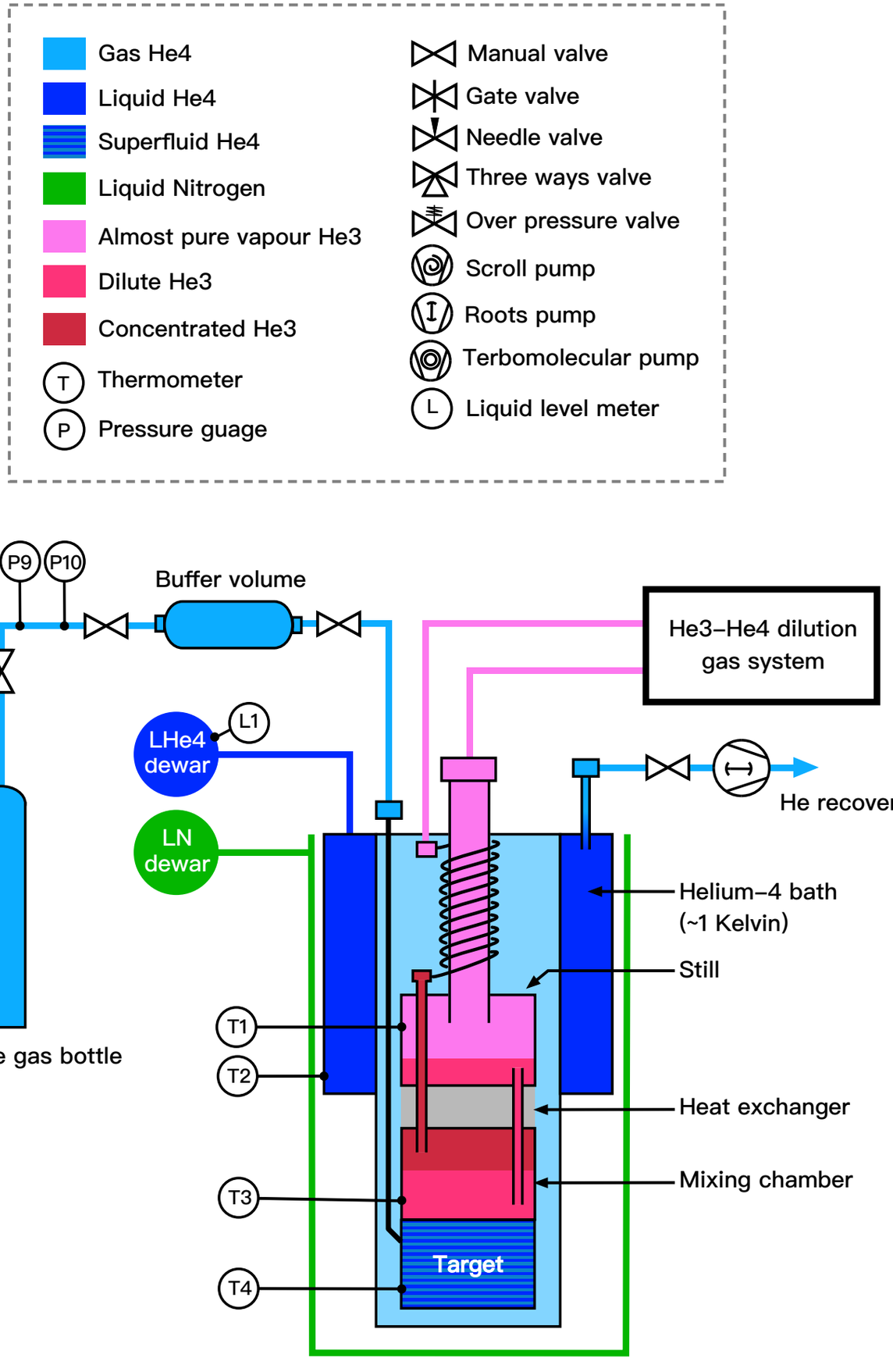
Gas He4
Liquid He4
Superfluid He4
Liquid Nitrogen
Almost pure vapour He3
Dilute He3
Concentrated He3
T Thermometer
P Pressure guage
Manual valve
Gate valve
Needle valve
Three ways valve
Over pressure valve
Scroll pump
Roots pump
Terbomolecular pump
L Liquid level meter
P9
P10
Buffer volume
He3–He4 dilution gas system
L1
LHe4 dewar
LN dewar
He recovery
Helium–4 bath (~1 Kelvin)
Still
T1
T2
Heat exchanger
T3
Mixing chamber
Target
T4
He gas bottle

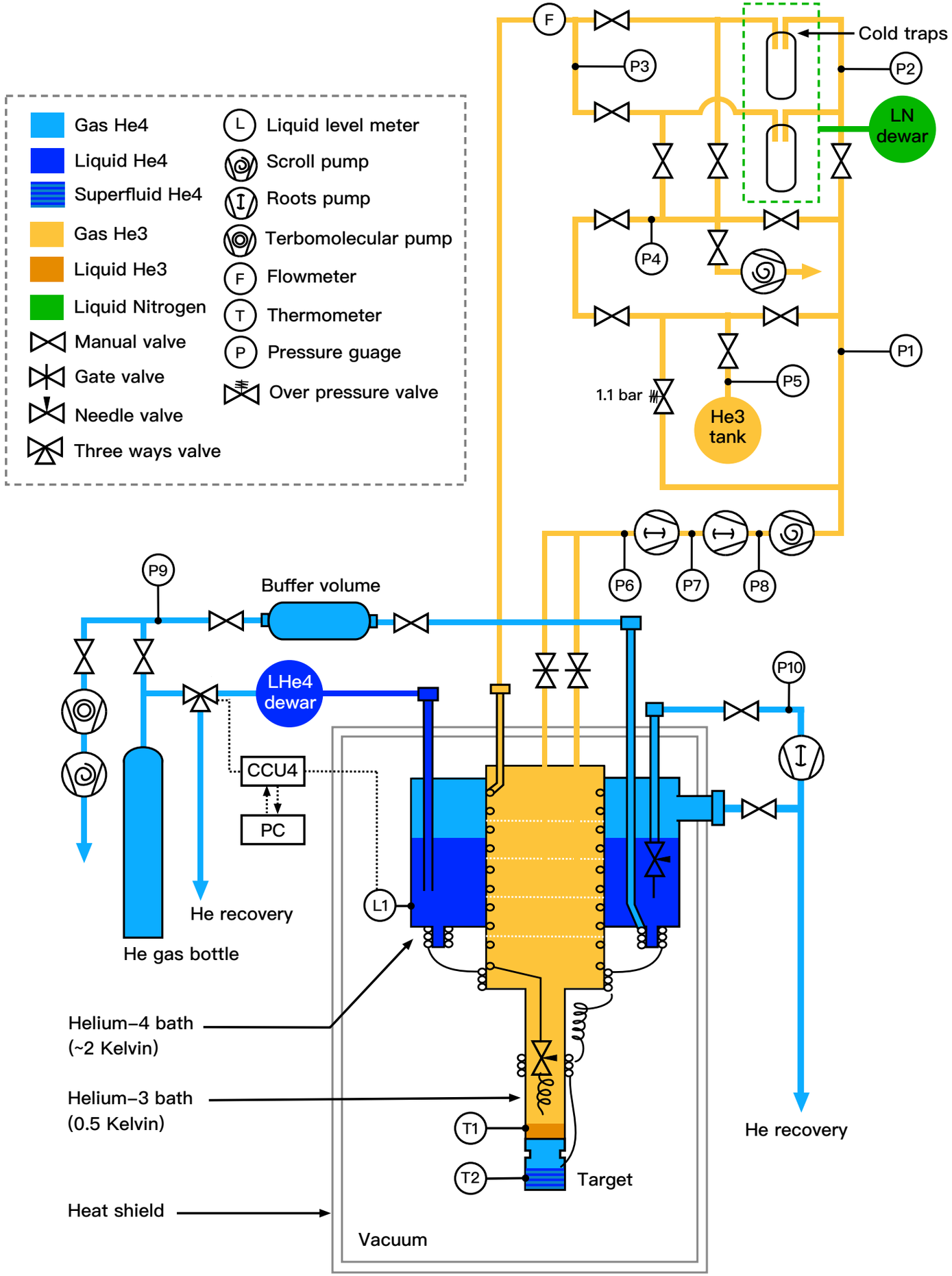
Gas He4
Liquid He4
Superfluid He4
Gas He3
Liquid He3
Liquid Nitrogen
Manual valve
Gate valve
Needle valve
Three ways valve
Liquid level meter
Scroll pump
Roots pump
Terbomolecular pump
Flowmeter
Thermometer
Pressure guage
Over pressure valve
F
P3
Cold traps
P2
LN dewar
P4
P1
1.1 bar
P5
He3 tank
P6
P7
P8
P9
Buffer volume
LHe4 dewar
P10
CCU4
PC
L1
He recovery
He gas bottle
Helium–4 bath
(~2 Kelvin)
Helium–3 bath
(0.5 Kelvin)
T1
T2
Target
He recovery
Heat shield
Vacuum

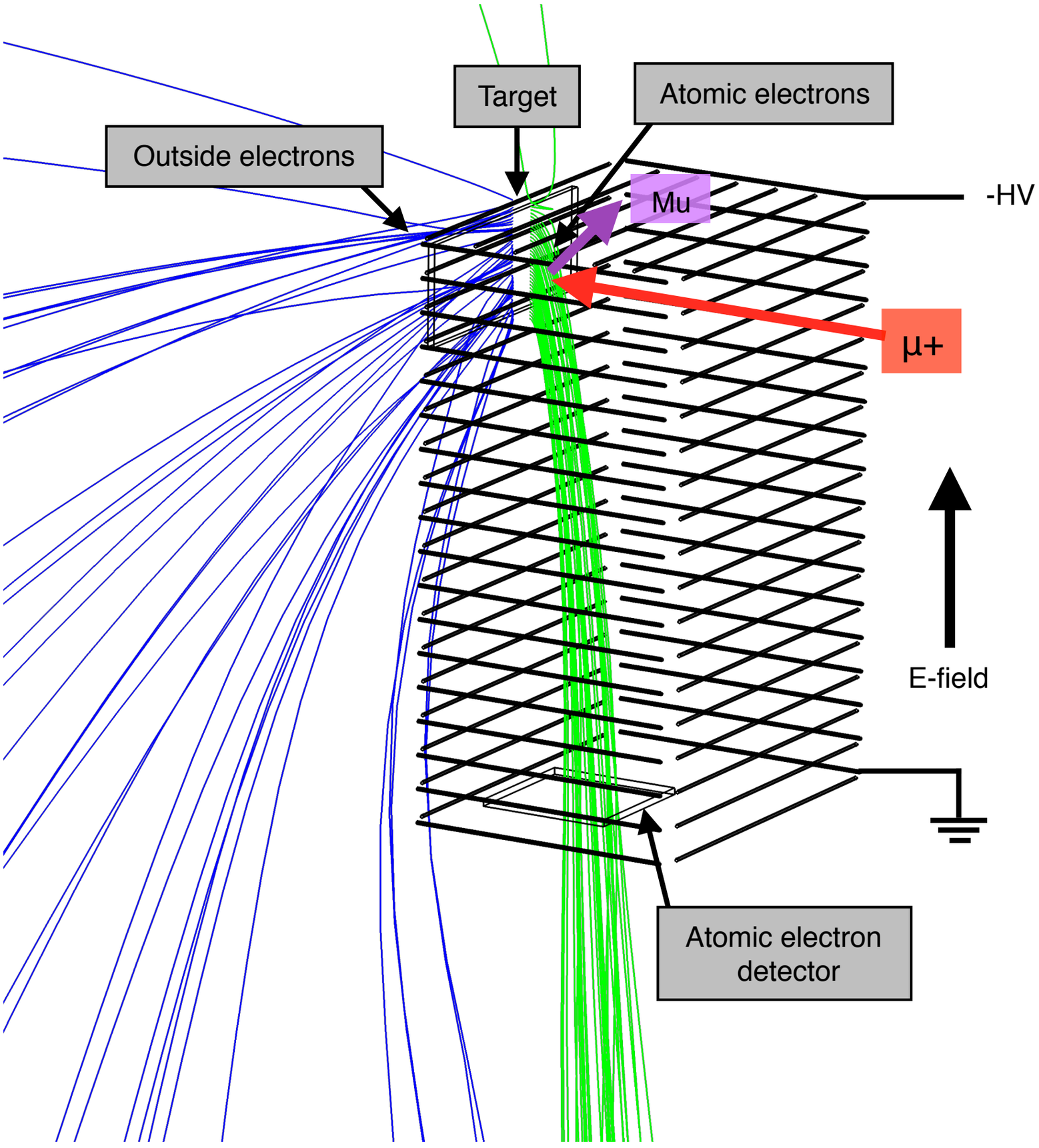
Target
Atomic electrons
Outside electrons
Mu
-HV
μ+
E-field
Atomic electron
detector

* The number of muonium signals detected by the middle detectors decreased when the pressure of helium increased
* The mean free path (l_{Mu}) of muonium can be calculated by

$$l_{Mu} = \frac{k_B T}{\sqrt{2}\pi P d_{Mu,He}^2}$$

* P~10^{-6} mbar, l_{Mu}~100 m
* P~0.01 mbar, l_{Mu}~1 cm
* P~0.1 mbar, l_{Mu}~1 mm

muCool

muCool principle

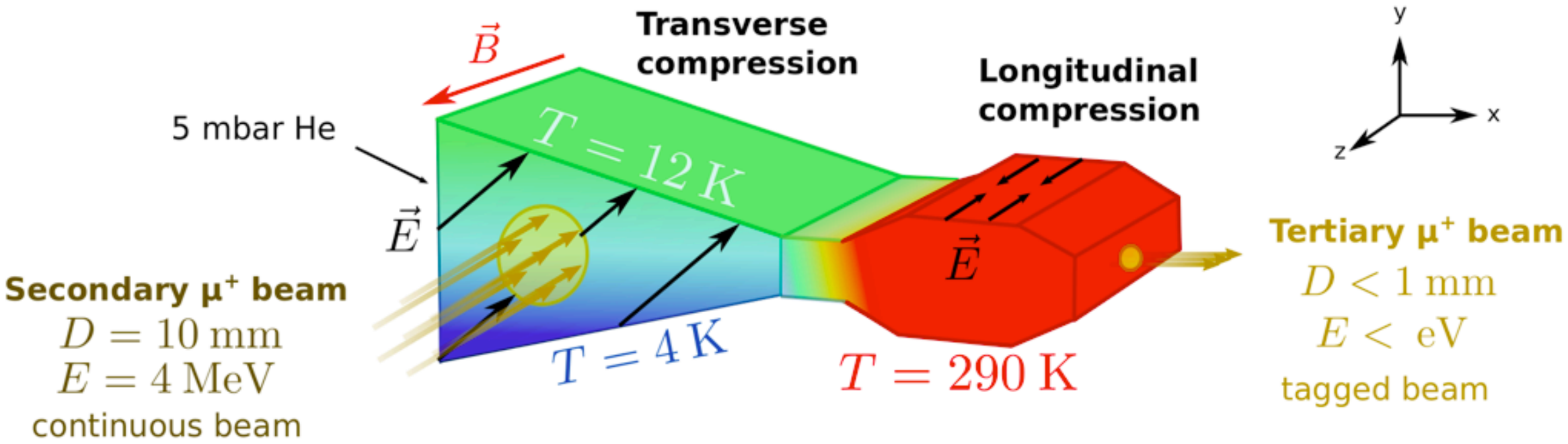

ω = eB/m: cyclotron frequency
μ = muon mobility
ν_{col} = collision frequency

$$\vec{v}_{drift} = \frac{\mu E}{1+\left(\frac{\omega}{\nu_{col}}\right)^2}\left[\hat{\mathbf{E}} + \frac{\omega}{\nu_{col}}\hat{\mathbf{E}}\times\hat{\mathbf{B}} + \left(\frac{\omega}{\nu_{col}}\right)^2\left(\hat{\mathbf{E}}\cdot\hat{\mathbf{B}}\right)\hat{\mathbf{B}}\right]$$

muCool: Transverse compression

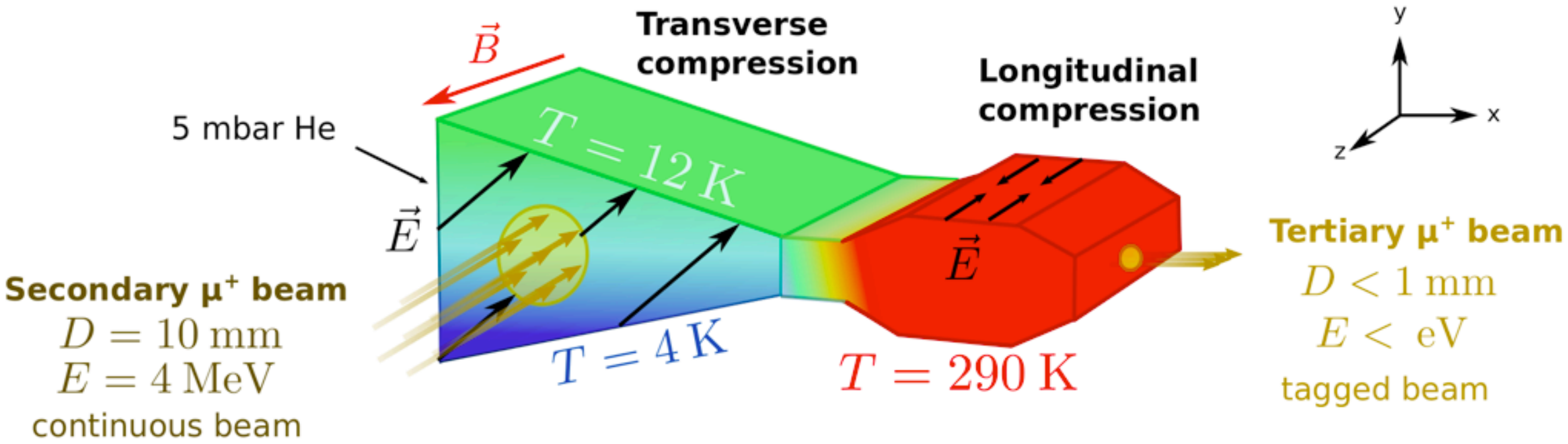

- 5 mbar He gas
- Cryogenic temperature
- Crossed E- and B-fields (E~ 1.5 kV/cm, B ~ 5 T)
- high density -> v_{col} large -> Ê dominates
- medium density -> v_{col} intermediate -> Ê x B dominates

$$\vec{v}_{drift} = \frac{\mu E}{1+\left(\frac{\omega}{\nu_{col}}\right)^2}\left[\hat{\mathbf{E}} + \frac{\omega}{\nu_{col}}\hat{\mathbf{E}}\times\hat{\mathbf{B}}\right]$$

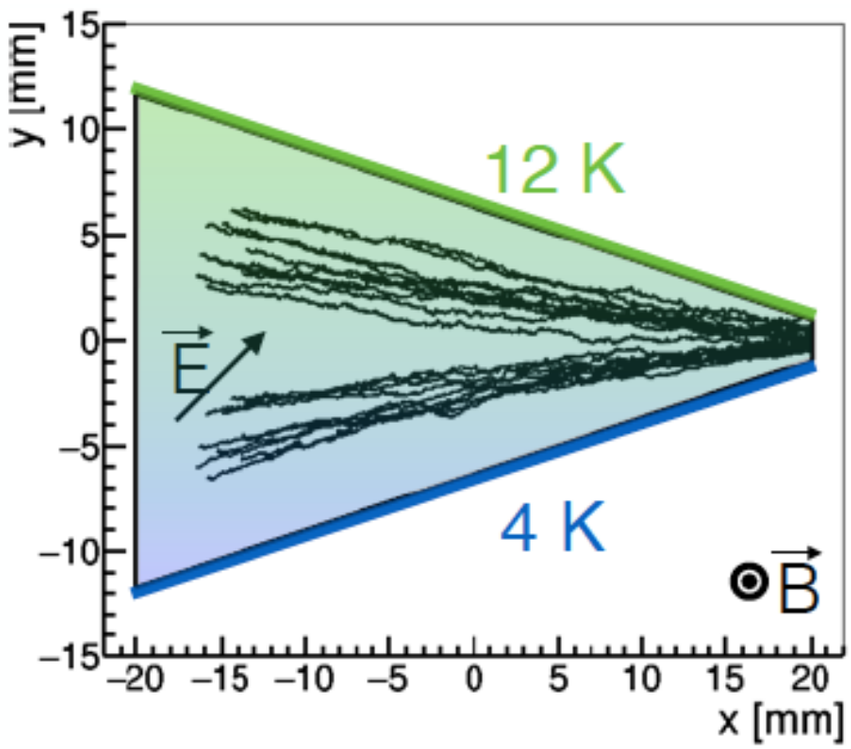

muCool: Longitudinal compression

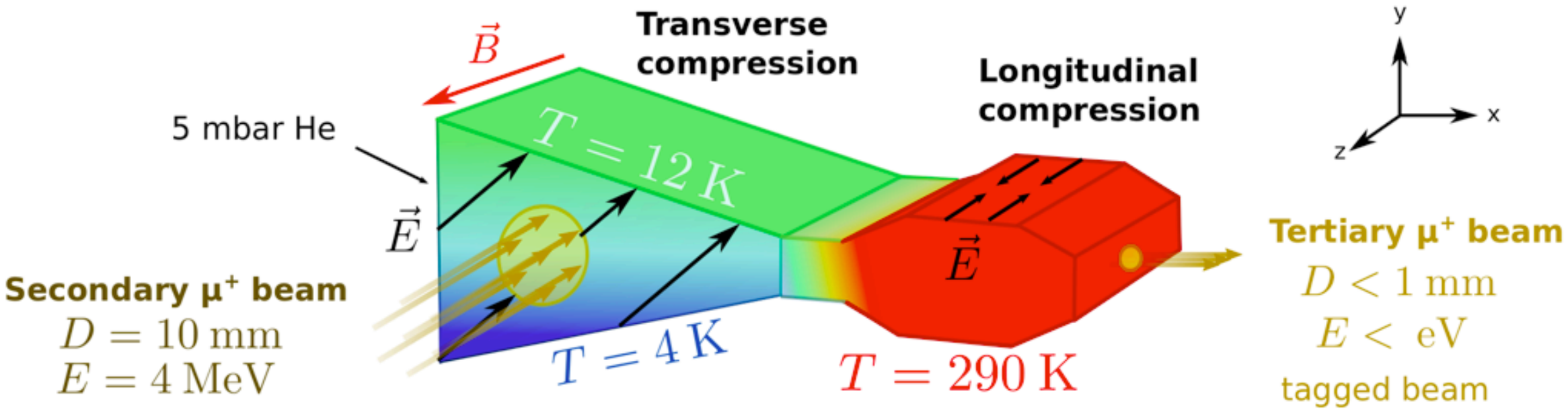

- 5 mbar He gas
- Room temperature
- Parallel E- and B-fields (E~ 60 V/cm, B ~ 5 T)
- low density -> v_{col} small -> B dominates

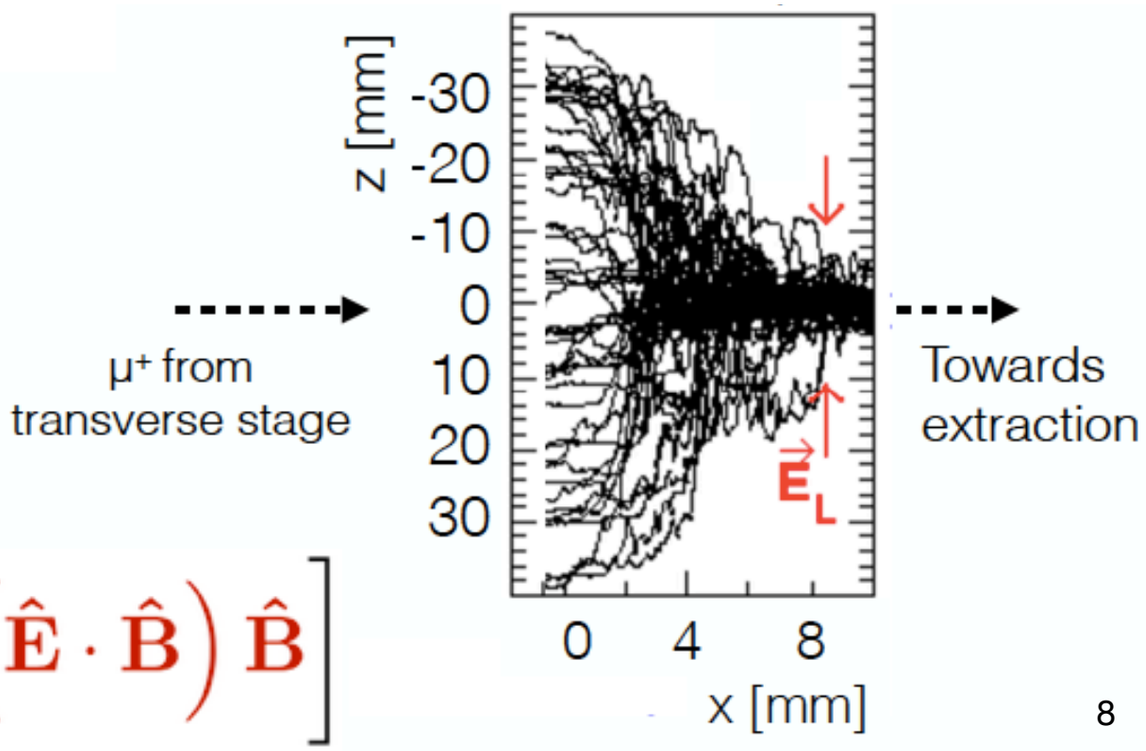

$$\vec{v}_{drift} = \frac{\mu E}{1+\left(\frac{\omega}{\nu_{col}}\right)^2}\left[\hat{\mathbf{E}} + \left(\frac{\omega}{\nu_{col}}\right)^2 \left(\hat{\mathbf{E}}\cdot\hat{\mathbf{B}}\right)\hat{\mathbf{B}}\right]$$

Interferometer

Experimental challenges

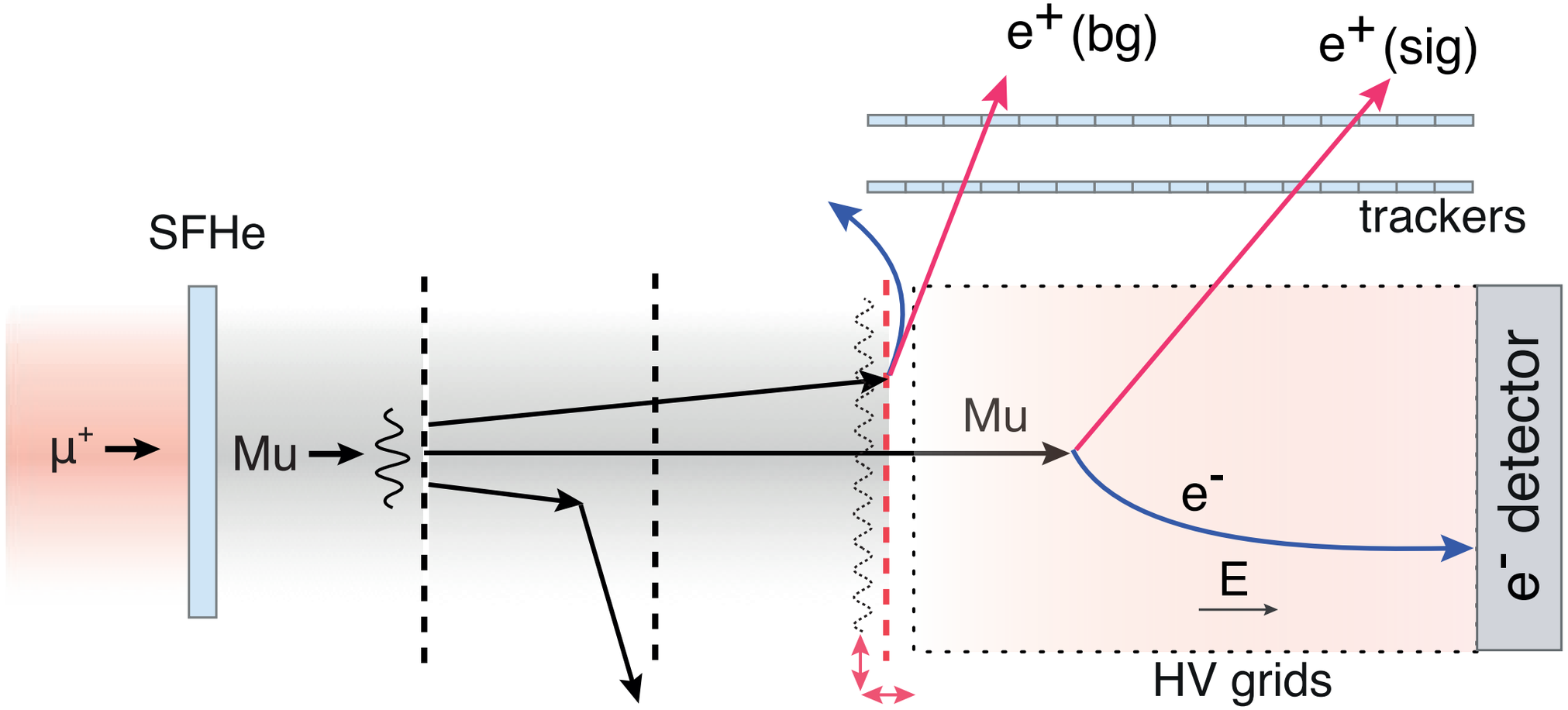

$\mu^+ \rightarrow$ vacuum Mu conversion

- efficient bulk production
- fast diffusion to surface
- vacuum emission
- horizontal beam geometry

Interferometer

- nm-precise fabrication over few mm
- alignment in cold
- stabilization in cold
- …

Detection

- efficient e^+ tracking
- coincident detection of atomic e^-
- high overall efficiency and low background

Gravity experiment using atomic Mu beams

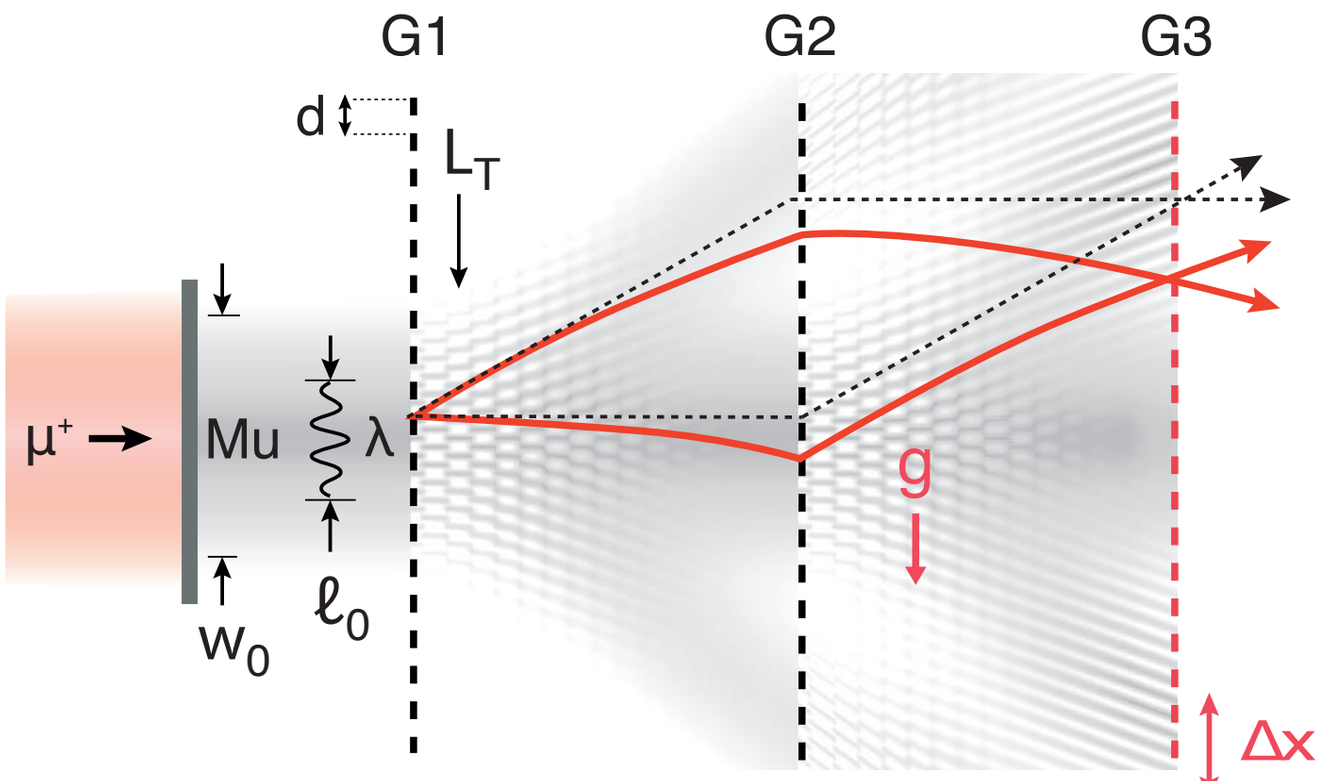

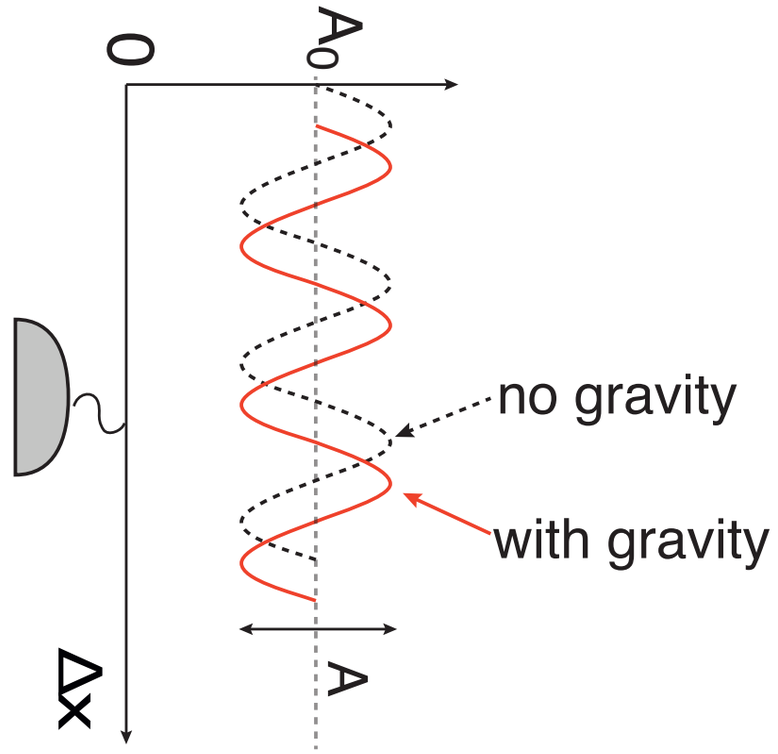

$$\Delta g \approx \frac{1}{2\pi T^2} \frac{d}{C\sqrt{N}}$$

Small grating period (~100 nm) to measure sub-nm shifts

Interaction time with gravity as τ = 2.2 μs ~ few μs !

Many atoms $N \sim N_0 b^3 e^{-(t_D+T)/\tau}$

Large contrast $C = A/A_0$

Inertial sensitivities

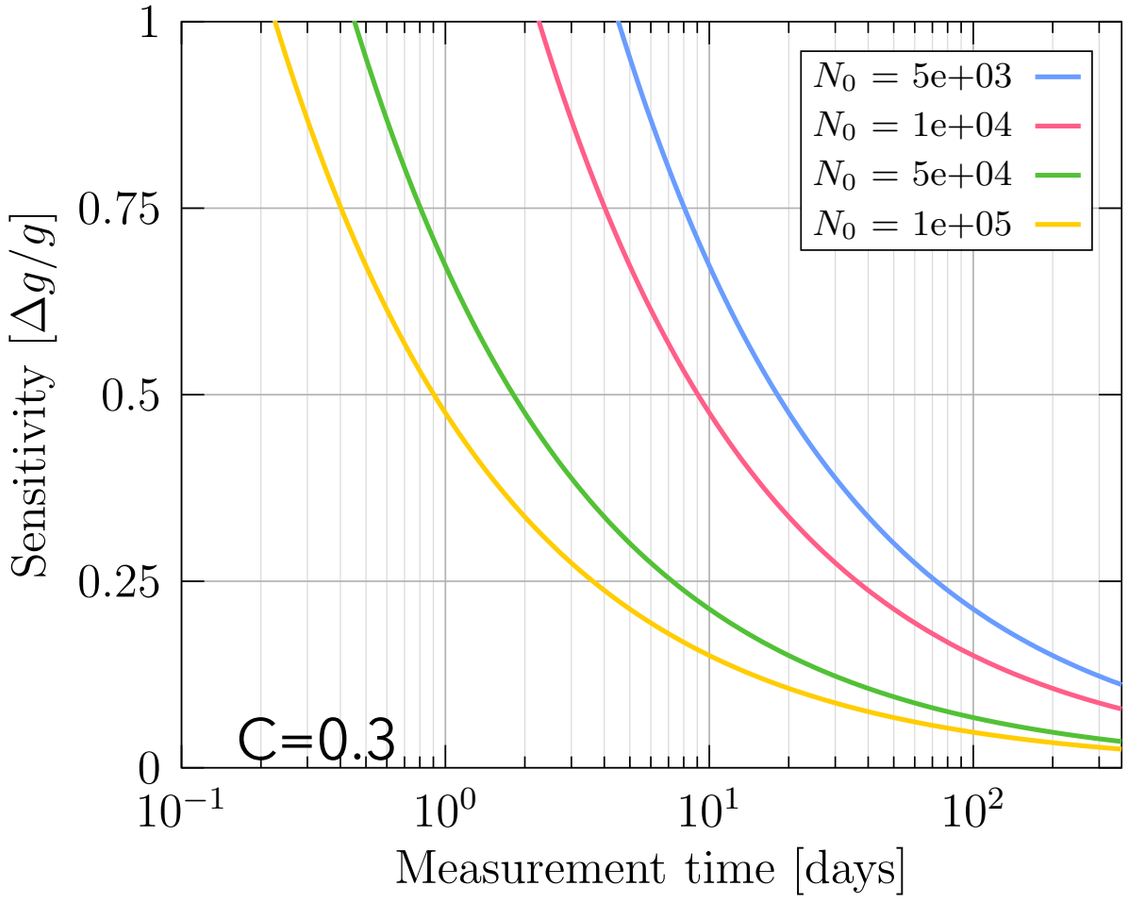

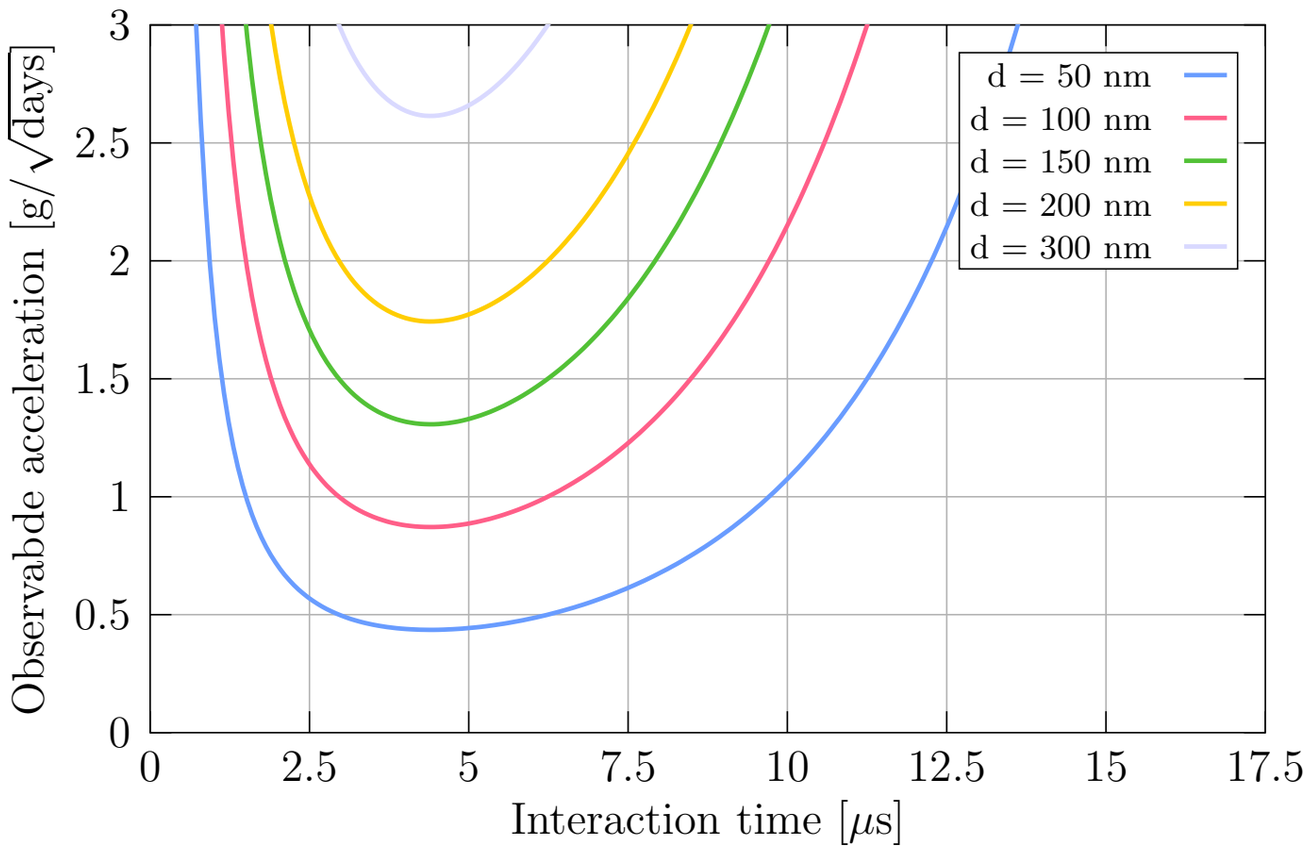

$$\Delta g \approx \frac{1}{C\sqrt{N_0 \cdot e^{-(t_D+T)/\tau}}} \frac{d}{2\pi} \frac{1}{T^2}$$

d = 100 nm, 70% loss on grids,
interaction time T = 8 μs

Determining sign of g:
1-2 days with Mu source of $N_0 = 5 \cdot 10^4$/s, C=0.3

Effects of beam quality on the gravity measurement

Same interferometer parameters (optimized for gravity):
L_0=5 mm, L=20 mm, d=100 nm

- Unrealistically narrow, fully coherent beam ($w_0 = \ell_0 = 30$ µm)

- realistic beam width and coherence length ($w_0 = 1$ mm, $\ell_0 = 10$ nm)

model used here based on:
McMorran et al., PRA 78 (2008)

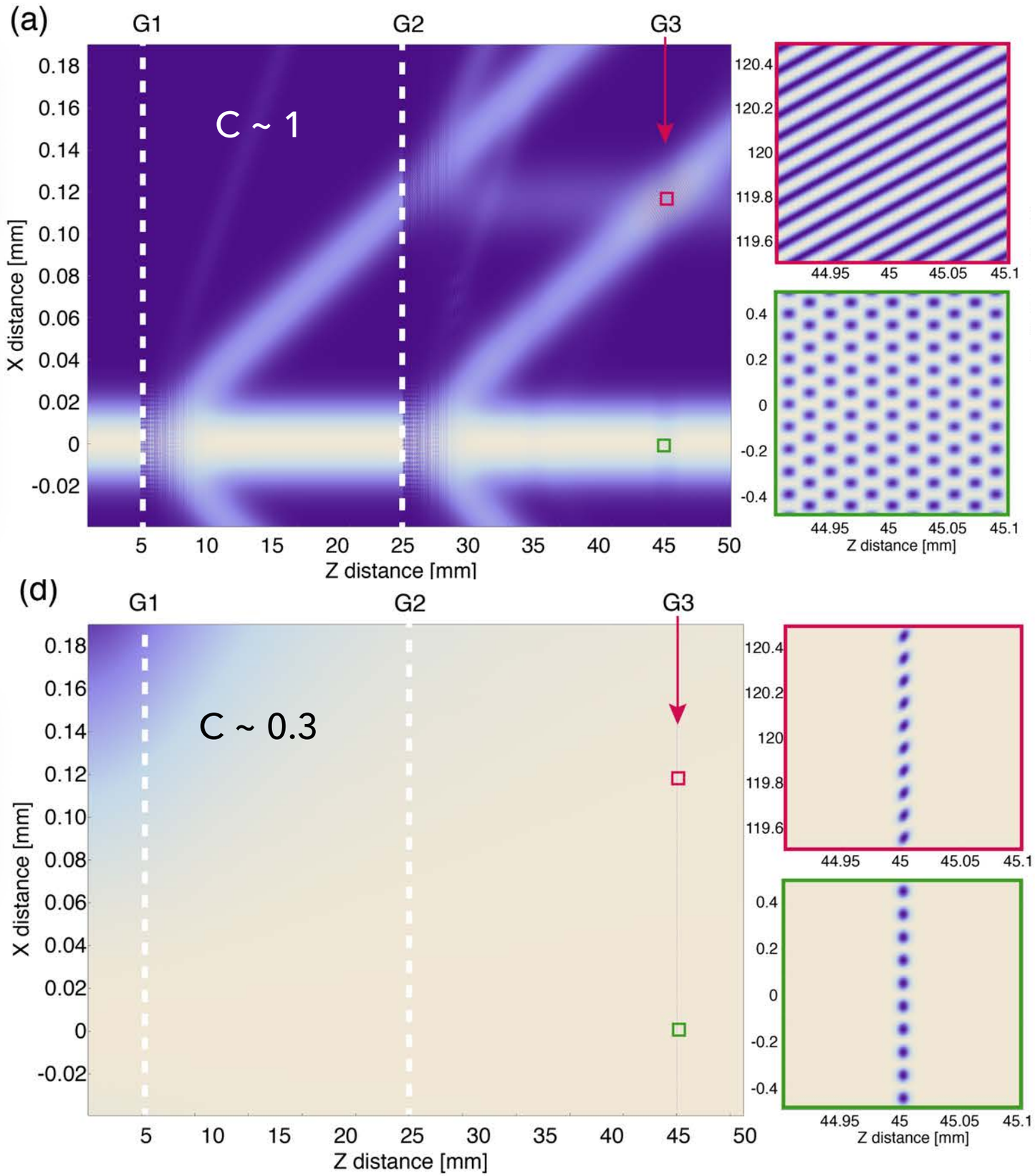

Mu formation processes

Mu formation processes in SFHe

PHYSICAL REVIEW B **66**, 035105 (2002)

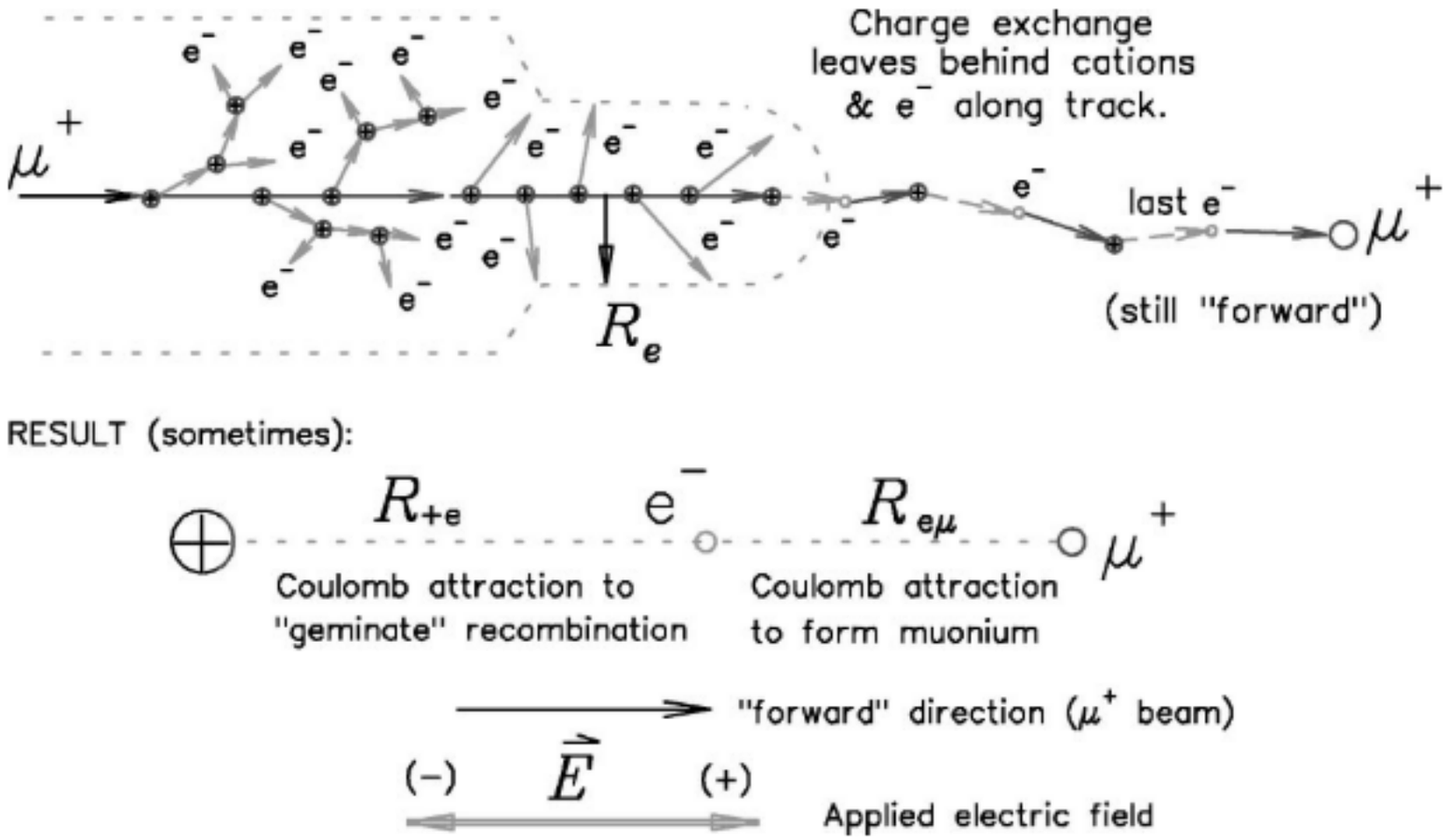

FIG. 1. Sketch of a general model of the end of the muon track in CRG. If the last "second stage" electron is to play a role in DMF, it must have $R_{+e} > R_{e\mu}$; otherwise it would recombine with the final positive ion before the μ^+.

Why Silica-types materials ?

Why SiO2 pourous thin film

To check if the value of the potential barrier height obtained above can be identified with the Mu work-function (W), Density Functional Theory calculations within GAUSSIAN 98 [116] were performed on clusters of SiO_2 containing up to eight silicon atoms and terminated by oxygen, capped with hydrogen atoms. We compute the total energy $E^{tot}_{SiO2+Mu}$ of the SiO_2 matrix with a Mu atom and the total energy of the SiO_2 fragment alone E^{tot}_{SiO2}. These computations yield $W = E^{tot}_{SiO2+Mu} - E^{tot}_{SiO2} - 13.6\text{eV} = (-0.6 \pm 0.3)$ eV. The main error for W originates from the uncertainty to locate the exact position of the interstitial Mu site with respect the Si and O atoms. Considering the over-simplification of the quantum diffusion model, it can be concluded that the experimental determination of the work-function is consistent with the theoretical estimation. Further experiments using other techniques and more precise measurements for Mu and Ps will be useful to gain a deeper understanding of this intriguing diffusion process in mesoporous films.

Kim Siang Khaw Thesis ETH Zurich

Formation processes

SFHe -> show the delay formation time -> need to ionize electron and mobility, come close to each other

Solid (SiO2, Zeolite powder,…) -> No delay time, electron is loosely-bounded by the solid and can form the bound-state with muon easily

Gas (Ar,Kr) -> Binding energy of Mu ~ 13.5 eV, Ionization energy of Ar ~ 15.8, of Kr ~ 13.9 eV, of Xe ~ 12.1 eV, no delay muonium fromation

Gas (He) -> Too high ionization energy ~ 24.5 eV, No muonium formation in He gas

Zeolite Powder

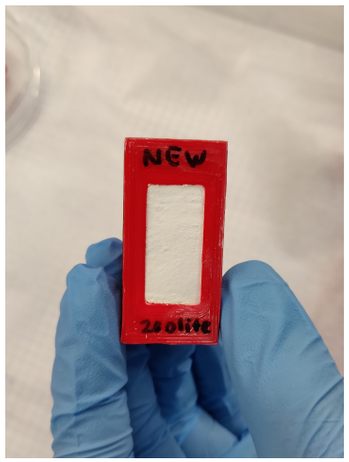

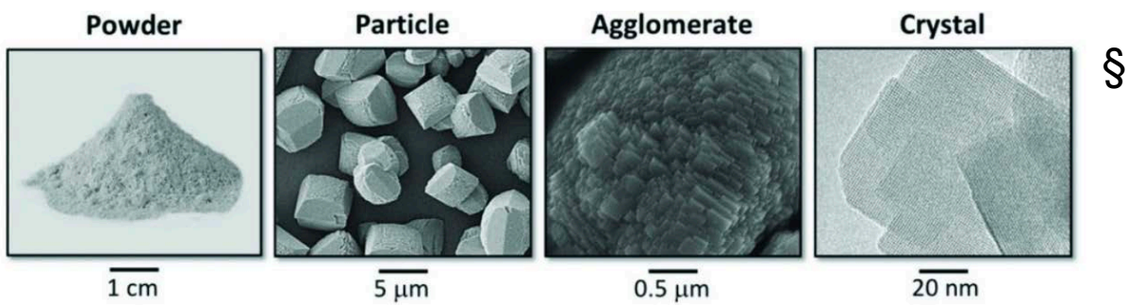

§

Name -> Ikaline treated CBV 712 faujassite zeolite (CBV712-B)

Normal Fabrication -> Slow crystallization of a silica-alumina gel in the presence of alkalis and organic templates, Sol-gel processing

Why? -> Nicely source of Ps, high yield

Ablated Aerogel

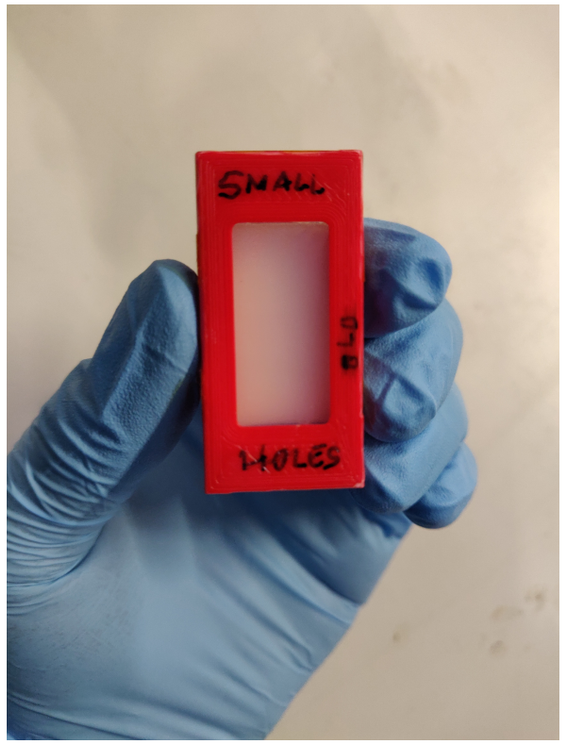

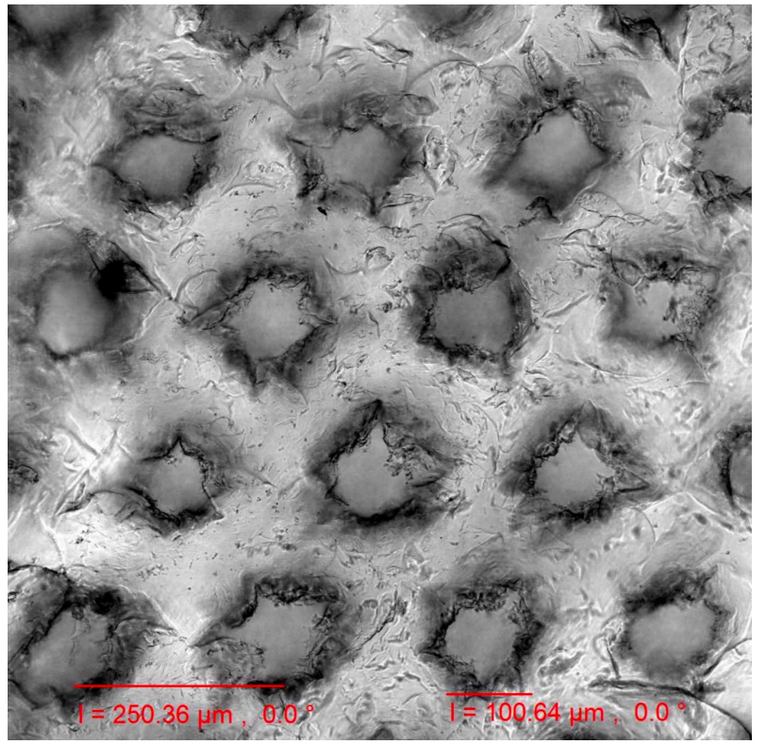

~100 um dimeter of holes
~250 um pitch
by TRIUMF

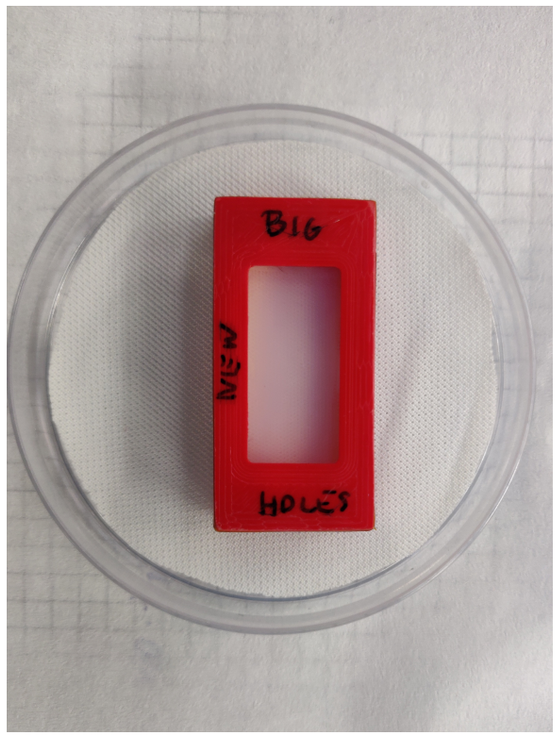

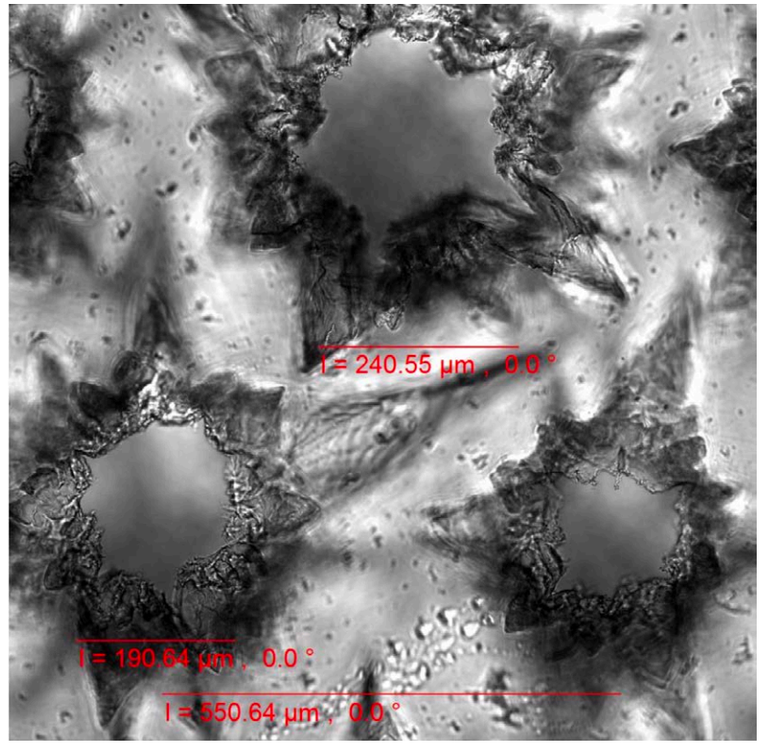

~240 um dimeter of holes

Helium Vapor Pressure

The observed saturated vapor pressure of liquid helium
R.J. Donnelly and C.F. Barenghi
Journal of Physical and Chemical Ref Data 27, 1217 (1998)

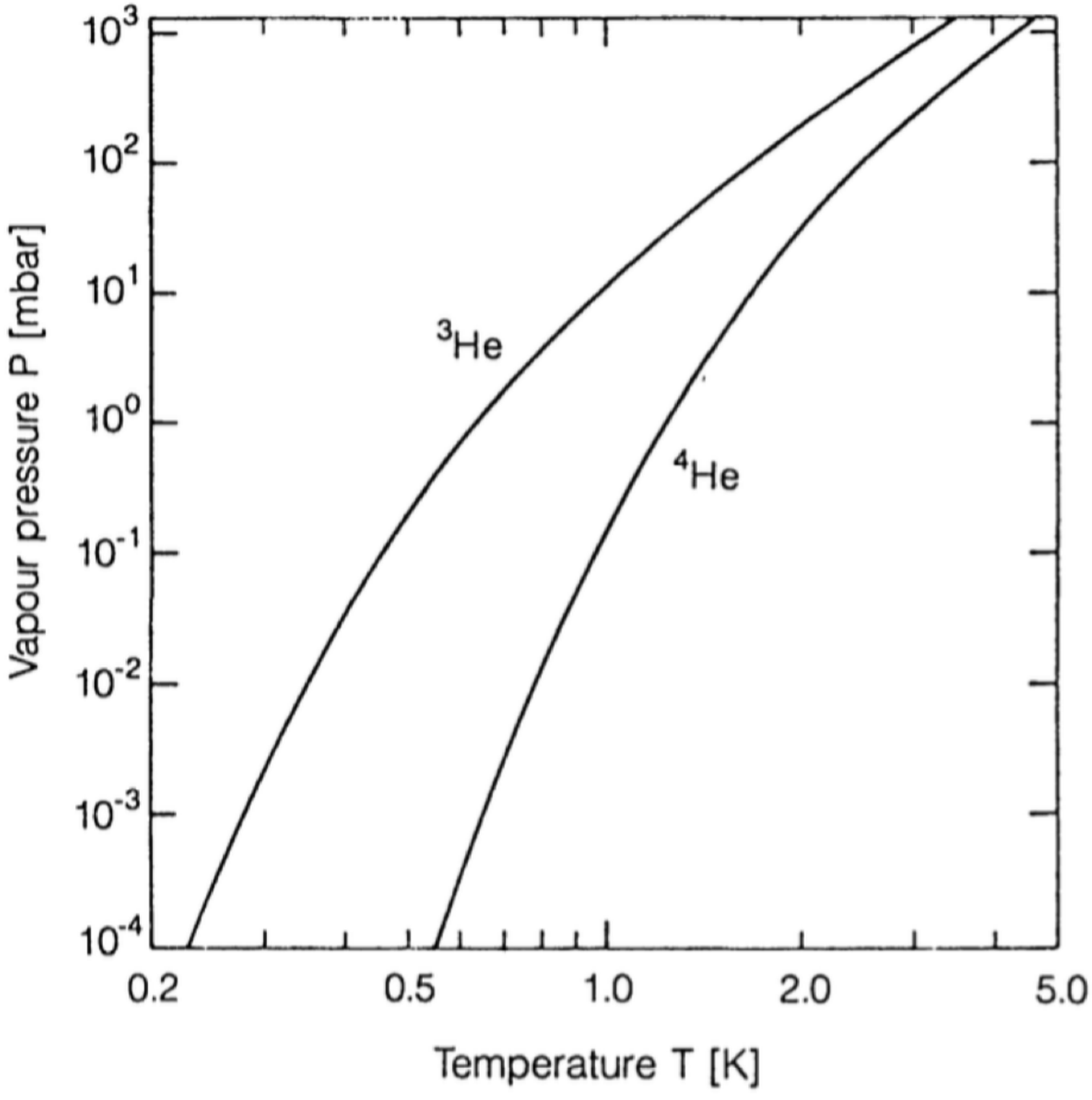

Fig.2.6. Vapour pressures of liquid ^{3}He and liquid ^{4}He

2nd Generation Particles

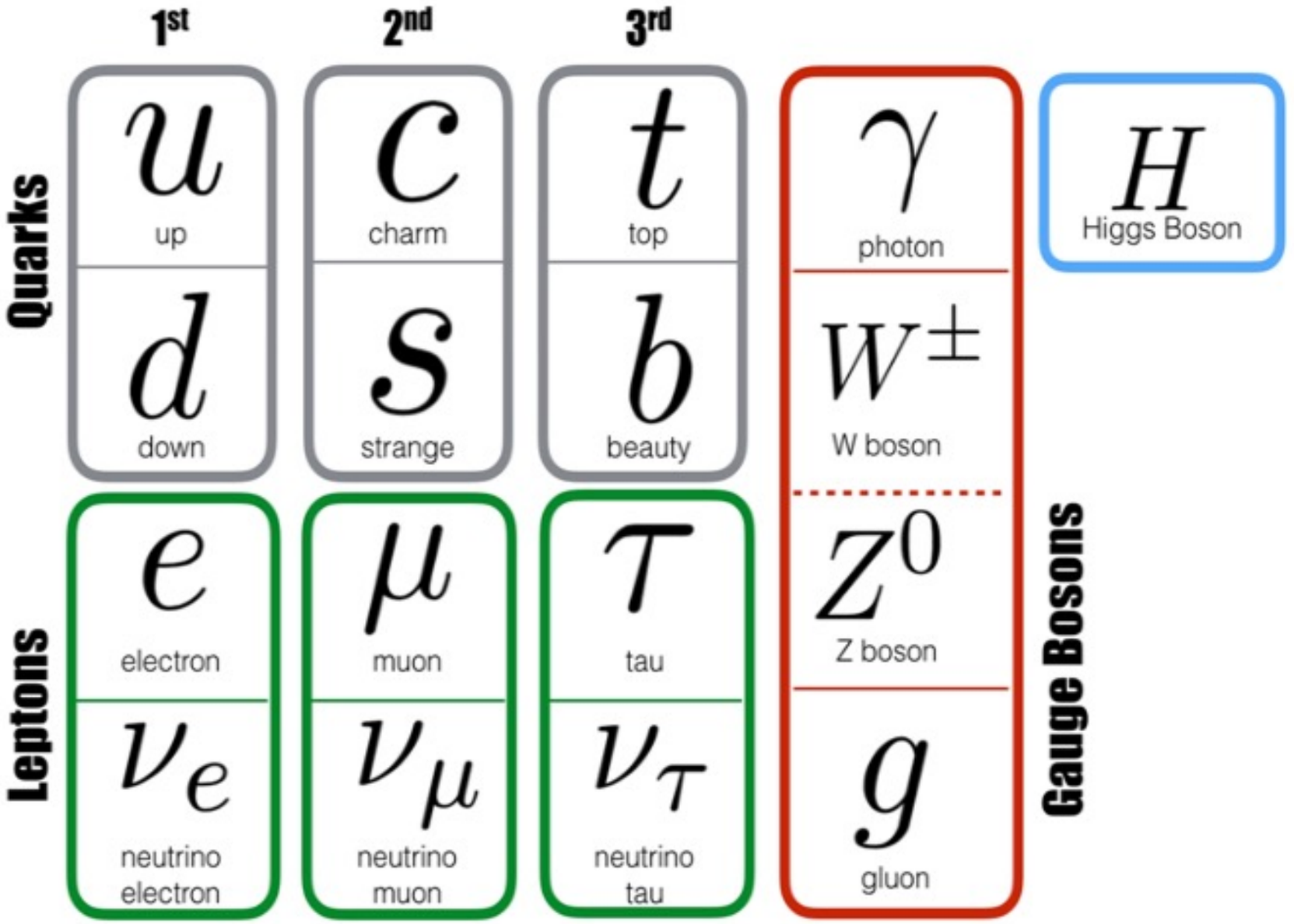
1st
2nd
3rd
Quarks
u
up
c
charm
t
top
d
down
s
strange
b
beauty
γ
photon
H
Higgs Boson
W±
W boson
Z0
Z boson
g
gluon
Gauge Bosons
e
electron
μ
muon
τ
tau
νe
neutrino electron
νμ
neutrino muon
ντ
neutrino tau
Leptons

3He Cryostat Cooling Power

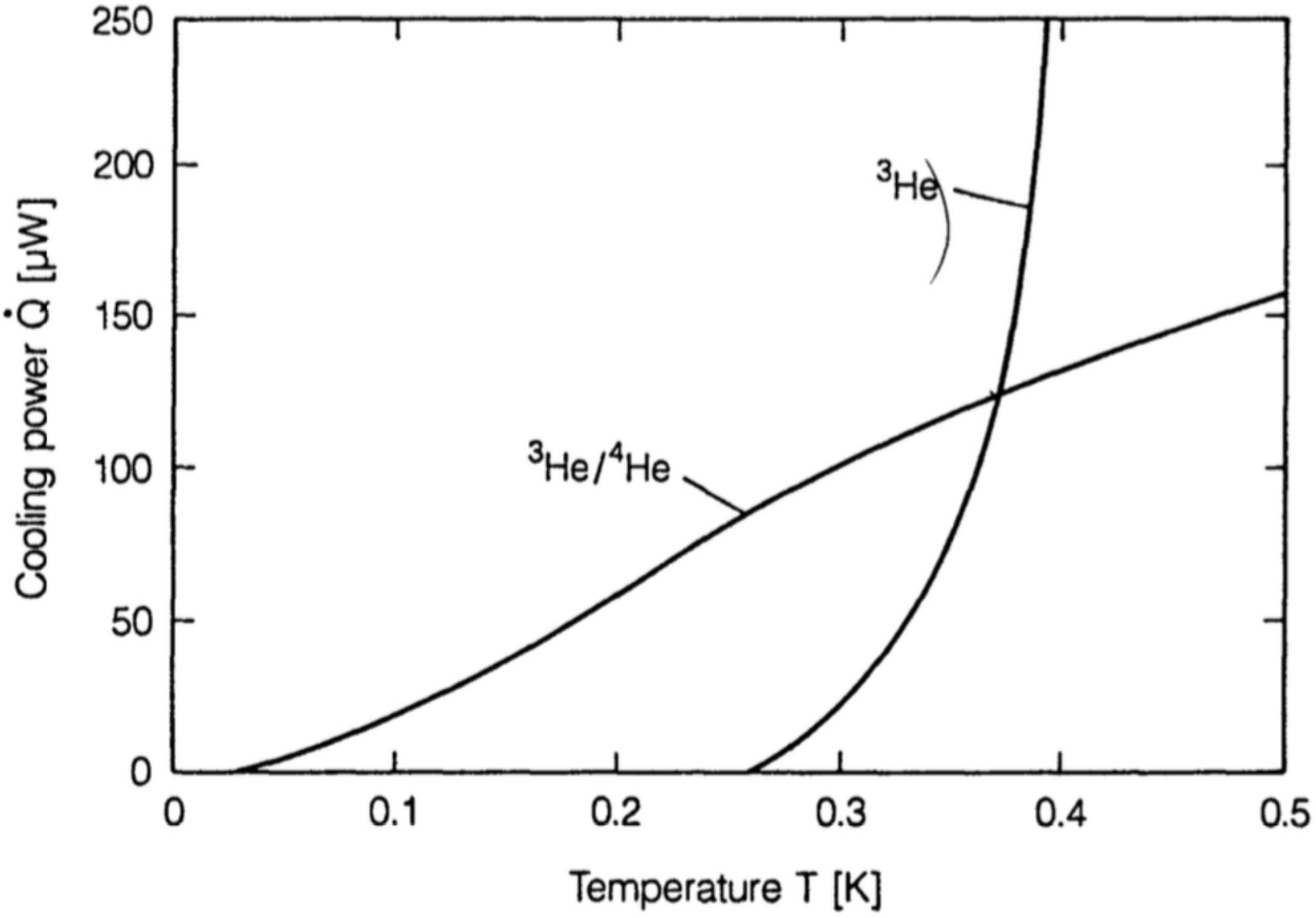
250
200
150
100
50
0
Cooling power Q̇ [μW]
^{3}He
^{3}He/^{4}He
0
0.1
0.2
0.3
0.4
0.5
Temperature T [K]

Slanted muon beam

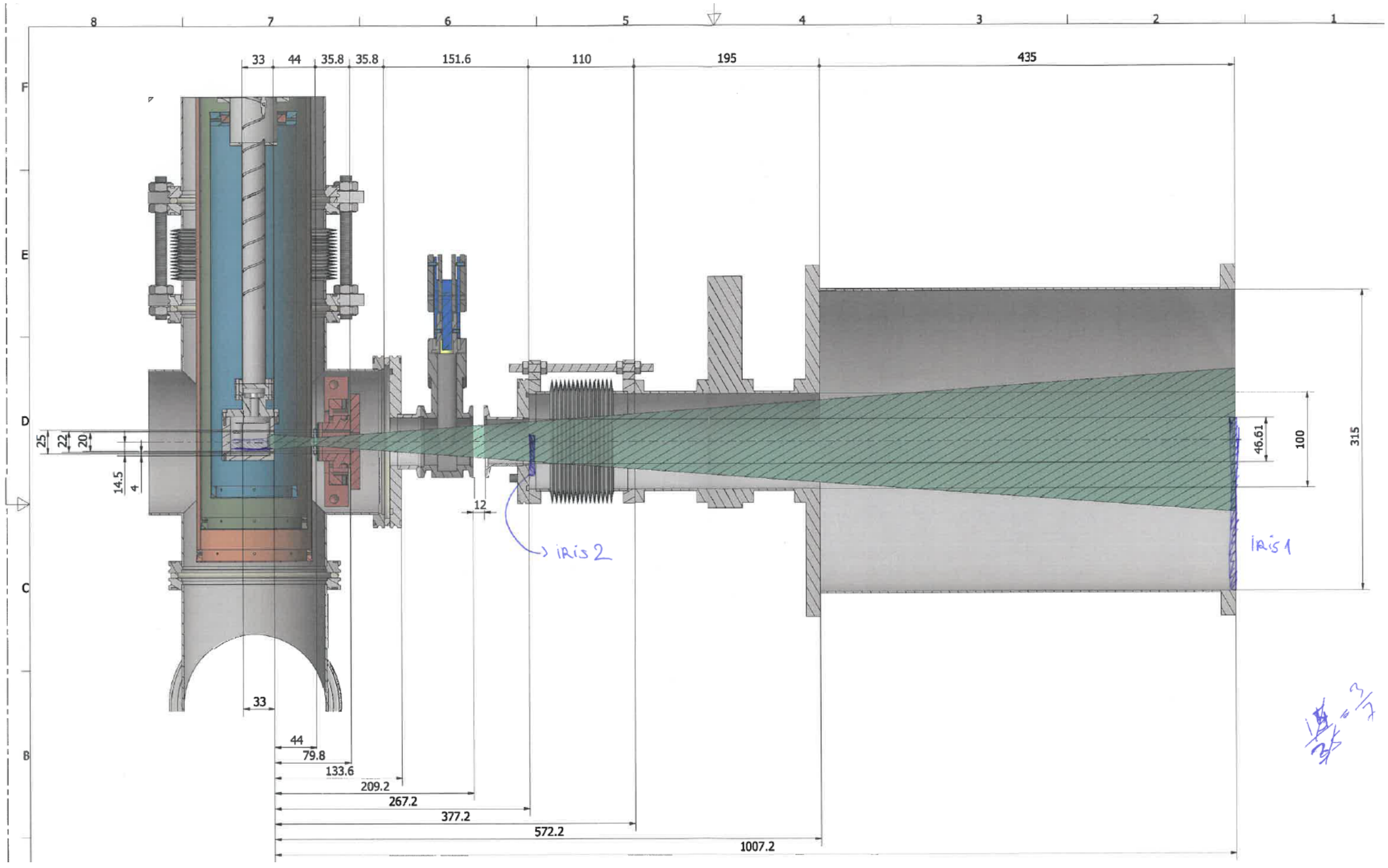
8
7
6
5
4
3
2
1
F
E
D
C
B
33
44
35.8
35.8
151.6
110
195
435
25
22
20
14.5
4
12
46.61
100
315
IRIS 2
IRIS 1
33
44
79.8
133.6
209.2
267.2
377.2
572.2
1007.2